8-2015

Natural polymer based composite scaffolds for tissue engineering applications

Marcos R. Villarreal
University of Texas-Pan American

NATURAL POLYMER BASED COMPOSITE SCAFFOLDS

FOR TISSUE ENGINEERING APPLICATIONS

A Thesis

By

MARCOS R. VILLARREAL

Submitted to the Graduate School of
The University of Texas-Pan American
In partial fulfillment of the requirements for the degree of

MASTER OF SCIENCE

August 2015

Major Subject: Mechanical Engineering

NATURAL POLYMER BASED COMPOSITE SCAFFOLDS

FOR TISSUE ENGINEERING APPLICATIONS

A Thesis
By
MARCOS R. VILLARREAL

COMMITTEE MEMBERS

Dr. Waseem Haider
Chair of Committee

Dr. Dumitru Caruntu, P.E.
Committee Member

Dr. Javier Macossay-Torres
Committee Member

August 2015

ABSTRACT

Villarreal, Marcos R., Polysaccharide Based Composite Scaffolds for Tissue Engineering Applications. Master of Science (MS), August, 2015, 90 pp., 8 tables, 28 figures, 101 references

The fabrication, characterization, and bio-assessment of two types of perspective tissue engineering (TE) scaffolds are presented. Principally derived of biopolymers, both types of scaffolds generally followed porous scaffold methodologies for synthesis. Differentiating the two scaffold varieties was chiefly driven by crosslinking attainment, where crosslinking is argued to add structural stability and aid in regulating biodegradability rates in TE scaffolds. Microwave irradiation via conventional microwave was one method used to prospectively crosslink cornstarch to chitosan and sodium alginate. Triethyl orthoformate, was used to prospectively crosslink collagen and chitosan. After the scaffolds were "crosslinked" they were subjected to freeze drying techniques in order to exploit the sublimation of ice crystals frozen within the scaffolds, to produce a porous-permeable microstructure, vital for promoting cellular processes. Osteoblast MC3T3 cells and fibroblast cells were used for the bio-assessment to suggest the scaffolds as viable candidates for tissue engineering applications for bone and skin regeneration programs.

DEDICATION

To Mom, Dad, Momo, Popo, Mariel, and Buddy Joe:

So passionately have you bestowed me with knowledge and an emphasis in education, that it has tailored me to never stop learning and in addition, to always appreciate the confines and multi-aspects of life. Moreover, that there is a degree of value to be taken from every experience, observation, and fraternization, no matter it's conclusion. I fell that this ideology has invoked limitless boundaries on me that I promise to pass on to OUR future children. In addition, the guidance, support, and love which has surrounded me throughout life, has unselfishly been irradiated from all of you, and also is promised to be passed to OUR children. With that, this thesis is dedicated to you.

To Candace, Zoe, and Ava:

The motivation, which facilitated the completion of this thesis, is owed to you. With its completion, I wish to demonstrate what perseverance and family support can ensure. I also promise to utilize the knowledge gained to acquire even more and to help establish our home. Candace, the burdens brought forth in accomplishing this degree are soon to be behind us. But I hope in the future we can reflect on the true provisions of life, which have recently been brought to light, and use this experience to help guide us through future struggles. Zoe and Ava, I promise to offer you the guidance, support, and love that were unselfishly bestowed upon me. With that, this thesis is dedicated to you.

ACKNOWLEDGMENTS

Luis Pompa, Andrea Flores, Alfonso Salinas, Lawrence Cano, Zia Raman, Jerry Contreras, Mr. Tom Eubanks, Lwei Lin, Hilario Cortez, Jessica Cruz, and Mr. Ed Villarreal

Dr. Lee Kramer, Dr. Chipara Dr. Mao, Dr. Pokhrel, Dr. Srivastave, Dr. S. Mohan, Dr. Debasish, Dr. John R. Villarreal, Dr. Jason Parsons, Dr. Caruntu, Dr. Maccosay-Torres, Dr. Tarawneh and most importantly, Dr. Haider for your perseverance and diligence.

The author would also like to acknowledge the US Army Research Office (W911NF-14-1-0100) for their support in the use of the XPS system.

TABLE OF CONTENTS

LIST OF TABLES

LIST OF FIGURES

CHAPTER I

INTRODUCTION

Biomedical engineering is a discipline utilizing engineering and scientific principles to resolve biological and physiological problems. More precisely, it entails the development of devices and procedures that solve medical and health-related issues (Florida Institute of Technology). A substantial list of sub-disciplines make up the field of biomedical engineering and it's thought that as technological advances improve, new niches of research may further expand the current biomedical engineering realm. For now, areas of research focus on computational and systems biology, biomedical imaging and optics, bio-nanotechnology, biosensors, neural engineering, biomechanics, healthcare systems engineering, regenerative engineering, biomaterials, and tissue engineering. Biomaterials is certainly one of the most imperative studies which is under extensive study where a biomaterial is defined as a nonviable material used in a medical device that is intended to interact with a biological system (Ratner, Hoffman, Schoen, & Lemons, 1996). Presently, there are a wide variety of biomaterials in application and under review with a range consisting of metals, polymers, ceramics, nano-materials, and composites. As broad as the scope of culprits may be, they all must exhibit certain qualities unique to biomaterial application. Some of the aspects that are critical in evaluation of biomaterials include toxicology, biocompatibility, healing, and consideration of the anatomical site of implantation, and mechanical and performance requirements. Initial thought in selecting a

material for biomaterial application must first include an assessment regarding the toxicology of the material being considered. It should be made certain to not possess toxic qualities or to produce toxic by-products in response to physiological conditions and degradation. This is vital in order to prevent any toxicity after implantation. Therefore, unless specifically engineered for such requirements, a biomaterial should not be toxic (Ratner, Hoffman, Schoen, & Lemons, 1996). Another key issue one must consider when selecting a suitable biomaterial is the materials degree of biocompatibility. Where biocompatibility, as defined by the European Society for Biomaterials, is the ability of a material to perform with an appropriate host response in a specific application. As in the definition, "specific application" is conceptually important in that biocompatibility may have to be uniquely defined for each application (Ratner, Hoffman, Schoen, & Lemons, 1996). Healing is also an important concern for a biomaterial scientist in that once a "foreign body" is implanted in vivo, special natural processes can invoke favorable or unfavorable responses. If tissue is subjected to injury or traumatic events (i.e during surgical implantation), stimulation of the inflammatory reaction sequence can be activated in order to heal the damaged tissue. Consequently, the rejection of an implant or tissue engineered scaffold may follow. If a foreign body, such as an implant or scaffold is involved, the reaction is referred to as the foreign body reaction, which in effect can trigger the inflammatory response of the body, resulting in possible increases of inflammatory intensity and duration (Ratner, Hoffman, Schoen, & Lemons, 1996) thus complicating healing. Another important consideration is, that of the anatomical site of implantation. The body is a product of different organs and systems functioning in unison. What complicates the selection of a universal biomaterial lies in

that each organ and system is composed of a unique cellular composition, resulting in different tissues, structures, and functions. Consequently, different tissues may have different degrees of acceptance for the same material. Organs are also very likely to be different shapes and sizes than adjacent organelle systems, or may be more dynamic in nature and functioning processes. Therefore biomedical engineers must consider the geometry, size, mechanical properties, and bioreactions, based on the anatomical site, for implementation for the biomaterial (Ratner, Hoffman, Schoen, & Lemons, 1996). Finally, a biomaterial engineer must select a material that more appropriately satisfies the mechanical and performance requirements necessary to serve its dynamic function as an implant.

Closely affiliated with biomaterials, tissue engineering (TE) involves the restoration or the improvement of defective tissues through biological tissue substitutes or by the synthesis of tissues. TE is usually conducted using in vitro techniques that involve the seeding of living cells on a scaffold or Scaffold, where cell proliferation and sorting can take place. Upon successful cell production and cell organization, the scaffold is then implanted "in vivo" to the appropriate anatomical site. Tissue engineering is just one branch underlying biomedical engineering, where the principles are based off the notion that the living body has the potential of regeneration through the use of engineering and cellular biological concepts (Yunos, Bretcanu, & Boccaccini, 2008) (Hubbell & Langer, 1995). It may be worth noting that TE differs from regenerative engineering in that regenerative engineering deals with the seeding of un differentiated cells called stem cells on tissue engineering scaffolds. The general process used by tissue engineering, usually starts with a biopsy of the tissue of interest and isolation of the tissue

cell. Cellular cultivation, proliferation, and differentiation are then carried out on a construct called a scaffold where tissue development commences at the cellular level. The reconstructed tissue is finally implanted into the patient (*in vivo)*; only after proper tissue formation is observed. To ensure that this is the case, cellular proliferation and sorting may take place in controlled devices known as bioreactors, which use mechanical stimuli to control cellular growth (Thayer, 2011) (Karp, 2003) (Chan & Leong, 2008) (Ackbar & al., 2007).

A tissue engineering bioreactor is a device that uses mechanical means to influence biological processes in the early stages involving in vitro development of new tissue (Martin, Wendt, & Heberer, 2004) (Martin & Vermette, 2005). This is done by providing biological and physical regulatory signals to cells, which encourage differentiation, and/or to stimulate production of extracellular matrix prior to in vivo implantation (Plunkett & O'Brian, 2011). In general, bioreactors, used in tissue engineering application, are designed to perform at least one of the following five functions; provide uniform cell distribution, maintain the desired concentration of gases and nutrients in the medium, provide mass transport to the tissue, expose tissue to physical stimuli, or provide information about the formation of 3D tissue (Mekala, Baadhe, & Parcha, 2011). As previously mentioned, engineering programs usually start with *in vitro* techniques and development, and only upon successful tissue growth, does it move to the *in vivo* phase. Thus the initial development of cell growth is essential for any tissue-engineering program. However, issues are present during culturing of cells on the scaffolds, primarily due to the static culture conditions. In particular, static culture conditions are found to allow cell necrosis and cell chemotaxis to occur *in vitro* on

scaffolds, leading to poor cell distribution or no cellular growth. Therefore, certain *in vitro* techniques must be invoked to foster a viable scaffold. Thus, by providing regulatory signals that mimic the natural physiological signals and conditions, healthier cellular activities are better attained. Bioreactors are also being used to increase the production of extra cellular matrix by providing mechanical stimulation to cells. For instance, it has been shown that increasing hydrostatic pressure in bioreactors, shows a significant improvement of culture growth over scaffolds (Martin, Martin, Plunkett, Mekala). Mechanical stimulation through the use of bioreactors can also increase cellular differentiation by encouraging stem cells to metastasize in a particular direction by providing biochemical and physical regulatory signals to the cells (Plunkett & O'Brian, 2011). While mechanical stimulation and chemical signaling is essential for the necessary biological and biochemical activities to occur, a viable material constituent is also needed to allow said biological activities to direct cellular activity on. Selecting an appropriate material for tissue engineering application is an entire different realm underlying biomedical engineering and is critical in finding a suitable scaffold for application.

The design and fabrication of tissue engineering (TE) scaffolds with the exact mechanical properties and replicated extracellular matrix microstructure to promote cellular attachment, growth, and new tissue formation, is one of the key challenges facing the tissue-engineering field today. Preceding studies have offered insight in the formulation of TE scaffolds and as a result have yielded base criterion necessary for the design of viable TE scaffolds. Unfortunately, the perfect candidate, which mimics that of natural tissue, does not exist and therefore retains only one or a few of the prescribed

characteristics research has implicated for TE practice. Accordingly, the physiological body may offer the greatest extent of insight into producing the most promising TE scaffolds. After all, the physiological body has perfected and adequately selected the ideal materials to use as its Scaffolds for cellular activity to take place. Science has labeled these materials as natural polymers, or more specifically, carbohydrates, lipids, proteins, and nucleic acids. The focus of the literature review will thus lie on prospective tissue engineering scaffolds that are principally derived of natural polymers and which are more aptly able to mimic the natural extracellular matrix for bone and skin synthesis using osteoblast MC3T3 and fibroblast cell lines.

Bone: Tissue and Growth

In order to better understand composites used in bone tissue engineering, its thought that a small section highlighting bone cells accompanied with an introduction of the processes involved in osseointergration would be useful, even though it may outside the scope of the objective. For instance, what is vascularization and why is it important in phase one of osseointergration? In addition, chemical growth factors involved in bone regeneration may be worthy of introduction and as a result are also included. Therefore this is only to offer a tangent path for further research prospect. In fact, its strongly encouraged to more closely study the growth factors involved in bone tissue engineering as well as the characteristics and chemical composition of bone and the processes involved with osseointergration. Bone formation is a complex process that involves a large number of hormones, cytokines, and growth factors that are regulated by multiple controlled molecular events. The diversity of size and physiological system of each bone type (long bone, skull, spinal bone, and mandibular bone), and fracture model (tibia,

radius, and calvarial defect, critical and noncritical-size defect) makes it difficult to choose an ideal delivery system for specific types of tissue to be restored. Therefore, it is imperative to choose particular bioactive molecules accordingly to enhance an ideal delivery system (Lee & Shin, 2007) (Fishman, et al., 2013) (Gartner & Hiatt, 2006) (Misch, 2008). A part of the following section is taken from *matrices and scaffolds for delivery of bioactive molecules in bone and cartilage tissue engineering*, to introduce some of the main growth factors associated with bone tissue regeneration. Overall some of the important roles of growth factors include, assistance in healing on the external adjacent tissues of bone, and to accelerate blood vessel growth into the scaffold from the host bone, a process called vascularization.

Osteoprogenitor Cells

Osteoprogenitor cells are undifferentiated-appearing cells located in the cellular layer of the periosteum, and the endosteum. They are also found at the lining of the haversian canals, where the housing of blood vessels are located and facilitate waste removal and introduce oxygen. They are also the cells that eventually give rise to the production of osteoblasts (Gartner, and Hiatt, 2006)

Osteoblasts are characterized by cuboidal to low-columnar cells and are primarily responsible for the production of bone matrix. During the synthesis and organization of the bone matrix, osteoblasts are surrounded by the matrix and subsequently become osteocytes (Gartner, and Hiatt, 2006). Osteocytes are thus spawned from osteoblasts and are responsible for the maintenance of bone. In addition these cells are also responsible for the short-term mitigation of calcium and phosphate homeostasis of the body.

Osteoclasts are multinucleated cells derived form monocytes, and are facilitate the reabsorption of bone. Cooperation between osteoclasts and osteoblasts is what dictates successful formation, remodeling, and repair of bone (Gartner, and Hiatt, 2006).

CHAPTER II

REVIEW OF LITERATURE

Tissue Engineering Scaffolds

Traditionally, the principal role of biomaterials and tissue engineering scaffolds was to provide an inert synthetic framework for cells. Today, research seems to lean more toward the notion that, biomaterials and scaffolds may need to go beyond this concept (Barbieri et al). Clearly put, that newly developed biomaterials and scaffolds should be designed with the intent of actively interacting with their biological surroundings (Barbieri et al). For instance, it has been observed that when stem cells attach to a biomaterial, the local surface characteristics of the material, such as the topography, roughness, surface stiffness, and chemistry can invoke certain and various cellular behaviors (Barbieri et al). Barbieri et al. cites as an example that micro- and nano-rough surfaces have larger surfaces areas, which promote and enhance specific protein absorption from surrounding body fluids. Thus giving rise to key protein motifs, which trigger various cell responses, such as the differentiation of cells into more specific tissue (Barbieri et al).

With this concept in mind, TE scaffolds should also possess certain properties and characteristics, fundamentally. Ideally, a scaffold should have the following characteristics: A three-dimensional porous and permeable network that accommodates

the necessary cell growth and allows flow transport of essential nutrients and metabolic waste (Loh & Choong, 2013) the scaffold should also be biocompatible and bio-resorbable, unless otherwise designed, with a controllable degradation and reabsorption rate to match cell/tissue growth in vitro and/or in vivo; it must also possess suitable surface chemistry for cell attachment, proliferation, and differentiation; finally, the scaffold should hold mechanical properties that closely mimic those of which the natural tissues exhibit at the site of implantation (Hutmacher) (Yang, Leong, Du, & Chua, 2001). In vivo, cells are supported both structurally and biochemically by the extracellular matrix (ECM), which is essentially a nano-scale fibrous protein mesh (Alisa morss Clyne Thermal Processing of TE scaffolds). Consequently, since scaffolds are intended to simulate a temporary artificial ECM, materials that most closely resemble the intended tissue replacement are the most promising candidates. Thus the challenges faced by tissue engineers are due to the complex combination of properties required in an ideal scaffold.

Currently, researchers have an extensive arsenal at their disposal in respect to the materials and fabrication methodologies involving the synthesis of TE scaffolds. Selection of materials is fundamentally based on the basis of if the scaffold should degrade or remain a permanent part of the tissue as it grows (Alisa), *in vivo* or not. Moreover, what further merit the selection of a material is the mechanical properties necessary for a successful implant. This can primarily be related to the physiological location in the body, geometry of the surrounding organ systems, and the nature of the surround tissues.

Metals presently being used include stainless steel, cobalt-based alloys, and titanium-based alloys (Alisa). Drawbacks of using these metals however, are related to their difficulty in processing and their lack of biodegradability. Therefore, orthopedic implants is usually what these materials are implemented as (Alisa). Ceramics on the other hand are used extensively in bone tissue engineering. Materials like calcium phosphate, silica, alumina, zirconia, bioglass, hydroxyapatite, and titanium dioxide, can be used alone or be utilized with other classes of materials in composite scaffolds (Alisa). The use of polymers, both natural and synthetic, is far fetching due to diversity in their composition, ease of bioactive factor conjugation, and ability to control both their mechanical properties and degradation rate (Alisa). Natural polymers employed include cellulose, chitosan, alginate, chitin, starch, fibrin, collagen, hyaluronic acid, glycosaminoglycan, and gelatin (Alisa) (Chung, H.J, and Park). Synthetic polymers include, polylactide (PLA), polyglycolide (PGA), poly(lactide-co-glycolide) (PLGA), polyanhydrides, and polyorthoesters (Alias) (Tuziakoglu) (Weigel, Schinkel).

While a variety in selection of material candidates is observed, so are the varieties of fabrication methods for making TE scaffolds. In addition, its found that properties of scaffolds such as structure and morphology can be invoked by altering specific thermal fabrication techniques and methodologies (Clyne). In Clyne's study, she separates scaffold fabrication into two types: fibrous scaffolds and porous scaffolds.

Fibrous Scaffolds and Techniques

Fibrous scaffolds may better mimic the natural extracellular matrix by possessing a nano-scale fibrous mesh. Also present in fibrous scaffolds, is a large surface area for

cell attachment in addition to high porosity for rapid nutrient diffusion (Clyne). However for load bearing application (i.e. tissues), fibrous scaffolds lack the structural stability and mechanical integrity. Still, fibrous scaffolds are highly sought as prospective culprits for many TE programs. Current active fibrous scaffold techniques include: fiber bonding, electro-spinning, and force-spinning.

Fiber Bonding. Fiber bonding is a fibrous scaffold type of technique that involves joining fibers at their crosspoints either through sintering the fibers or melting a secondary polymer in order to join them together (Clyne). Unfortunately, scaffold porosity is limited and often ranges from 50% to 81% and proves difficult to control. Also harsh solvents are sometimes needed, that can in turn harm cellular progression if residual solvent is not present (Clyne) (Chung J.J and Park) (Weigel). PGA poly(L-lactic acid) (PLLA) seem to be used extensively in studies. In one, PLLA was used as the bonding agent (Kim, Mooney) and the PGA fibers matrices were sprayed with atomized PLLA and annealed at 195°C to melt the PLLA (Clyne). The PLLA then condensed at the PGA fiber crosspoints (Clyne). In the study it was concluded that extensive fiber bonding increased scaffold compressive modulus, slowed degradation, improved cell interaction, and prevented matrix contraction with seeded cells (Clyne). Clyne further details a study where fiber bonding was applied to increase the integrity of electrospun scaffolds by bonding PCL electrospun fibers in Pluronic F127 (Clyne) (Lee, Oh, Liu). It was determined that scaffold mechanical properties such as shrinkage, ultimate tensile strength, and burst pressure improved (Clyne). Overall, Fiber bonding scaffolds produce fibrous morphologies similar to native extracellular matrix, exhibit

beter mechanical properties than electrospun scaffolds, and yield high porosity scaffolds (Clyne). On the flipside however, porosity varies greatly, there are limited polymers and solvents available for use, and solvents may have toxic effects (Clyne).

Electrospinning. Developed primarily as a textile and filtration fabrication method, electrospinning was introduced as a viable way of producing TE scaffolds after it was demonstrated that organic polymers could be electrically spun (Clyne). Simply put, electrospinning involves the extrusion of a polymer melt from a nozzle using gravity, mechanical, and high voltage electric fields (10-20kV) (Clyne). Nano-fibers are created (extruded) when the applied electric field causes a greater electric force that surpasses the polymer surface tension yielding the extruded nanofibers (Clyne). Studies indicate variances in fiber morphology are related to polymer viscosity, conductivity, surface tension, molecular weight, flow rate, tip to collector distance, and nozzle tip design (Clyne) (Murugan, Huang). Synthetic polymers have been successfully electrospun including: PLGA (18 kV, 20cm between needle tip and plate, fiber diameter 500-800nm), PCL (13 kV, fiber diameters from 20 nm to 5 micrometers (Clyne). Alternatively, natural polymers have also been spun and include: fibrinogen (22 kV, average diameter nanofiber of 80nm) (Wnek, Carr) and dissolved silk (15 kV, 13 nm-120 nm) (Min, Lee). Other natural polymers successfully spun include chitin and alginate. Also, Li et al. fabricated electrospun blends of synthetic and natural polymer blends that improved mechanical properties while maintaining cell affinity (Clyne) (Li, Mondrinos). Overall, studies show that fibrous scaffolds are more similar to native extracellular matrix, nanoscale fibers can be created from both synthetic and natural polymers, and high surface area and porosities are obtained, from electrospinning fabrication (Clyne).

Disadvantages include low mechanical performance in regards to integrity and pore size that may be too small for cellular penetration (Clyne).

Forcespinning®. Where electrospinning uses electrostatic forces to draw nano-sized fibers, Forcespinning® utilizes centrifugal forces to extrude nano-fibers, resulting in a significant increase in yield and ease of production (Lozano) (Pardon, Fuentes, Caruntu). The method has often been compared to the mechanics behind the production of cotton candy. Another upside benefit to using forcespinning®, is that both conductive and non-conductive polymer solutions and melts can yield fibers without implementing electric fields (Lozano). Finally, the production rate of Forcespinning®, has yielded a production rate of 1g per min, per nozzle in comparison to electrospinning which produces up to only 0.3g per hour (Lozano)(Sarkar, Gomez) (Lozano & Sarkar) (Ramakrishna, S). Unfortunately, due to the infancy of the forcespinning® method, a lot of research has not been done. However, Fenghua et al., successfully mass produced chitosan/polyvinyle alcohol binary and tannic acid/chitosan/polyvinyle alcohol ternary composite nanofiber membranes from chitosan citric acid salt aqueous solutions without toxic solvents (Fenghua & Lozano). The study produced a novel ternary composite membrane, which promoted fibroblast cell adhesion while providing a 3D structure that mimicked the natural extracellular matrix of skin (Fenghua & Lozano). It was also noted that antibacterial properties, against gram-negative bacteria *E. coli,* were as well present, thus offering promise for wound dressing applications (Fenghua & Lozano).

Porous Scaffolds andTechniques

Porous scaffolds are typically used to exploit their porous and permeable morphology, which is adequate for allowing cell and cellular function mobility and dynamics. Studies indicate that optimum pore size for tissue growth varies with tissue type (Clyne)(Cima). Current methods for creating porous scaffolds include emulsion freeze drying, solvent casting, gas foaming, high pressure processing, and thermally induced phase separation (Clyne).

Emulsion Freeze Drying. Emulsion freeze-drying is conducted by producing a homogenous solution consisting of a dispersed water phase and a continuous polymer-solvent phase. The mixture is then frozen at very low temperatures and subsequently lyophilized (freeze-dried), which consequently leave behind a porous and permeable morphology (Clyne). Variability in pore size are influenced by emulsion characteristics, polymer weight percentage, molecular weight, dispersed phase volume fraction, and freezing temperature (Clyne). Moreover, pore size range from 20 micrometers to 200 micrometers and can yield overall porosities exceeding 90% (Clyne). A few cases where emulsion freeze drying was used, were found in Clyness' work as well. Conclusions yielded by studies include, that increasing polymer volume fraction in a polymer-methylen chloride solution of PLA or PLGA, increased porosity and pore size. Also mentioned was that scaffolds with pore size less than 50 micrometers show improved bone defect healing (Clynes) (Whang, Thomas) (Whang, Thomas). Baker et al. also produced PLGA and PLA scaffolds by emulsion freeze drying. That study included a surfactant call Span 80, to stabilize the emulsion. Pore size yielded ranged from 20 micrometers to 50 micrometers (Clyne)(Baker). Also, a hydrogel of poly(vinyle

alcohol)(PVA) and poly(vinylpyrrolidone) (PVP) was added to a PLGA emulsion and made homogenous. Solvents where removed by submerging in water, and it was freeze dried and subsequently yielding mechanical properties similar to native cartilage (Clynes)(Spiller). Overall, emulsion freeze dried scaffolds yield highly porous with high pore size morphology and are safe for protein and bioactive factor incorporation into scaffolds. However, the variance in pore size can be difficult to control (Clyne). Also troubling is the stabilizing surfactant that may need to be employed for effective emulsion to take place (Clyne). In some cases, these surfactants can possess toxic qualities that may hinder quality of the scaffold.

Lyophilization (Freeze Drying). Freeze drying is similar to emulsion freeze drying but differs in that the polymer is dissolved, rather than suspended, and mixed with a water solution. Where as the emulsion freeze drying incorporates a stabilizing agent, this method usually involves a dissolving agent for the polymer. Therefore care should be taken as some polymers may require toxic solvents, and proper removal of residuals is needed. Nevertheless, the sample is also frozen and subsequently freeze dried to sublime ice water crystals, which leave a porous structure. Hydrogels are typically used in this method due to their ability to retain high amounts of water. After freezing and freeze drying, hydrogels are shown to provide high porous and permeable morphologies. Studies have left us with some important observations. For instance, fast freezing rate produces smaller pores (Sacholos and Czernuszka) (Dagalakis) (Doillon), and unidirectional solidification has been used to create a homogenous 3D-pore structure (Sacholos and Czernuszka) (Schoof et al, 2000) (Schoof et al, 2001).

Solvent Casting/Particulate Leaching. Solvent casting/Particulate leaching can produce scaffolds with defined pore size by modifying particulate diameter and concentrations. Basically, a polymer is cast with mineral or organic particles dispersed in a solution. Consequently the solvent is evaporated out while the particles are left to dissolve or be leached out (Clyne). Pore size range from 100 micrometers to 600 micrometers with values of porosity exceeding 90% (Clyne). Overall, advantages of using solvent casting/particulate leaching include defined pre size with high porosity, independent control of pore size and porosity, and can be utilized to make porous ceramics as well (Clyne). Disadvantages include possibilities of having to use toxic solvents and producing nonporous skin layers, which can consequently stop or disrupt cellular penetration (Clyne).

Gas Foaming/Particulate Leaching. Similar to solvent casting/particulate leaching, this method involving fabricating tissue engineering scaffolds uses an effervescent salt as its porogen which produces gas as it is leached out of the polymer (Clyne). Monney et al., saturated the biodegradable polymer PLGA with carbon dioxide at high pressures. Successively, bringing the carbon dioxide pressure back to atmospheric level then rapidly decreased the solubility of the gas in the polymer. This resulted in nucleation and growth of gas bubbles, yielding pores between 100-500 micrometers in the polymer (Sachlos) (Mooney, 1996). Clyne adds that the process is rather quick and that the fabricated scaffolds do not have an impermeable skin layer as in solvent casting (Clyne). Porosities of 90% can also be attained as well as having control of both porosity and mechanical stretch by controlling gas evolution reactions (Clyne). Overall, Clyne concludes that favorable attributes of gas foaming/particulate leaching

include no skin layer and high porosity, and that downfalls lie in that toxic solvents may be required and that difficulty lies in controlling pore shape and interconnectivity (Clyne).

Biocomposites

Many of our modern technologies require materials with unusual combinations of properties that cannot be met by the conventional metal alloys, ceramics, and polymeric materials alone (Callister, 2007) (Yusop, Bakir, Shaharo, Kadir, & Hermanwan, 2012) (Yoshida, Dhandayuthapani, Maekawa, & Kumar, 2011). For instance, metals exhibit extraordinary mechanical properties with respect to strength and toughness. Under normal circumstance however, they require surface modification in order to obtain favorable biological responses. Needless to say, machining metals to meet biomaterial needs can result in costly manufacturing procedures. Bioactive ceramics have the great advantage of accepting and encouraging bone ingrowth, a condition referred to as osseointegration. One the other hand, bioactive ceramics fall short of some of their mechanical properties; specifically the toughness associated with them. Polymers generally have good toughness, but their bioactivity is normally not comparable with that of bioactive ceramics.

The "pros and cons" debate between metals, ceramics, and polymers may never end, however it doesn't mean we can't get beyond the offense. Like many other industries biomaterial scientist and engineers are incorporating the best of both worlds. As an example D. Barbieri et al. cites that in attempting to design biomaterials that are able to support and trigger bone tissue regeneration, in addition to mechanically

facilitating and supporting the physiological stresses, research has resorted to fully or partially mimicking the biphasic composition of bone (Barbieri et al.). Bone, which is a natural composite material, is macroscopically a collagen matrix with nano-apatite particulates (Barbieri et al.). As another example the physiological composition of the extracellular matrix, is that of a matrix composed primarily of polysaccharide gels reinforced with fibrous proteins, to accommodate the natural stresses produced from cellular proliferation and differentiation.

For our study in biomaterials and tissue engineering, an appropriate definition for composites is a material consisting of two or more chemically distinct constituents, on a macro-scale, having a distinct interface separating them. The two chemically distinct materials are often referred to as the matrix and dispersed phases. The matrix phase is the continuous phase of the material that makes up the majority of the volume. The matrix encompasses the second member known as the dispersed phase, which can also be thought of as the reinforcing constituent of the composite. The properties of composites are therefore strongly influenced by the constituent materials, their distribution, the interaction among them, and the geometry and nature of the dispersed phase (Ratner, Hoffman, Schoen, & Lemons, 1996).

Fiber-reinforced and particle-reinforced composite materials are of primary importance for use as a biomaterial. For particle-reinforced composites, the dispersed particles are equiaxed. By comparison, for fiber-reinforced composites, the dispersed phase has the geometry of a fiber (Callister, 2007). The main reinforcing materials currently being used in biomedical composites are carbon fibers, polymer fibers, ceramics, and glass. Also, depending upon the application, the reinforcements can been

inert or absorbable (Ratner, Hoffman, Schoen, & Lemons, 1996). With regards to the matrix, absorbable and non-absorbable matrix composites are used. Absorbable matrix composites have been used in situations where absorption of the matrix is desired such as to expose surfaces to tissue or to release admixed materials such as antibiotics or growth factors. However, the most common reasons for using absorbable matrix composites is to accomplish time-varying mechanical properties and ensure complete dissolution of the implant. Non-absorbable matrix composites are typically used in instances where specific mechanical properties are desired but unattainable using homogeneous materials. Designing a composite material to mimic the structure and properties of tissue to be replaced offers a great potential for solving problems due to the advantage of utilizing the good qualities of different materials (Huang, et al.). It's now up to research to offer us insight into implementing the optimal combination of constituents to produce an ideal composite for a proper tissue engineering scaffold for particular use (Yoshida, Dhandayuthapani and Maekawa).

Biopolymers as Biomaterials

Biopolymers encompass a wide variety of bioorganic compounds, which exist in nature and which are synthesized by natural processes. Alternatively known as natural polymers, biopolymers serve a variety of functions throughout nature, which include offering structural integrity, serving as metabolic energy, and providing recognition sites on cellular surfaces (Bruice) (Solomans). In a physical sense, some natural polymers must exhibit unique and complicated structures, due to the fact that specific recognition on certain physiological surfaces is needed, for natural and vital biological processes to

occur. Known as molecular recognition (Bruice) (Solomans), this is what is responsible for key events such as a sperm cell recognizing the specific carbohydrate surface of an unfertilized egg. Thus, to offer an analogy, if the body used a specific language to dictate specific physiological sequences, biopolymers may offer the best capability of communication, by understanding the language. Another formidable attribute of natural polymers lies in the fact they are typically composed of a polymeric network, which can contain up to 99 percent or higher water content, thus giving rise to exhibit environments resembling the highly hydrated state of natural tissues (Hsu-Feng Ko, et al) (Ratner & Bryant, 2004). As a result the term 'hydrogels' has also been used to describe the swelling capacity demonstrated through the absorption abilities of water (Hsu-Feng Ko). Gutowska et al. adds that gelatinous onset of natural polymers vary and are dependent on the polymer it self and include; changing temperature or pH, ionic cross-linking, solvent exchange or crystallization, and viscosity modification in polymer solution (Hsu-Feng Ko). Hence, with the utilization of bio-inertness and ability of communicating with the body, the underlying interest in the understanding and implementation of natural polymers as tissue engineering scaffolds.

Classifications of Biopolymers

Scientific literature has bestowed names and classes upon natural polymers through which recognition may also be more aptly attained. Proteins, nucleic acids, lipids and carbohydrates make up the familiar natural polymers that are present amongst algal, plant, microbial, and animal life (Bruice) (Solomans). In some literature, lipids and carbohydrates are combined under one class called polysaccharides, therefore yielding

three main groups of natural polymers: proteins, nucleic acids, and polysaccharides. Proteins have the greatest diversity in respect to physiological function, which encompass the regulation of reactions in the body, being the prime constituent of muscle, which is necessary for physical motor function, and also making up antibodies, which protect living systems from disease. In comparison, nucleic acids serve two major purposes that include the storage and transmission of biological information. Finally, polysaccharides are considered to be the main polymers behind energy reserves for living systems, providing biochemical labels on cellular surfaces, and in providing structural support for certain organisms and plants (Bruice) (Solomans).

Nucleic Acids and Lipids. Lipids are a group of natural polymers that consist of a variety of constituents including tricylglycerolds, terpenes and terpenoids, steroids, prostaglandins, and phospholipids. Lipids are compounds of biological origin that dissolve in nonpolar solvents (Bruice) (Solomans). An important and abundant type of lipid is the variety known as triacylglycerols, or the oils of plants and the fats of animals. Tricylglycerols that are liquids at room temperatures are labeled as oils, compared to those that are solids at room temperatures, which are known as fats (Bruice) (Solomans). In animals, tricylglycerols are primarily used as energy reserves. When metabolized, triacylglycerols yield more than twice as many kilocarlories per gram as do carbohydrates or proteins, due to the high proportion of carbon-hydrogen bonds per molecule (Bruice) (Solomans). The steroids group is another variety of lipids present in physiological bodies that can be described as “biological regulators”. Important steroid types include male and female sex hormones, adrenocortical hormones, D vitamins, and bile acids. Phospholipids are structurally derived from a glycerol derivative known as phosphatidic

acid. What makes this variety of lipids so important is the fact that phosphatides main biological functions includes, providing a structural interface between organic and aqueous environments such as the case in cellular walls and cellular membranes. This is possible because of the polar and non-polar structure of the polymer that creates both a hydrophilic and hydrophobic end, opposite of each other (Bruice) (Solomans).

Carbohydrates. Representing 50% of the biomass on earth, carbohydrates are the most abundant class of compounds in the biological world (Bruice) (Solomans). In addition, carbohydrates are among one of the most essential natural polymers of all living entities, in that they participate in a variety of roles and functions. For instance, carbohydrates; contribute to cellular structure and support, provide a resource for metabolic energy, and characterize cellular surfaces by invoking specific recognition sites on cells (Bruice) (Solomans). For example, in *Organic Chemistry,* by Bruice, the first event in any of our lives was that of a sperm cell recognizing a specific type of carbohydrate on the outer surface of an egg.

While extensive in variety, carbohydrates can ultimately be classified as either a simple or complex carbohydrate. Simple forms of carbohydrates are referred to as monosaccharides or alternatively, simple sugars. When two or more monosaccharides are linked together, a complex carbohydrate is then formed. Complex carbohydrates can further be sub-classified as disaccharides, oligosaccharides, and finally polysaccharides. Specifically, disaccharides consist of two simple sugars linked together, whereas, oligosaccharides have three to ten simple sugars linked together. In contrast those labeled as polysaccharides, refer to a complex carbohydrate with ten or more simple sugars linked together. Interestingly however, all of the aforementioned complex

carbohydrates can be disassembled through hydrolysis to form a simple carbohydrate, for instance glucose. Existing in both plants and animals, glucose is found to be the most abundant type of all carbohydrates throughout nature (Bruice) (Solomans). When an animal has an excess amount of glucose from the consumption of plants, the glucose is converted into a polymer know as glycogen. In comparison, when a plant has produced an excess of glucose from photosynthesis, the glucose is converted into the carbohydrate (polymer) we know as starch. To metabolize the newly formed "stored" polymer, both the animal and plant consequently break down the glycogen or starch back to its simpler form of glucose to use as energy. Conversely, natural polymers are assembled through a chemical mechanism called dehydration synthesis. Dehydration synthesis consequently attributes to the formation of oligosaccharides and polysaccharides.

Many physiological events take place as a result of communication between different participants in the body and their surroundings. Communication involves the interaction, recognition, and linking between cells, viruses, bacteria, and tissues, and is possible through the surface recognition between each participating aforementioned constituent. Carbohydrates such as oligosaccharides and polysaccharides are prevalent on many cellular surfaces giving rise for communication between cells and their environment, if compatibility permits. Oligosaccharides chains are linked to cellular surfaces by the reaction of an OH or an NH_2 group of a cell-membrane protein with the anomeric carbon of a cyclic sugar (Bruice), consequently enabling the cells to recognize and interact with other cells, or with invading viruses and bacteria (Bruice) (Solomans). Proteins that are bonded to oligosaccharides are referred to as glycoproteins and are found to vary in composition percentage of carbohydrate. Types of glycoproteins include

collagen, immunoglobulin, follicle-stimulating hormones, and blood plasma proteins (Bruice). Additionally, an important function of the oligosaccharide chains of glycoproteins is the fact that they act as receptor sites on the cell surface, enabling signal transmissions from hormones and other molecules into the cell. Such cellular signaling may be key in supporting good cellular differentiation and proliferation to occur, a vital requirement for any successful tissue-engineering scaffold. Physiological responses such as infection, prevention of infection, inflammatory responses, and blood clotting are also related to the surface interactions between carbohydrates and glycoproteins, which are also of important concerns for any successful tissue-engineering scaffold program. Thus underlying the interest of implementing natural polymers as tissue-engineering scaffolds, for they may literally hold the molecular key for locking and unlocking favorable and unfavorable physiological conditions to support a viable scaffold which mimics the ECM which could in turn foster cellular differentiation and proliferation.

Polysaccharides. Polysaccharides have attracted interest in medical and scientific studies pertaining to tissue engineering scaffolds due to their biodegradability, low toxicity, low manufacture cost, low disposal costs, and prospect in renewability (Khan). In addition, the biochemical nature polysaccharides possess, mimics components of the human extracellular matrix, thus are readily recognized and accepted by the body (Shelke) (K.M. Colvin). Another factor contributing to polysaccharides as prospective scaffolds is their ability to undergo enzymatic and/or hydrolytic degradation in biologic environments, yielding the release of physiological degradable derivatives (Shelke) (M.M. H. Huisman) (I. Mkedder). However, complications and setbacks for polysaccharides do exist and can include their susceptibility to rapid degradation during

storage, which can foster the loss of biological properties necessary for successful implementation programs (Khan). Moreover, microbial contamination, uncontrolled water uptake, poor mechanical strength, and unpredictable degradation patterns, are also undesirable drawbacks that pertain to polysaccharides as tissue-engineering scaffolds [Shelke]. Despite the setbacks brought forth, polysaccharides continue to be investigated as viable candidates for scaffolds. Namely, due to their biocompatibility and bioactivity, which can be related to the structural characteristics of the polysaccharides, such as degree of substitution and molecular weights [Khan] [M.G. Peter]. Other properties, which are governed by the structural characteristics of polysaccharides, include the chemical reactivity, solubility, and physiological activities.

Cellulose, chitosan, and sodium alginate are among the most studied polysaccharides for tissue engineering application, such as in bases, coatings, drug delivery vehicles, cell encapsulation, and tissue engineering scaffolds. Each of the following polysaccharides about to be introduced are all derived from either flora or fauna, and include cellulose, chitin and its derivative chitosan, and sodium alginate. Many polysaccharides used for tissue engineering application are utilized as hydrogels in order to exploit the high water content and hydrophilic properties of hydrogels, which also mimic the natural "wetness" of tissue. The main approach in forming hydrogels is the chemical and/or physical cross-linking of hydrophilic polymers. Where, the physiological properties of hydrogels are strongly dependent on the cross-linking type and the cross-linking density, in addition to the molecular weight and chemical composition of the polymer.

Moreover, viable tissue engineering scaffolds must posses a porous and permeable network of voids to facilitate the penetration of cells and natural processes, which foster and invoke production of natural tissues. In many instances the process of lyophilization, commonly known as freeze-drying, is incorporated in the synthesis of tissue engineering scaffolds, particularly with hydrogels. By freezing hydrogels, (which can have 99% or more water) often as low as -$80^{o}C$, its hoped that by immediately lyophilizing them, the sublimation of the water in said hydrogels will consequently leave voids in place of ice crystals through out the scaffold, yielding a porous or sponge like material.

Cellulose and its derivatives are the most abundant naturally occurring polysaccharides in the world. Where its primary function is serving as the main structural component of cell walls in plants, algae, fungi, and bacteria (Namdev B Shelke)(Hsu-Feng Ko). High water-holding capacity, high crystallinity, fine fibre network, ease of mold ability and high tensile strength (Svensson et al. 2005), and the biodegradable limits is what makes cellulose such a lucrative culprit for scaffold implementation (Hsu-Feng Ko). Varieties of cellulose and its derivatives most commonly used include: carboxymethylcellulose (CMC), hydroxyethylcellulose (HEC), hydroxypropylcellulose, hydroxypropyl methylcellulose (HPMC), cellulose acetate and bacterial cellulose (Hsu-Feng Ko). Applications are also far fetching for cellulose ands its derivatives. Studies have implicated an abundance of promise including through the implementation into gel bases, film coatings, binders, bio-adhesives, controllers of drug release and thickeners and stabilizers (Hsu-Feng Ko, Novel synthesis strategies for natural polymers). Approaches involving cellulose primarily use the natural polymer

matrix components in scaffolds. Fang et al., prepared hydroxyapatite/bacterial cellulose nanocomposite scaffolds using a biomimetic technique to investigate the proliferation and osteoblastic differentiation of stromal cells derived from human bone marrow (Fang). Cells were found to adhere and subsequently spread on the scaffold through characterization using scanning electro microscopy (Fang). It was also found that the adhesion of cells were more apparent on the hydroxyapatite/bacterial cellulose scaffolds in comparison to scaffolds made solely bacterial cellulose. Proliferation was also more prevalent on the hydroxyapatite/bacterial cellulose scaffold as made clear using Alamar Blue Assay (Fang), concluding that the development of biocompatible scaffold with potential in bone tissue engineering was attained (Fang). Gao et al. (Gao) prepared bacterial cellulose sponges, through emulsion freeze-drying technique. Sponges with hierarchical pore structure were produced and shown to possess large pores and nano sized pores. In addition a porosity of about 90% was attained (Gao). Using inverted microscopy and the MTT assay, it was determined the bacterial cellulose sponges exhibited excellent cell compatibility as the fibrous synovium derived MSCs were shown to proliferate well and grown at least 150 micrometers into the sponge (Gao).

Chitin, poly (Beta-(1-4)-N-acetyle-D-glucosamine), is a biopolymer synthesized by arthropods, insects, and the cell walls of fungi and yeast (R.jayakumar, biomedical applications of chitin and chitosan). Primarily used in nature where strength and reinforcement is necessary, chitin it is considered to be the second most abundant polymer in the world, behind cellulose (R. Jayakumar, biomedical application). Unfortunately, due to its structure, chitin does not readily dissolve in common organic solvents and as a result, merits limited application. Consequently, toxic and harsh

chemical solvents are necessary in order to merit scaffold grade material. In addition, another set back is due to the large amount of time needed for solvent treatments. However, few solvents where solubility is possible for chitin include N, N-dimethylacetamide (DMAC)-LiCl (Cho et al, 2000) (R. Jayakumar M. Prabaharan), Hexafluoroacetone, 1,1,1,3,3,3-hexafluoro-2-prpanol (HFIP) (Kurita, 2001) and Saturated calcium solvent (jayakumar and Tamura, 2008) and (Nagahama et al, 2008) (Jayakumar Novel chitin and chitosan). Utilizing a different methodology, Min et al. prepared chitin nano-fibers by thoughtfully de-polymerizing chitin with gamma radiation and subsequently using HFIP solvent before electro-spinning, fibers with diameters less than 100nm were yielded (Min et al) (Jayakuma, Novel chitin and chitosan). R. Jayakumar et al., has generously provided the science and engineering community with a great chart highlighting chitin and chitosan polymers with their respective solvents, degrees of deacetylation (%), and average fiber diameter yielded, in Novel chitin and chitosan nano-fibers in biomedical applications, which should be referred to for quick reference (R.Jayakumar, Novel chitin chitosan). Despite the troubles with solubility of chitin, much research still implicates it as a viable candidate for tissue engineering application due to its biocompatibility, non-toxic and, anti-microbial properties (R. Jayakumar, Biomedical application of chitin and chitosan).

Chitosan is a biocompatible, biodegradable, non-toxic, and a biofunctional deacetylated derivative of chitin (Hsu-Feng Ko) (R. Jayakuma biomedical appl). Its through the deacetylation process, where a linear structure of glucosamine and N-acetyl-glucosamine are linked in a beta-1, 4 manner (Hsu-Feng Ko)(Di Martino et al. 2005). Reports indicate that chitosan is soluble at pH levels lower than 5.5, thus acetic acid and

hydrochloric acid are often used to dissolve chitosan. In addition, raising the pH levels to 6 or higher, forms chitosan gels (Suh & Matthew 200) (Hsu-Feng Ko). Gelation can also be achieved by interacting chitosan with a variety of divalent and polyvalent anions (Hsu-Feng Ko)(Hejazi & Amiji 2003). Applications involving the incorporation of chitosan as biomaterial include drug delivery (Hsu-Feng Ko) (Li & Xu 2002) (Zhang & Zhang 2001) (Hejazi & Amiji), growth factor encapsulation (Hsu-Feng Ko)(Kim et al. 2003), and gene delivery by forming complexes between cationic chitosan and negatively charged DNA (Kim et al)(Lee et al. 1998) (Roy et al. 1999).

Chitin and chitosan inherently have poor mechanical properties, therefore when used for TE bone scaffolds, bone substitutes, or bone repair, mechanical properties must be improved (Jayakuma, Deepthy, A Short Review). Specifically, chitin and chitosan are shown to exhibit mechanical weakness, instability, and difficulty in maintaining a predefined shape (Khan & Ahmad). Consequently, other biomaterials such as hydroxyapatite (HAp) and bioactive glass ceramic (BGC), alginate, calcium phosphate, hyaluronic acid (HA), and poly(L-lactic acid) (PLLA) have been utilized and implemented in the material design parameters for scaffolds made of natural polymers (Jayakuma, Deepthy, A Short Review) (Khan & Ahmad). Moreover, in many cases using these reinforcing materials have shown promise as to not effect the good traits chitosan and chitin scaffolds attain, such as porosities and biocompatibility properties. As an example, CS-gelatin (CG) with nBGC (Peter, Binulol, Nair, et al, 2010) (Jayakuma, Deepthy) and chitosan-gelatin/nanophase hydroxyapatite (nHAp) (peter et al.) were produced (Jayakuma, Deepthy). It was shown that both composites exhibited pore size ranges of 150-300 micrometers, and both exhibited decreases in degradation

rates in comparison to their non-nanoparticle constituents. In addition, it was reported that the incorporation of both nBGC and nHAp, also increased cell attachment and cellular spreading (Jayakuma). Kong et al., also prepared CS/nHAp scaffolds, and studied their bioactivity by examining apatite formation on the scaffolds after incubation in simulated body fluid (SBF), as well as to the activity of preosteoblasts when cultured on the scaffolds. They concluded that the (CS/HAp) composite formed apatite more readily during the biomimetic process, compared to pure CS scaffolds (Khan & Ahmad)(Kong et al). Aside from HAp and BGC, silica, which is a component of bioactive glass, has merit for utilization with chitosan for also improving scaffold properties. It has been shown through numerous studies that silica is found to have apatite forming ability in simulated body fluid (SBF) (panjian, Ohtsuki, kokubo, Nakanishi, and Soga), specifically by aiding in nucleation and the growth of apatite layers from body fluids (Hench, 1991), by forming an essential step in the formation and mineralization of hard tissues, and by providing sufficient atomic distance to accommodate crystal structure of bone apatite (Karlsson, Froberg, and Ringbom). Also Lee et al., from Jayakuma et al, noted that addition of a material like silica can also improve the bioactivity and biocompatibility of chitin. Another ceramic of interest that is sometimes utilized in natural polymer scaffolds is zirconium (ZrO2). R.Jayakumar, Ramachandran, et al, in fabrication of chitin-chitosan/nano ZrO2 composite scaffolds for tissue engineering applications, synthesized chitin-chitosan scaffolds with nano ZrO2 R. (Jayakumar). The idea was based off the notion that osteogenesis properties would increase as a result of adding the ZrO2 nano particles. It was shown that the scaffolds produced by lyophilization technique, exhibited better swelling and controlled

degradation in comparison to a control scaffold made only of chitin and chitosan. Cell studies revealed a non-toxic nature of the synthesized scaffolds suggesting that the prerequisites for tissue engineering application were present (R. Jayakumar, Ramachandran, ZrO2).

Alginate is a naturally occurring anionic polymer (Kuen young lee & Mooney), derived from brown algae, certain seaweeds, or bacteria. Used primarily for its biocompatibility, low toxicity, relatively low cost, and mild gelation through the addition of divalent cations such as Ca^{2+} (Lee & Mooney), alginate found to be a linear polysaccharide copolymer of (1,4)-linked beta-D-mannuronic acid (M) and alpha-L-guluronic acid (G) monomers. Where the composition and arrangement of the M and G monomers determine the structural properties. Namely, alginates richer in blocks of G monomers: have higher elastic modulus and higher solute diffusivity (Ko, Hsu-Feng). Applications for alginate vary from drug, antibody, and growth factor delivery systems, cell encapsulation and seeding, gene delivery in plants and mammals in the form of microspheres (Ko, Hsu-Feng). Alginate is also typically used in the form of hydrogels specifically in would healing, drug delivery and tissue engineering (lee & Mooney).

In a new calcium releasing nano-composite biomaterial for bone tissue engineering scaffolds, Cattalini et al. developed nano-composite, biodegradable and bioactive films and scaffolds with Ca(2+) releasing ability as multifunctional substrates for bone tissue engineering (J.P., J, A.R., S., & Mourino, 2013). The incorporation of bioactive glass nanoparticles into alginate films significantly improved the tensile strength of the scaffolds. Biomineralization studies revealed deposition of apatite on the films surface, suggesting their bioactive behavior, which is a consequence of the high

bioreactivity of the added bioactive glass nanoparticles. It was also found that stability was met due to the films resistance of degradation after 60 days. The release of Ca(2+) is seen to be controlled and without an initial burst effect, which might be an advantage when cellular in vitro studies, are envisaged (J.P., J, A.R., S., & Mourino, 2013).

Marsich et al. recognized the potential of undesired microbial attachment on synthetic biomaterial implants, and therefore conducted research on incorporating silver nanoparticles on alginate/HA composite scaffolds to exploit the antibacterial properties silver possesses. The composites were made by internal gelation followed by freeze-drying to obtain a porous structure. The nanoparticles were prepared in presence of a lactose modified-chitosan and this colloidal solution was absorbed on the scaffolds by exploiting electrostatic interactions. Micro-computed tomography analysis of the scaffolds showed a homogeneous porous structure with average pore size of 341.5 micrometers and porosity of 80% (Marsich, Bellomo, Turco, Travan, Donati, & Paoletti, 2013). In vitro analytical tests revealed the silver doesn't affect the scaffolds ability to promote osteoblasts proliferation. Also, it was shown that it was effective against Gram+ and Gram- bacterial strains (Marsich, Bellomo, Turco, Travan, Donati, & Paoletti, 2013). The overall consensus of the study showed that the biocompatible antimicrobial scaffolds possess ideal characteristics for tissue engineering applications (Marsich, Bellomo, Turco, Travan, Donati, & Paoletti, 2013).

Exploiting the Dispersed Phase for Scaffold Design

In Polymer-Bioceramic Composites for Tissue Engineering, Yunos, Bretcanu, and Boccaccini report on an important class of scaffolds for bone tissue engineering that are based on biodegradable and bioactive ceramics and glasses, including hydroxyapatite (HA), bioactive silicate glasses and calcium phosphates. They also discuss efforts in producing scaffolds from non-biodegradable oxide ceramics, notably alumina, titania, and zirconia. The drawback from using all of these materials, and ceramics generally is their low resistance to fracture under loads in addition to their high brittleness. These disadvantages are exacerbated by the fact that optimal scaffolds must be highly porous (90% porosity). Therefore, the study to incorporate polymer coatings and the formation of interpenetrating polymer-bioceramic scaffolds to develop bioactive composites with enhanced structural integrity, fracture strength and toughness of bioceramic scaffolds is of interest (Yunos, Bretcanu, & Boccaccini, 2008). Carbonated HA is the inorganic component of bone thus, many calcium phosphate-based scaffolds have also been studied and have exhibited the promising characteristic of inducing a strong bond to bone when implanted. Bioactive glasses and related silicate glass-ceramics constitute another group of bioactive materials being highly considered in tissue engineering scaffold development because of their high bioactivity, specifically their ability to rapidly form fast tissue bonding without the formation of scar tissue. Also, bioactive glass of composition 45S5 Bioglass exposes critical concentrations of Ca, Si, Na, and P ions which have been shown to activate genes in osteoblast cells thus stimulating new bone formation in vivo (Yunos, Bretcanu, & Boccaccini, 2008). A method being used to enhance mechanical properties in inorganic scaffolds made of HA and other bioactive glass and bioceramics, is coating

them in polymer layers. The aim is to fill existing cracks during fracture thus increasing the overall scaffold toughness. This is analogous to the natural method in which collagen fibers enhance the fracture toughness of bone. As well as with coating treatments, this approach has been extended to include scaffolds with interpenetrating network structures, where the polymer is made to penetrate and infiltrate the pore walls of the scaffold via remaining porosity or micro-cracks (Yunos, Bretcanu, & Boccaccini, 2008). Its also being considered that the polymer phase may have other functions. For instance, the polymer phase being used as a drug or biomolecule carrier to enhance functionality and bioactivity of the scaffold (Yunos, Bretcanu, & Boccaccini, 2008).

To better understand the effect of interpenetrating network microstructures in scaffold optimization, Yunos et al. investigated the infiltration of a biodegradable polymer phase (PDLLA) into a partially sintered Bioglass glass-ceramic scaffold prepared by the foam replica technique. The results showed that the mechanical properties of the interpenetrating microstructure of the 45S5 Bioglass/PDLLA composites significantly increased; the compressive strength of the coated scaffold was up to 7 times higher than the value for the non-coated scaffolds (figures are shown in Polymer-bioceramic composites for tissue engineering) (Yunos, Bretcanu, & Boccaccini, 2008). This result indicates that PDLLA films have effectively infiltrated the micro-pores of the partially sintered struts. The bioactivity of the PDLLA-coated 45S5 Bioglass scaffolds was investigated by immersion in a cellular 1.5SBF and by subsequently determining the formation of hydroxyapatite on the surfaces. HA was clearly detected after 7 days of immersion in concentrated SBF (1.5SBF) and the layer thickness increased with increasing time in the medium, reaching a dense, continuous HA layer

after 28 days in 1.5 SBF. This result suggests that the PDLLA coating does not affect negatively the bioactive character of the 45S5 Bioglass-based scaffolds, as also discussed elsewhere (Yunos, Bretcanu, & Boccaccini, 2008). Yunos et al. conclude by making key points in their findings. A significant toughening effect by the polymer incorporation, especially in scaffolds exhibiting interpenetrating network microstructure, was found. Also, the addition of a polymer phase might have extra functions, e.g. the biodegradable polymer can act as carrier for biomolecules, growth factors and antibiotics, hence increasing the capability of tissue engineering constructs. Moreover addition of nanoparticles or carbon nanotubes to the polymer coating will induce nano-topographical surface features, which should be relevant for enhancing cell attachment and subsequent cellular behavior in contact with the scaffold (Yunos, Bretcanu, & Boccaccini, 2008).

In a study conducted by Huang et al. nano-sized hydroxyapatite (nanoHA) reinforced composites, simulating natural bone, were produced. Examination revealed that nanoHA particles had a rod-like shape, 20-30 nm in width and 50-80 nm in length. These nanoHA particles were incorporated into poly-2-hydroxethylmethacrylate (PHEMA)/polycaprolactone (PCL) matrix to make new nanocomposites: nanoHA-PHEMA/PCL. Porous nanocomposite scaffolds were then synthesized using a porogen leaching method, leading to a porosity of 84% with pore sizes around 300-400 micrometers. It was observed that the produced nanocomposites were indeed bioactive as indicated by the formation of a bone-like apatite layer after immersion in simulated body fluid as well as being capable of supporting the growth and proliferation of primary human osteoblast cells. The human osteoblast cells developed a well organized actin

cytoskeletal protein on the nanocomposite stoking the premise of possible application of nanocomposite scaffolds for tissue engineering for bone repair (Huang, et al.).

Chen et al. experimented with in situ grown fibrous composites of poly(DL-lactide) and hydroxyapatite, for the use as tissue engineering scaffolds. The tensile strength of the in situ grown composite (IGC) was 8.2 plus or minus 1.1 MPa and Young's Moduli for the IGC was 63.5 plus or minus 5.6 MPa, which proved to be higher in comparison to blend electrospun composites (BEC) with 25.2% of HA inoculation (Chen, Li, Cui, Xie, Zou, & Zou, 2010). Interactions at the matrix polymer and formed HA and high HA loadings enhanced the mechanical performances and stable interfaces. Apatite localization on the fibrous surface of the IGC was determined to improve biomineralization ability after incubation into simulated body fluids (SBF), whose ionic composition mimicked blood plasma (Chen, Li, Cui, Xie, Zou, & Zou, 2010). It was also shown to enhance the morphological stability of the fibers and fibrous mats during incubation into the degradation media. The non-stoichiometric HA particles existed on the fiber surface was able to maintain desirable cell-substrate interactions, provide favorable conditions for cell proliferation and stimulate to undergo osteogenic differentiation, thus showing that in situ grown fibrous composites showed potentials as coating materials on medical devices and scaffolds for tissue regeneration (Chen, Li, Cui, Xie, Zou, & Zou, 2010).

Nejati et al. proposed the possible use of synthesized nano-hydroxyapatite (nHAP) rods/poly(L-lactide acid) composite scaffolds for bone tissue engineering applications (nHAP/PLLA). Identification and morphology of synthesized nHAP particles was done and found to be in forms of rods that had a average size of 37-65 nm

in width and 100-400nm in length. It was also seen to resemble natural bone apatite particles in chemical composition and structure. Then nHAP and micro sized HAP particles were utilized to engineer HAP filled PLLA (HAP/PLLA) composite scaffolds using thermally induced phase separation method (Nejati, Mirzadeh, & Zandi, 2008). The result was a scaffold with 85.06 porosity and average macropore diameter of 64-175 micrometers. Upon testing and comparison of the compression strengths between the nanocomposite scaffolds (nHAP/PLLA), pure PLLA, and microcomposite scaffold (mHAP/PLLA), the results yielded values of 14.9, 1.79, and 13.68 MPa, respectfully (Nejati, Mirzadeh, & Zandi, 2008). Also the cell affinity and biocompatibility of the nano scaffold were found to also be higher than the other two specimen scaffold samples. Finally, it was concluded that the nHAP/PLLA composite scaffold was in fact comparable with cancellous bone in terms of microstructure and mechanical strength (Nejati, Mirzadeh, & Zandi, 2008).

In Structure and properties of nano-hydroxyapatite/polymer composite scaffolds for bone tissue engineering, the objective was to find a scaffold that would better mimic the mineral component and microstructure of natural bone. The solution was to use thermally induced phase separation (TIPS) techniques to synthesize novel nano-hydroxyapatite (NHAP)/polymer composite scaffolds. The technique yielded high porosity (90% and above) and well controlled pore architectures (Wei & Ma, 2004). Morphologies, mechanical properties, and protein absorption capacities of the scaffolds were studied (Wei & Ma, 2004). Introduction of HAP was shown to increase mechanical properties and improve protein absorption capabilities. Finally, using a dioxane/water mixture solvent system, NHAP-incorporated PLLA scaffolds produced a fibrous

morphology that increased protein absorption three fold over non fibrous scaffolds suggesting the new NHAP/polymer composite scaffolds may serve as an excellent 3D substrate for cell attachment and migration in bone tissue engineering (Wei & Ma, 2004).

Lu Zhang et al. experimented with graphene/hydroxyapatite (HA) composite made using spark plasma sintering (SPS). Mechanical properties as well as in vitro biocompatibility were researched. It was seen that graphene nanosheets (GNSs) survived the processing conditions of the SPS processing parameters (Zhang, et al., 2013). A 1.0 wt.% GNS/HA composite exhibits around 80% improvement in fracture toughness as compared to pure HA, due to grain bridging by GNS, crack bridging and crack deflection (Zhang, et al., 2013). Enhancement of osteoblast adhesion and apatite mineralization in vitro osteoblast growth signifies GNS/HA composites may be a viable candidate for load bearing orthopedic implants (Zhang, et al., 2013).

In Compositional dependence of hematopoietic stem cells expansion on bioceramic composite scaffolds for bone tissue engineering Mishra et al., as the name literally implies, studied the compositional dependence of hematopoietic stem cells (HSCs) expansion on bioceramic composite scaffolds for bone tissue engineering. The study focused on the expansion of HSCs on as-synthesized composite scaffolds from HA and beta-tricalcium phosphate for bone tissue engineering, in adequate load bearing functions. Indications show that response of HSCs varies with change in stoichiometry of composite scaffolds (Mishra, Rajyalakshmi, & Balasubramanian, 2012). Researchers suggest that H2T2 composite can be a potential strategic bone-graft substitute in contrast to monolithic bioceramics, indicating bioresorbability and enhanced load-bearing

capacity (Yoshida, Dhandayuthapani, Maekawa, & Kumar, 2011), (Mishra, Rajyalakshmi, & Balasubramanian, 2012).

In Fluorescent PLLA-nanodiamond composites for bone tissue engineering, Zhang et al. exploited the excellent mechanical properties of diamond nano-particles. Using biodegradable polymer, poly(L-lactic acid) (PLLA), and octadecylamine-functionalized nanodiamond (ND-ODA), the researchers produced a multifunctional fluorescent composite bone scaffold. The introduction of a uniform distribution of nanoparticles (10% wt.) in the polymer leads to a drastic increase in both hardness and Young's Modulus of the composites by 200% and 800%, respectively. This resulted in the respective properties similar to that of human cortical bone and also was seen to have no negative effects on cell proliferation (Zhang, et al., 2011).

The following is a study conducted by Barbieri, et al. and is taken from Influence of polymer molecular weight in osteoinductive composites for bone tissue engineering (Barbieri, Yuan, Luo, Grijpma, & Bruijn, 2013). It was determined through experimentation that the molecular weight of L-lactide/D,L-lactide copolymer in composite materials can implicitly control surface phenomena occurring at the interface, dictating whether osteoinduction occurs or not. It was seen that composites with low molecular weight polymer absorbed more body fluids, activating a surface events including larger exposure of apatite particles and higher serum protein absorption. Improved cell colonization on the surface may have lead to heterotopic bone formation through absorbed protein motifs (Barbieri, Yuan, Luo, Grijpma, & Bruijn, 2013). The authors emphasize the importance to note that in vivo bone formation may have occurred after surface mineralization, which highlights the importance of surface bioactivity. This

supports the suggestion that surface mineralization is a necessary condition, but it is not the driver, for heterotopic bone formation in composites (Barbieri, Yuan, Luo, Grijpma, & Bruijn, 2013). However, the main triggers of material-related osteoinduction mechanism and their interconnection still need to be unraveled. It was also observed that improving the osteoinductive property by virtue of controlling the polymer molecular weight did not lead to materials with sufficient mechanical properties. In fact, osteoinduction was obtained at the cost of elastic properties worsening. Concluding that there is need for a balance between the various material factors to obtain proper tuning of both mechanical characteristics and osteoinduction (Barbieri, Yuan, Luo, Grijpma, & Bruijn, 2013).

Another type of composite recently synthesized utilized plasma treated poly(etherimide) (PEI) films, gold nanoparticles (GNPs), and the amino acid lysine. The synthesis was possible through a layer-by-layer assembly of the three constituents and demonstrated to be good for cell attachment and proliferation. The thought is that the surface roughness provided by the gold nanoparticles capped by lysine molecules presents the "rough" feature necessary for cell attachment and proliferation (Britto, et al., 2009). The cells used in the study were Chinese hamster ovary (CHO) cells and in one part of the study were placed on several different treated surfaces, such as polystyrene culture plate, poly-L-lysine coated polystyrene culture plate, untreated PEI film, plasma treated PEI film, plasma treated PEI film incubated with GNPs for 24 hours, and plasma treated PEI film layered with GNPs and thereafter with lysine. The percent mitochondrial activity was compared on each of the surfaces and graphed for easy comparison, with results of 100, 163,4 189,181, and 228, respectively. In addition,

statistical data comparing the number of cells on untreated PEI film, plasma treated PEI film, plasma treated PEI film incubated with GNPs for 24 hours and plasma treated PEI film layered with GNPs and thereafter with lysine. These results yielded a high cell count on the PEI film layered with GNPs and thereafter with lysine with a cell count of around 400,000 with the runner up specimen being plasma treated PEI film at only a cell count of 100,000 (Britto, et al., 2009).

In a novel study from China, Yang et al. experimented with composite scaffolds made of silk fibroin/gelatin (SF/G). The aim of the study was to investigate the cytotoxicity of SF/G composite scaffolds in vitro and vivo, with liver tissue engineering application in mind (Yang, et al., 2012). Silk fibroin has high histocompatibility and mechanical characteristics as well as great workability. Due to hydrogen bonding nature of the silk fibroin, a hydrophobic character is observed in the material, and makes it insoluble in solvents such as dilute acid, alkali and water, thus in pure form making it not useful for cell adherence, and possessing a slow rate of degradation (Yang, et al., 2012). The gelatin in this study was derived from natural collagen, which is a natural biopolymer. Studies show that gelatin promotes cell differentiation and adhesion, as well as use as an extracellular matrix (Yang, et al., 2012). Three-dimensional SF/G scaffolds of three different ratios (i.e. diameter of 10 mm, thickness of 1mm) where implanted into subcutaneous pockets on male Sprauge-Dawley rats. After the 7th, 14th, and 30th days of implantation, the surrounding tissues and scaffold area were retrieved. Significant cell attachment and proliferation were observed, noting that increased gelatin concentrations became more amenable to cell adhesion and faster degradation rate. Also immunological rejection tests showed slight inflammation in the SD rats and that on day 30, each

scaffold had been completely infiltrated and organized by fibroblasts and inflamed cells. The group concludes by offering the suggestion that SF/G scaffolds are promising candidates for implantable bio-artificial livers (Yang, et al., 2012).

A literature review on natural polymer based composite tissue engineering scaffolds was conducted. Research involving natural and synthetic polymers as matrices for composite based scaffolds were primarily of focus, in addition, various dispersed phase constituents were also studied such as: gold nanoparticles, diamond nanoparticles, silver nanoparticles, silk and various ceramics. The primarily interest in utilizing composite scaffolds, lie in the opportunity of exploiting the mechanical properties of two different materials. In addition, composites are also being used as scaffolds for their ability to contain internal materials that can be exposed to certain tissues as degradation of the polymer matrix unfolds. This capability thus gives rise to either novel "drug delivery systems" or the facilitation of exposing a desired morphology, such as a particular surface roughness to promote cell adhesion. Also brought to light, were properties of individual scaffold constituents as well as the composites themselves, and methodologies to fabricate various types of scaffolds. It's hoped, that after studied, this article will provide an "out of box" approach in future research endeavors involving prospective tissue engineering programs. Unfortunately, the ideal scaffold has not been invented for an appropriate and specific use. However, headway is underway. What we do know in respect to producing an ideal scaffold is the necessity of a high degree of biocompatibility, and a biodegradable rate resembling that of the in situ tissue formation. Also, the mechanical competence of the scaffold must be sufficient in order to provide mechanical stability and integrity in load bearing sites prior to and during regeneration of

new tissue. And finally, a three-dimensional interconnected porous structure with porosity of 90% and pore size between 300 and 500 micrometers is essential to permit cell penetration, tissue in growth, and vascularization.

CHAPTER III

METHODOLOGY AND FINDINGS

Materials

Corn Starch Microwave (MW) Irradiated Scaffolds

For the corn starch MW irradiated scaffolds the following materials were used for the their fabrication. Agro brand 100% pure corn starch (for cooking and baking) was purchased through a local supermarket store. Practical grade chitosan derived from shrimp shells (greater than 75% deacetylated chitin, Poly(D-glucosamine) was purchased from Sigma Aldrich. The estimated molecular weight of the chitosan according to sigma Aldrich was 190,000 to 375,000. Sodium alginate was purchased through MP Biomedicals, LLC. Acetic acid solution 1N solution was purchased from Fisher Scientific. Other necessary equipment used in the synthesis process included 25 cm^2 tissue culture dish, Falcon 25 mL serological pipets, tweezers, a Drummond pipet-aid, a Labconco 4.5 Freezone Freeze Dryer, a conventional microwave {power insert} by Sharp, an ACCULAB AL-64 balance, 24 well plate culture dish, deionized water, and an assortment of beakers and glassware for mixing, stirring, and holding and a ½ inch diameter steel leather punch (stamp).

TEO Treated Scaffolds

For the TEO treated Scaffolds, the following materials were used for their fabrication. Collagen of bovine achilles tendon origin was purchased through Worthington Biochemical Corporation. Practical grade chitosan derived from shrimp shells (greater than 75% deacetylated chitin, Poly(D-glucosamine) was purchased from Sigma Aldrich. Where the estimated molecular weight of the chitosan according to sigma Aldrich was 190,000 to 375,000. Acetic acid solution 1N solution was purchased from Fisher Scientific. Also purchased through Fisher Scientific was H_2SO_4 and NaOH. Triethyl orthoformate was purchased through TCI and had a MW of 148.20. Other necessary equipment used in the synthesis process included an ACCULAB AL-64 balance, Falcon 25 mL serological pipets, tweezers, a Drummond pipet-aid, a Labconco 4.5 Freezone Freeze Dryer, a conventional microwave {power insert}, 24 well plate culture dish, deionized water, and an assortment of beakers and glassware for mixing, stirring, and holding.

Scaffold Synthesis

Corn Starch Microwave Irradiated Scaffolds

Corn Starch Sodium Alginate MW Scaffolds. The sodium alginate powder was dissolved in deionized water to yield a two per cent weight to volume ratio solution. To ensure a homogenous solution, the mixture was stirred for 15 minutes with a glass rod and then left covered with aluminum foil for one hour under a disinfected laminar flow hood. While homogeneity was being attained, the cornstarch preparation was carried out. Thirteen grams of cornstarch was weighed out and subsequently mixed with 40 mL of

deionized water in a small beaker and mixed with a glass rod. This solution was also covered and set aside for an hour. It may be worth noting that after an hour, the cornstarch solution will not completely dissolve. Therefore excess cornstarch should be present at the bottom of the beaker.

After an hour the two mixtures were combined. To prepare the final solution, the cornstarch deionized water mixture was stirred vigorously with a glass rod to distribute the settled cornstarch throughout the entire mixture. Immediately following the stirring, 10 mL of the cornstarch solution was poured into a small 40 mL beaker. Then 5 mL of the dissolved sodium alginate solution was added to the 10 mL of the cornstarch solution yielding a 15 mL cornstarch sodium alginate solution. The new solution was mixed for about one minute and poured into a 25 cm^2culture dish and immediately placed into the microwave for 20 seconds (with the culture dish lid on). After the microwaving process, the entire culture dish was placed into a -80ºC freezer for two minutes in order to cool the gel down and make it more favorable for stamping out specimens. Using the leather punch, ½ inch diameter specimen coupons were punched out of the newly formed cornstarch sodium alginate gel (approximately 24 coupons can be attained from one 24 inch culture flask). Each coupon was then placed into its own well in a 24 well plate culture dish. The well plate was covered and wrapped in aluminum foil and placed in the -80ºC freezer for 24 hours. After 24 hours the culture dish (without the lid) was placed in a 900 mL Labconco vacuum flask and freeze dried for 72 hours using the Labconco freeze dryer. Upon removal from the freeze dryer the Scaffolds were placed under a disinfected laminar flow hood. 2 mL of deionized water were added to each cell to soak the Scaffolds for one day. This was done to help draw in water thus swelling the

Scaffold for another freeze drying process in hopes of yielding larger pores in the microstructure. After the one day soak, the access water was syphoned out using a pipet and pipet aspirator. The entire culture plate with Scaffolds inside, were again frozen for 24 hours and subsequently freeze dried for 72 hours. After freeze drying the Scaffold coupons were placed in a vial which was label accordingly and stored in a refrigerator until experimental tests were ready.

Cornstarch Chitosan MW Scaffolds. The chitosan powder was dissolved in 1 N acetic acid solution to yield a .75 per cent weight to volume ratio solution. To ensure a homogenous solution, the mixture was stirred for 15 minutes with a glass rod and then left covered with aluminum foil for one hour under a disinfected laminar flow hood. While homogeneity was being attained, the cornstarch preparation was carried out. Thirteen grams of cornstarch was weighed out and subsequently mixed with 40 mL of deionized water in a small beaker and mixed with a glass rod. This solution was also covered and set aside for an hour. As aforementioned, the cornstarch will not completely dissolve and cornstarch sediment should be present at the bottom of the beaker after the hour.

After an hour the two mixtures were combined. To prepare the final solution, the cornstarch deionized water mixture was stirred vigorously with a glass rod to distribute the settled cornstarch throughout the entire mixture. Immediately following the stirring, 10 mL of the cornstarch solution was poured into a small 40 mL beaker. Then 5 mL of the dissolved chitosan and acetic acid solution was added to the 10 mL of the cornstarch solution yielding a 15 mL cornstarch chitosan solution. The new solution was mixed for about one minute and poured into a 25 cm^2culture dish and immediately placed into the

microwave for 20 seconds (with the culture dish lid on). After the microwaving process, the entire culture dish was placed into a -80ºC freezer for two minutes in order to cool the gel down and make it more favorable for stamping out specimens. Using the leather punch, ½ inch diameter specimen coupons were punched out of the newly formed cornstarch chitosan gel (approximately 24 coupons can be attained from one 24 inch culture flask). Each coupon was then placed into its own well in a 24 well plate culture dish. The well plate was covered and wrapped in aluminum foil and placed in the -80ºC freezer for 24 hours. After 24 hours the culture dish (without the lid) was placed in a 900 mL Labconco vacuum flask and freeze dried for 72 hours using the Labconco freeze dryer. Upon removal from the freeze dryer the Scaffolds were placed under a disinfected laminar flow hood. 2 mL of deionized water were added to each cell to soak the Scaffolds for a three-day period where the water was drained and replaced everyday. In comparison to the cornstarch sodium alginate Scaffolds, this was done for two reasons. First, to help draw in water to swelling the Scaffold for another freeze drying process in hopes of yielding larger pores in the microstructure. Second, upon initial inspection of the Scaffolds, it was noticed that a strong presence of acetic acid was present in their odor. Thus the three-day soak of the Scaffolds was implemented where each day the deionized water was replaced with fresh deionized water. After the three-day soak, the access water was syphoned out using a pipet and pipet aspirator. It may be worth noting that at the end of the soak, there was no acetic acid aroma present from the Scaffolds. Indicating the majority if not all of the acetic acid was removed. The entire culture plate with Scaffolds inside, were again frozen for 24 hours and subsequently freeze dried for

72 hours. After freeze drying the Scaffold coupons were placed in a vial which was label accordingly and stored in a refrigerator until the commencement of experimental tests.

Triethyl Orthoformate Treated Scaffolds

TEO Treated Chitosan Scaffolds. Chitosan powder was dissolved in 1 N acetic acid solution so that a 1% chitosan acetic acid solution (w/v) was made. The mixture was first stirred using a glass rod for about 10 minutes and then set under a disinfected laminar flow hood for one hour to fully dissolve. After one hour under the flow hood, approximately 2 mL of the mixture were cast in molds using the culture wells of a 24 well culture plate yielding 24 future Scaffolds. The culture plate was covered with its lid and wrapped in aluminum foil and placed in an -80º freezer for 24 hours. After the 24 hours the Scaffolds were removed from the freezer and promptly placed in a freeze dryer for lypholization for 72 hours. Upon completion of freeze drying, the Scaffolds were rehydrated and then treated with 2.5% (w/v) triethyl orthoformate solution with 17% (w/v) $H_2SO_{4(aq)}$ solution for 24 hours, hopefully crosslinking the Scaffolds. Subsequently, the samples were soaked in a 12% (w/v) NaOH solution for 1 hour at room temperature. Next, the samples were washed thrice with distilled water and dried at room temperature. Now looking more like a hydrogel membranes, the Scaffolds were soaked in distilled water for 24 hours. Then the soaked membranes were kept in a freezer at -80 °C for 24 hours and finally subjected to the 2nd lyophilization to get a hydrogel Scaffold for further characterization and biological testing.

TEO Treated Collagen Scaffolds. Collagen fiber was dissolved in 1 N acetic acid solution so that a 1% collagen acetic acid solution (w/v) was made. The mixture was first stirred using a glass rod for about 10 minutes and then set under a disinfected laminar flow hood for one hour to fully dissolve. After one hour under the flow hood, approximately 2 mL of the mixture were cast in molds using the culture wells of a 24 well culture plate yielding 24 future Scaffolds. The culture plate was covered with its lid and wrapped in aluminum foil and placed in an -80º freezer for 24 hours. After the 24 hours the Scaffolds were removed from the freezer and promptly placed in a freeze dryer for lypholization for 72 hours. Upon completion of freeze drying, the Scaffolds were rehydrated and then treated with 2.5% (w/v) triethyl orthoformate solution with 17% (w/v) $H_2SO_{4(aq)}$ solution for 24 hours, hopefully crosslinking the Scaffolds. Subsequently, the samples were soaked in a 12% (w/v) NaOH solution for 1 hour at room temperature. Next, the samples were washed thrice with distilled water and dried at room temperature. Now looking more like a hydrogel membranes, the Scaffolds were soaked in distilled water for 24 hours. Then the soaked membranes were kept in a freezer at -80 °C for 24 hours and finally subjected to the 2nd lyophilization to get a hydrogel Scaffold for further characterization and biological testing.

TEO Treated Chitosan-Collagen Scaffolds. Chitosan powder was dissolved in 1 N acetic acid solution so that a 1% chitosan acetic acid solution (w/v) was made. In addition, collagen fiber was dissolved in 1 N acetic acid solution so that a 1% collagen acetic acid solution (w/v) was made. Both mixtures was independently stirred using a glass rod for about 10 minutes in their respective beakers, and set under a disinfected

laminar flow hood for one hour to fully dissolve. After one hour, the two mixtures were combined in one beaker yielding a 1% collagen and 1% chitosan (1:1 v/v) solution. The mixture was mixed well to yield a homogenous solution. Again, approximately 2 mL of the final mixture were cast in molds using the culture wells of a 24 well culture plate, yielding 24 future Scaffolds. The culture plate was covered with its lid and wrapped in aluminum foil and placed in an -80º freezer for 24 hours. After the 24 hours the Scaffolds were removed from the freezer and promptly placed in a freeze dryer for lypholization for 72 hours. Upon completion of freeze drying, the Scaffolds were rehydrated and then treated with 2.5% (w/v) triethyl orthoformate solution with 17% (w/v) $H_2SO_{4(aq)}$ solution for 24 hours, hopefully crosslinking the Scaffolds. Subsequently, the samples were soaked in a 12% (w/v) NaOH solution for 1 hour at room temperature. Next, the samples were washed thrice with distilled water and dried at room temperature. Now looking more like a hydrogel membranes, the Scaffolds were soaked in distilled water for 24 hours. Then the soaked membranes were kept in a freezer at -80 °C for 24 hours and finally subjected to the 2^{nd} lyophilization to get a hydrogel Scaffold for further characterization and biological testing.

Experimental Tests and Analysis

Scaffold Characterization

In order to ascertain a more concise understanding of the synthesized Scaffolds, an extensive characterization study was implemented using traditional characterization techniques. X-ray photoelectron microscopy (XPS), Fourier transform infrared

spectroscopy (FTIR), Raman spectroscopy, scanning electron microscopy (SEM), and energy-dispersive spectroscopy (EDS), were among the techniques used to establish elemental constituents, molecular characteristics, surface chemistry, morphologies, and surface interactions with simulated body fluids to conclude some bio-assessments.

X-ray Photoelectron Spectroscopy. The surface chemistry was analyzed by using X-ray photoelectron spectroscopy (XPS, K-Alpha, ThermoFisher, UK). Survey spectra were recorded in a range of -10 to 1350 eV with a pass energy of 100 eV, step size of 1.0 eV and dwell time of 10 ms yielding an atomic composition (%) for each scaffold specimen. High-resolution spectra were also acquired for all samples which included C 1s, N 1s, O 1s and S 2p regions and were collected in the fixed analyzer transmission mode with a pass energy of 100 eV, step size of 1 eV and dwell time of 10 ms. The acquired data was converted using Avantage software.

XPS Corn Starch Scaffold. XPS survey spectra for the corn starch scaffold is presented in figure 1 below. Its purpose is to provide an elemental list of constituency present at the surface of the scaffold (atomic percentage), and to give detail as to what functional groups are present as well. Carbon peak was present at 285.75 eV. Oxygen was present at a binding energy level at 532.85 eV. Atomic percentage data rendered a presences of carbon at 61.41% and oxygen at 38.59%.

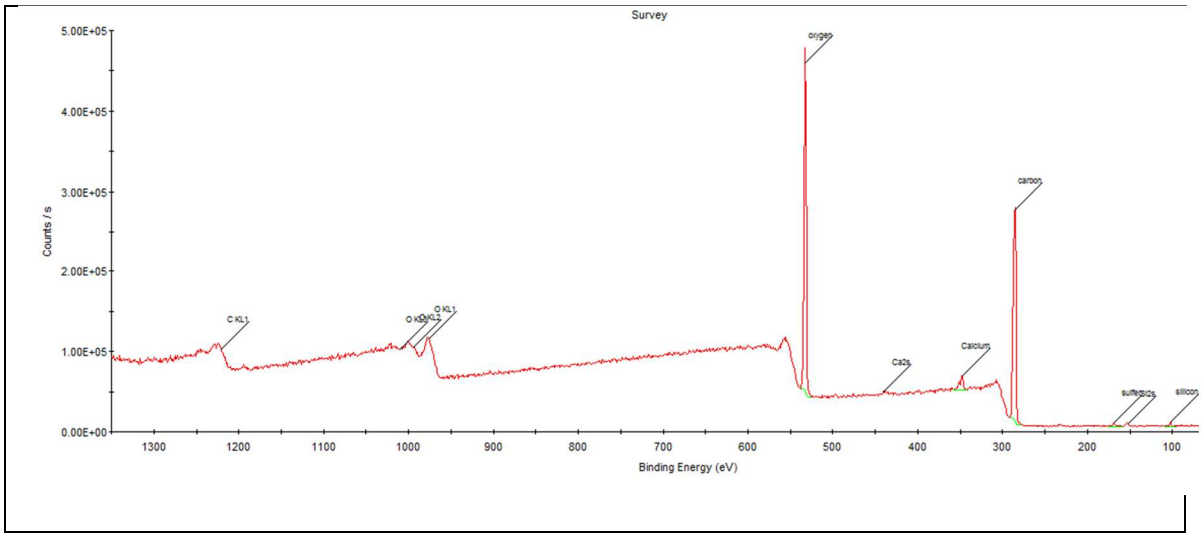

Figure 1: XPS survey spectra for corn starch scaffold.

XPS Corn Starch-Sodium Alginate Scaffold. XPS spectra (figure 2) revealed the elemental composition of the surface for each scaffold with a depth range between 6-8 nm. CS-SA Scaffold spectra indicate carbon, oxygen, and sodium as the main constituents on the scaffold surface with binding energies at 285.53, 532.79, and 1071.70 eV, respectively. The atomic percentage analysis indicate that carbon is by far the most prevalent of the elements with a 62.48% association, followed by oxygen and sodium at 29.09% and .99% respectively. Thus, yielding 92.56% of total atomic percentage at the surface of the Scaffold. The remaining 7.44% of atomic percentage was found to be composed trace amounts of silicon, sulfur, nitrogen, and fluorine. Where it's projected that Scaffold synthesis pertaining to the incorporation of water and culture plates may be the cause of such trace amounts. Spectral regions under close consideration, were that of carbon and oxygen.

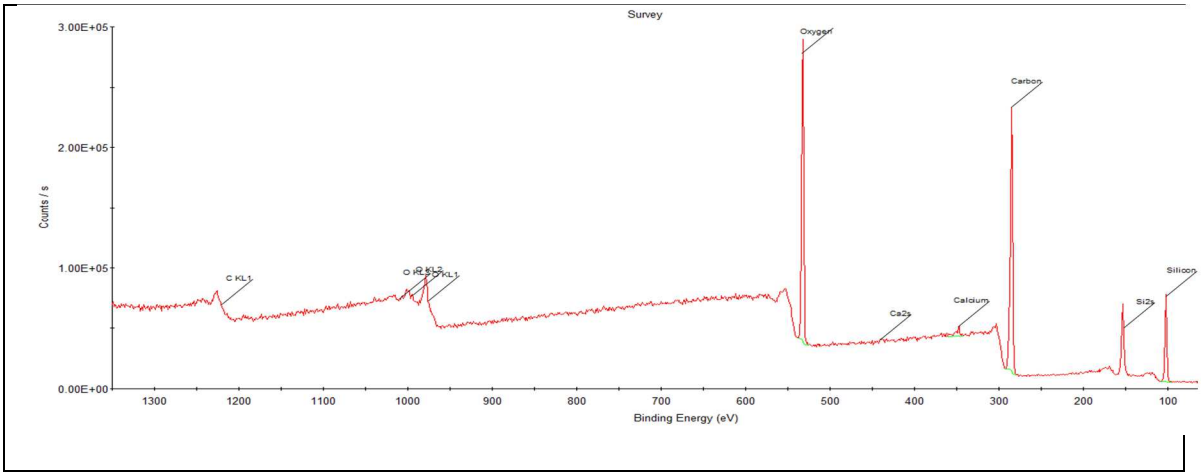

Figure 2: XPS survey spectra for corn starch-sodium alginate scaffold.

XPS Corn Starch-Chitosan Scaffolds. CS-CH XPS studies indicate that 98.5% of the surface elemental composition is that of carbon (48.01%), oxygen (30.92%), and sodium (19.57%). Thus a substantial decrease in carbon presence and increase of sodium presence as opposed to the CS-SA surface characterization. Trace amount of sulfur was also present in the surface with an atomic percentage of 1.23%.

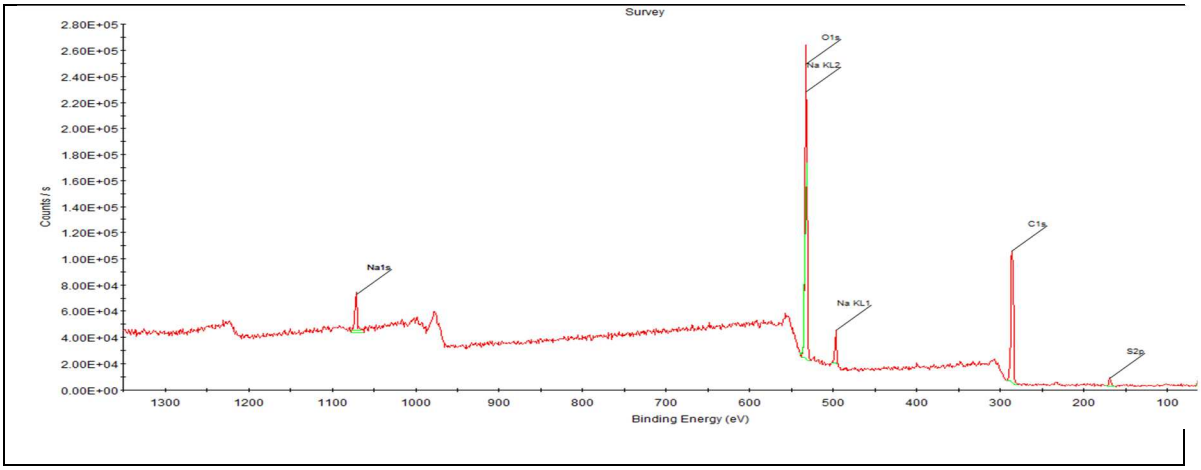

Figure 3: XPS survey spectra for corn starch-chitosan scaffold

XPS Chitosan Treated Scaffolds. XPS spectra of chitosan TEO Scaffolds for the most part, indicate the same elemental composition as that of the corn starch based irradiated specimen varieties. Much as the CS-CH Scaffold aforementioned, the CH-TEO Scaffold

contained 48.36% carbon, 27.85% oxygen, and 9.79% sodium, making up 86% of the total atomic percentage. However, analysis reveals higher levels of nitrogen and silicon, with atomic presence of 5.04% and 5.22%, respectively. Moreover, a much greater atomic percentage was marked for elemental sulfur at 3.74%, possibly from the TEO/H_2SO_4 treatment used for crosslinking.

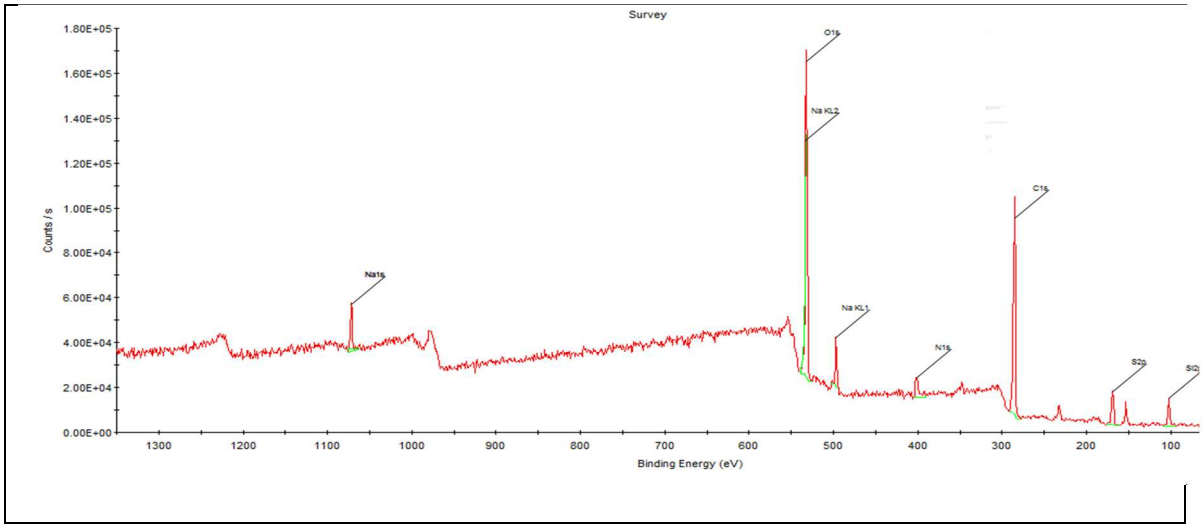

Figure 4: XPS survey spectra for TEO treated chitosan scaffold

XPS Chitosan-Collagen TEO Treated Scaffolds. The spectra for Ch-Coll TEO treated Scaffolds ascertained low levels of carbon and oxygen, compared to all aforementioned Scaffolds thus far. Carbon presence was found to be 28.02% of the surface composition and oxygen presence was determined to be 26.81%. Sodium atomic percentage was 31.79% and sulfur accounted for 3.14% atomic percentage, also higher than the corn starch irradiated Scaffolds. Therefore, carbon, oxygen, sodium, and sulfur comprised of 89.76% of the atomic weight. A relatively large amount of fluorine was also observed by the analysis at 7.27%.

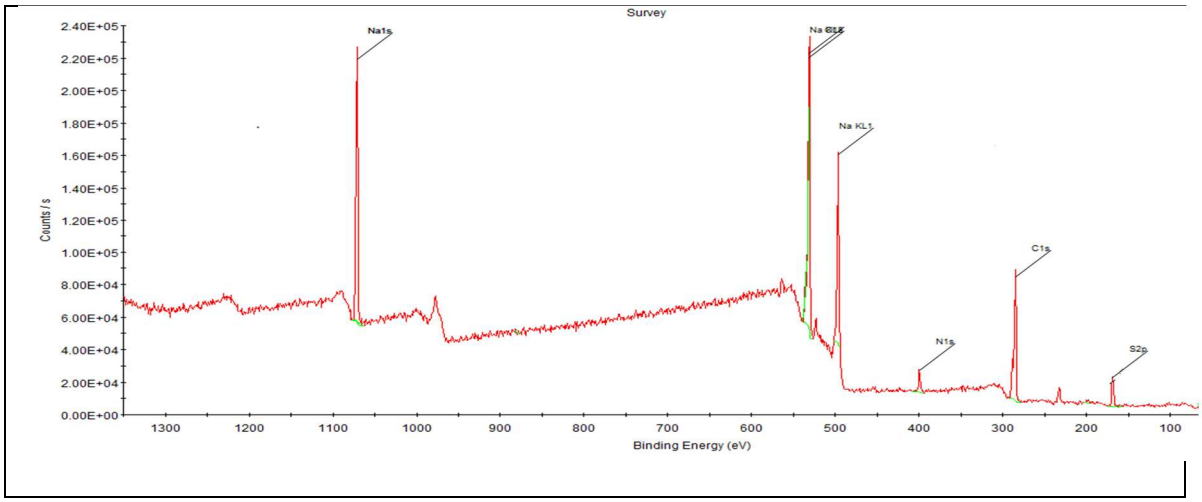

Figure 5: XPS survey spectra for TEO treated chitosan-collagen scaffolds.

XPS Collagen TEO Treated Scaffolds. Atomic percentage results on the surface of collagen TEO treated Scaffolds reveal carbon at 37.23%, oxygen at 41.01%, and a significantly larger atomic percentage of nitrogen at 12.24%. Sulfur levels were again observed though XPS analysis with a 3.30% of the atomic surface composition, which seems to be in the realm their TEO treated counterparts.

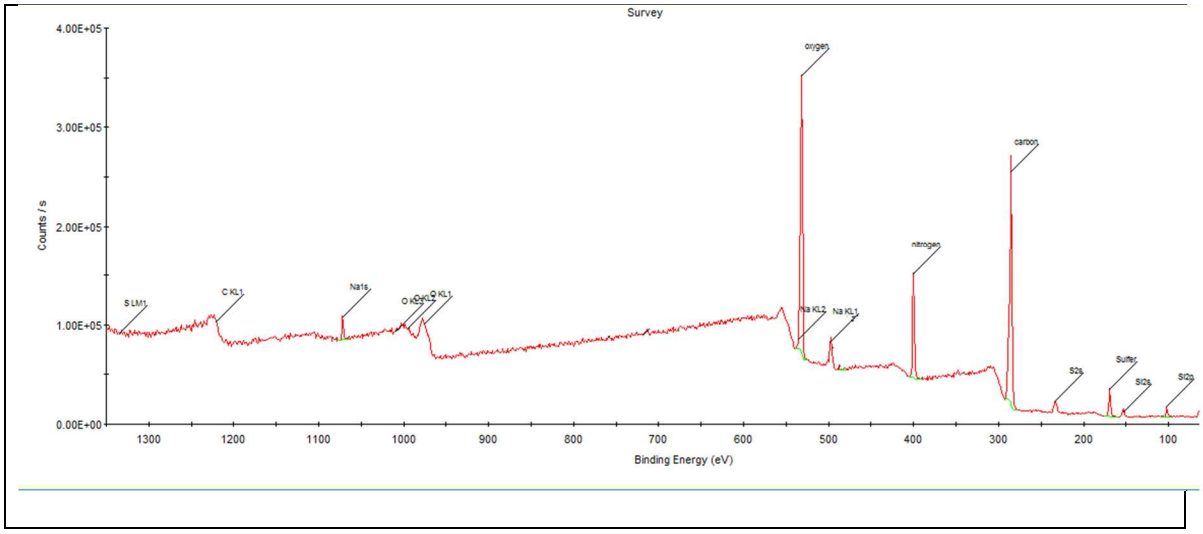

Figure 6: XPS spectra for TEO treated collagen scaffolds.

Fourier Transform Infrared Spectroscopy Analysis. Characterization of the Scaffolds by Fourier Transform Infrared Spectroscopy (FTIR) was carried out using a Thermo Nicolet Nexus 470 FT-IR E.S.P instrument and OMNIC software to interpret the initial readings. Origin data interpretation software was then used to superimpose the spectra of the parent polymers atop that of the scaffold spectra to analyze the data more conveniently. Moreover, Raman spectroscopy technique was utilized as a complementary measure to help characterize the Scaffolds..

Corn Starch Sodium Alginate Scaffold. FTIR spectra of the parent polymers and that of the CS-SA scaffold are presented in figure 7, A and B. The resemblance between the CS and CS-SA scaffold spectra is strikingly similar. However, considering that the CS amount outweighs that of the SA, the CS may be masking that of the SA. C-O stretch is present in all three spectra from 1000 cm^{-1} to 1300 cm^{-1}, with 1010 cm^{-1} for CS, 1050 cm^{-1} for SA, and 1000 cm^{-1} for the CS-SA scaffold. O-H stretch is also present in all three spectra, as well, around 3400 cm^{-1} , where the wider absorbance bands in the CS and CS-SA scaffold are attributed most likely to H2O absorbance. On the other hand, the possibility of physical hydrogen bonding (OH) between the cornstarch and sodium alginate may also be indicative of the variance in the O-H spectra region, but is less likely than the projection made of that of the absorbance of H_2O. Finally C-H stretch is shown particularly more so in the CS and CS-SA scaffold, at around 2940 cm^{-1} and 2920 cm^{-1} respectively. The amide band represented by peaks around 1640 cm^{-1} is present in all three spectra. Where it should be present in the sodium alginate spectra especially, the presence of the amide band on the cornstarch spectra, initially stoked some confusion. It was researched that some spectra and molecular structures for corn starch, did not

recognize an amide group present. However, other studies indicated contrary to this and identified amide I presence in cornstarch. Raman spectra of the corn starch used in the experiment were shown to agree well with published work and verified a slight peak at 1640 cm^{-1} as well. Therefore it seems that this particular type of corn starch used for this study, did in fact have amide groups in its contents. Some studies indicating amide groups in cornstarch are present in particularly in waxy corn starch molecular structure and spectra Liu et al. and Kizil et al. (Liu et al.) (Kizil et al.). Another possibility for the presence of a peak at 1640 cm^{-1} could be H_2O absorbance.

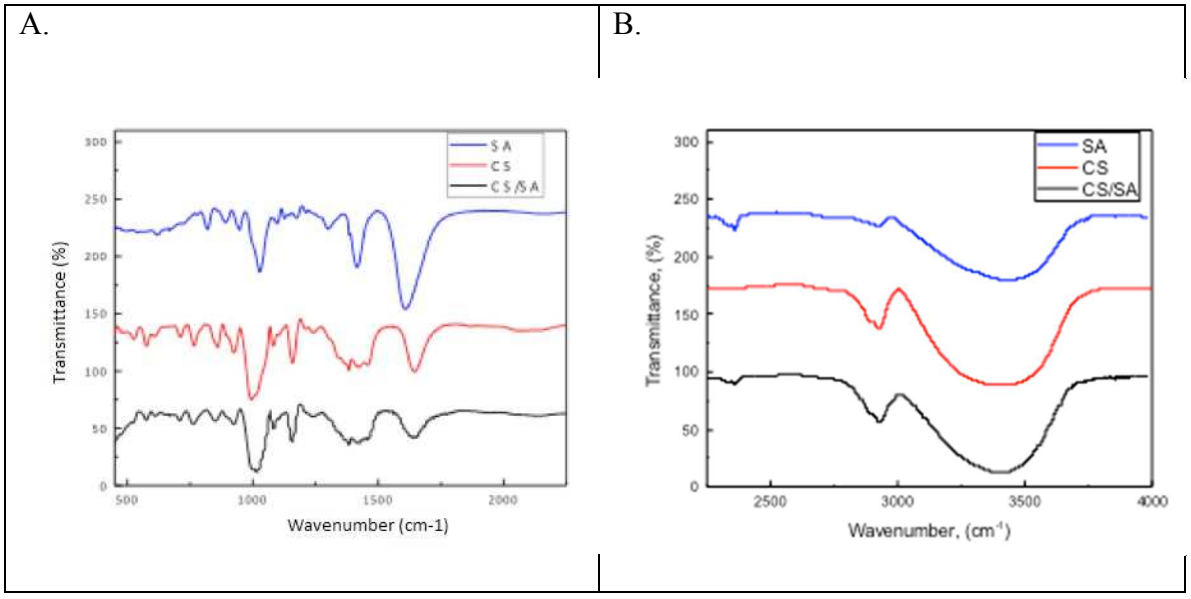

Figure 7: FTIR stacked spectra comparison of SA, CS, and CS-SA. (A) higher spectra (B) lower spectra

Corn Starch-Chitosan Scaffold. As with the CS-SA scaffold, the CS-CH scaffold and CS spectra bear nearly identical resemblance. This is thought again to be due to the predominant amount of CS over CH in the scaffold. O-H regions are present in both parent polymers and CS-SA scaffold, and all share nearly the same broad width in

wavelength, indicating H_2O absorbance. C-O stretch is present in CH, CS-CH, and CS with peaks at 1130 cm^{-1}, 1160 cm^{-1}, and 1170 cm^{-1}, respectively. Also, the amide I band peak is apparent in the spectra as well. Chitosan is known to contain an amide group in its molecular structure, therefore its presence at 1630 cm^{-1} was expected.

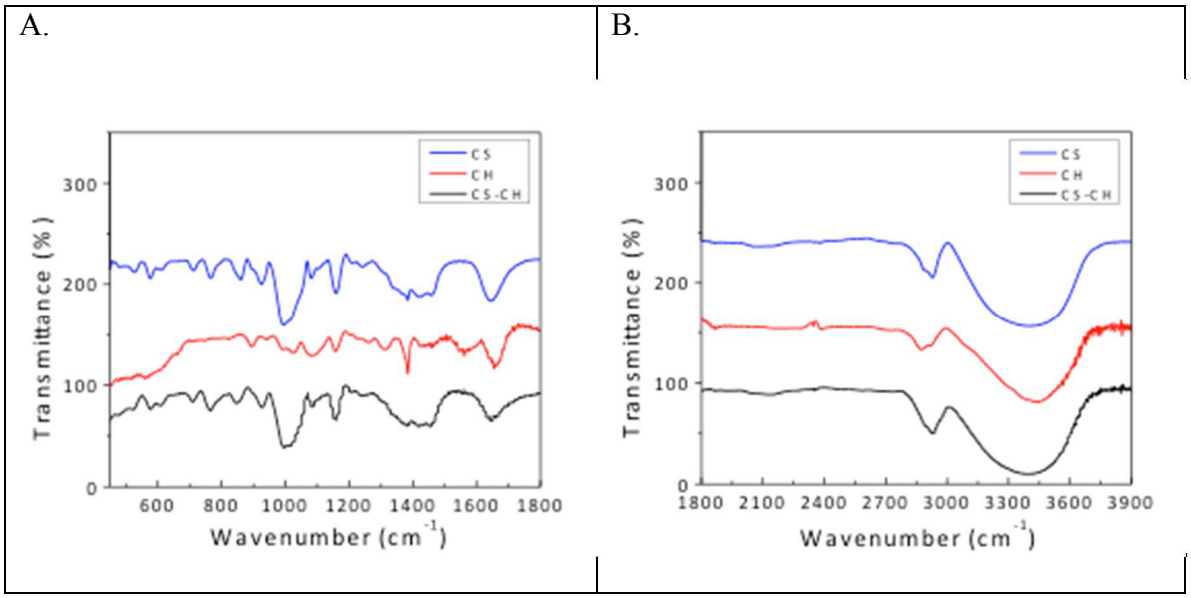

Figure 8: FTIR stacked spectra comparison of CS powder, CH powder, CS-CH scaffold. (A) higher spectra (B)lower spectra

Chitosan TEO Treated. Amide I bands are shown by peak values at 1643 cm^{-1} for both CH and CH treated spectra as expected, with a slight broadening as a result of the TEO treatment. Also noticed is a broad emergence of a peak at 1066 cm^{-1} in the CH TEO spectra. This is indicative of C-O-C stretching and may be due to hydrogen bonding from water absorbance which is backed up by a wide broadening also in the O-H region from 2400 cm^{-1} to 3500 cm^{-1}.

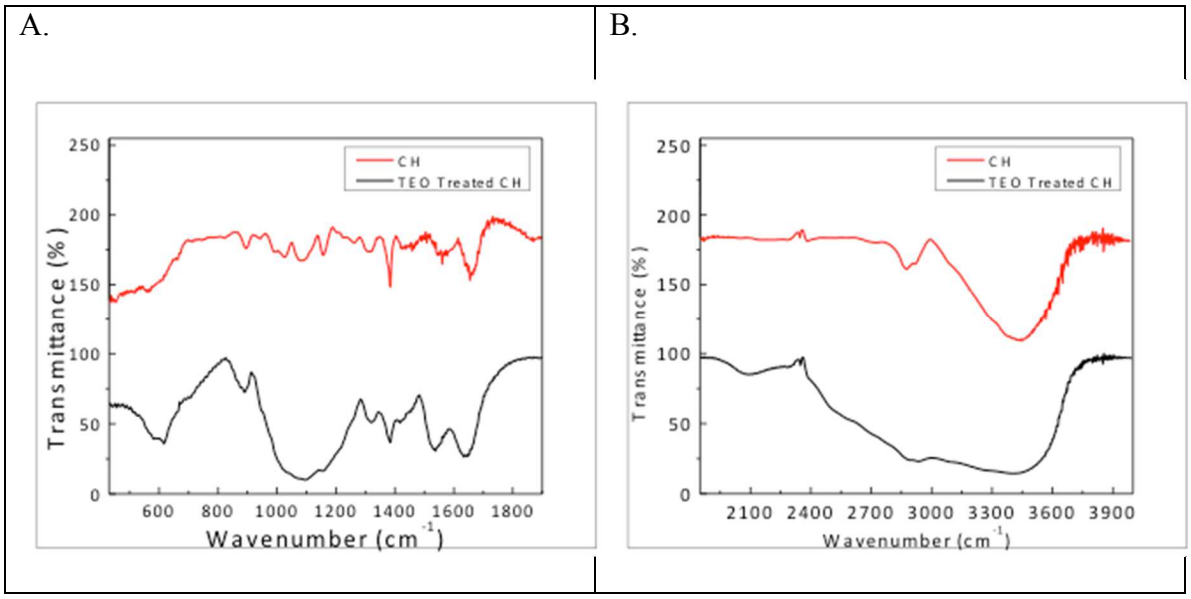

Figure 9: FTIR stacked spectra comparison of CH powder and TEO treated CH scaffold. (A) higher spectra (B) lower spectra

Chitosan Collagen TOS Treated. Perhaps more interesting in regards to discrepancies amongst the spectra pertain to those of the CH-Col TEO treated members. Complete peak development at 2480 cm^{-1}, 2103 cm^{-1}, 1764 cm^{-1}, 744 cm^{-1}, 617 cm^{-1}, all must evolve from the TEO treatment and are shown on the spectra of CH-Coll Treated scaffolds. In addition, extremely large broadening of C-H bending and C-O stretch take place at 1429 cm^{-1} and 1120 cm^{-1} , respectively.

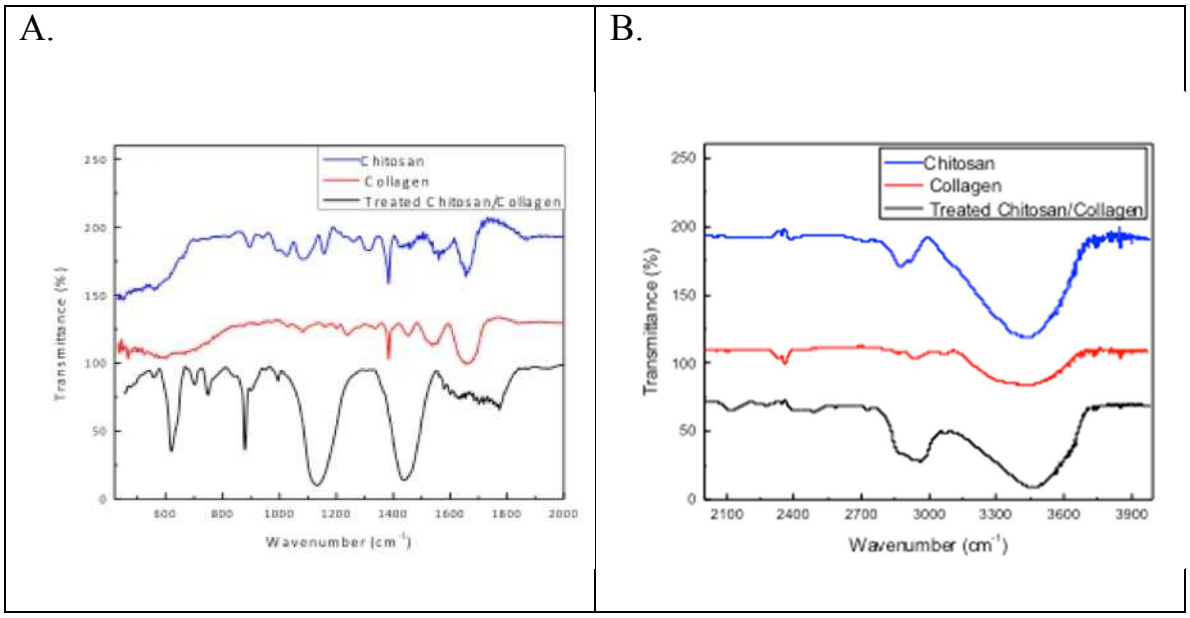

Figure 10: FTIR stacked spectra comparison of, CH powder, Coll fiber, TEO treated CH-Coll scaffold. (A) higher spectra, (B) lower spectra

Collagen TEO Treated. Spectra for the collagen TEO treated scaffold appear to be inconclusive due to poor spectra attainment. Additional spectra must be taken to make better judgment for this group.

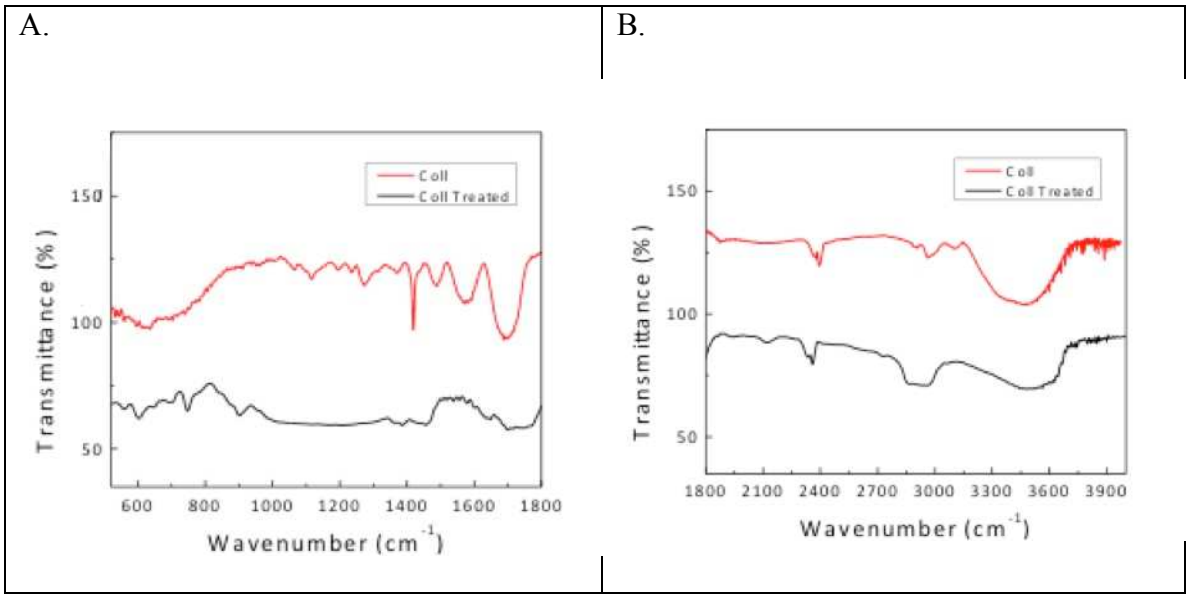

Figure 11: FTIR stacked spectra comparison of, (top) coll fiber, (bottom) TEO treated coll scaffold.

Scanning Electron Microscopy (SEM)

Scanning electron microscopy was carried out using an SEM Sigma VP model EDAX Octane Super, Carl Zeiss, Germany. Its hoped that SEM testing will aptly detail the scaffold morphologies and help determine if the scaffolds would permit favorable cellular processes to occur. All samples were submerged in liquid nitrogen for 2 minutes and subsequently pulled apart with two sets of tweezers to retain the actual morphology due to a brittle fracture as a result of the sub-freezing temperature. EDS characterization is hoped to offer an alternative means of defining elemental composition at the surface. Additionally, EDS results are expected to offer deeper elemental analysis where up to 3 μm of depth may be accounted for, as compared with only 6-8 nm from XPS results.

SEM/EDS Corn Starch Scaffold. The first SEM images of discussion is that of the corn starch scaffold and cornstarch polymer itself, as can be seen in the following figure. A porous morphology does seem to be present in the scaffold; however, pore size seems to be limited in comparison to CS-SA and CS-CH samples, as can be compared with future figures. Limitations on pore size seem to be constrained under the magnitudes of 30 μm. Present nonetheless, is indications of pore-pore communication. This is an indication that some degree of permeability is existent within the scaffold bulk material. The surface of the scaffold may also give rise to cell attachment, as sharp edges and peaks of valleys are shown. These height variations can create prospective dwellings for initial cells by offering hook like platforms for cells to grab to stage proliferation processes. EDS results also indicate significant percentages of carbon and oxygen within the surface of the scaffold.

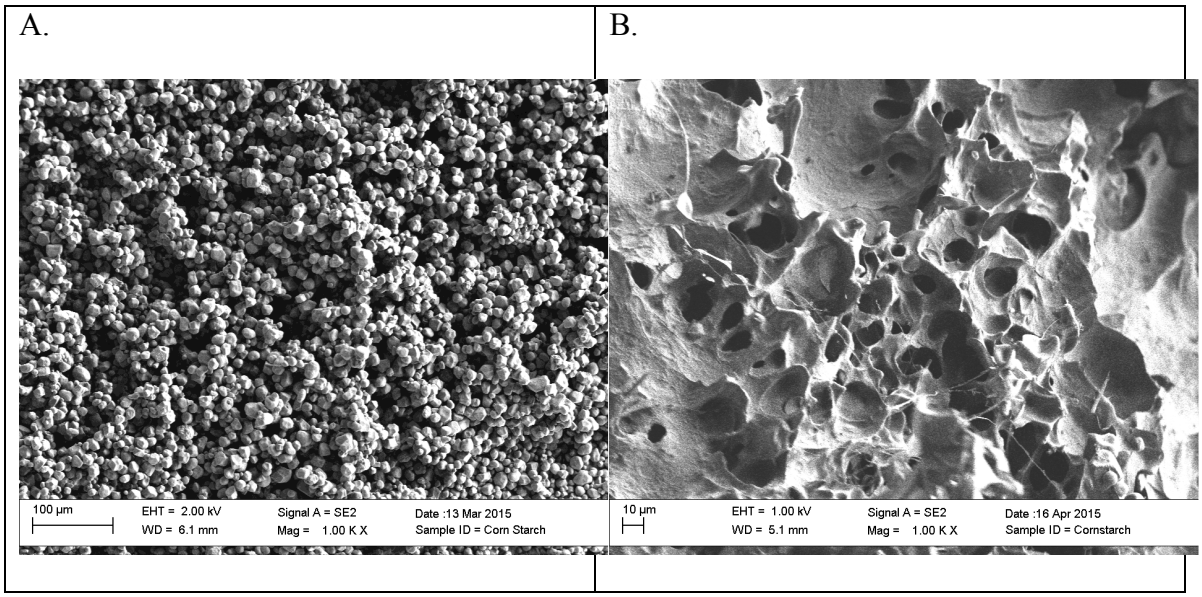

Figure 12: SEM images pertaining to CS scaffold. (A) CS powder and (B) CS scaffold.

SEM/EDS Corn Starch Sodium Alginate. Morphology of the CS-SA scaffold in figures 13-C, reveals a somewhat layered organization form the side view of the scaffold. This profile is analogous to a floor and ceiling scheme of a multi-storied building. Clearance between "floor and ceiling" varies in distance throughout the view, where 20 µm to over 100 µm is observed. Figure 13-D, shows the top view of the scaffold where initial cell attachment should take place. The surface of the scaffold offers many opportunities for cells to "hook" onto for attachment due to its rough nature. In addition, pores are present throughout the scaffold exterior surface with pores easily observed over 15 µm in diameter. This, would give rise to cellular penetration into the scaffold, where average cell diameter is around 10µm. Figures 13-A and B show the parent polymers used in the synthesis of this particular scaffold. Figures 14-A and B show a closer view of the side and top views. A porous and permeable morphology is indicative of figure 14-F, due to the communication and observance of pores within pores, another important

trait necessary for cell proliferation to occur. EDS results reveal carbon and oxygen at the surface.

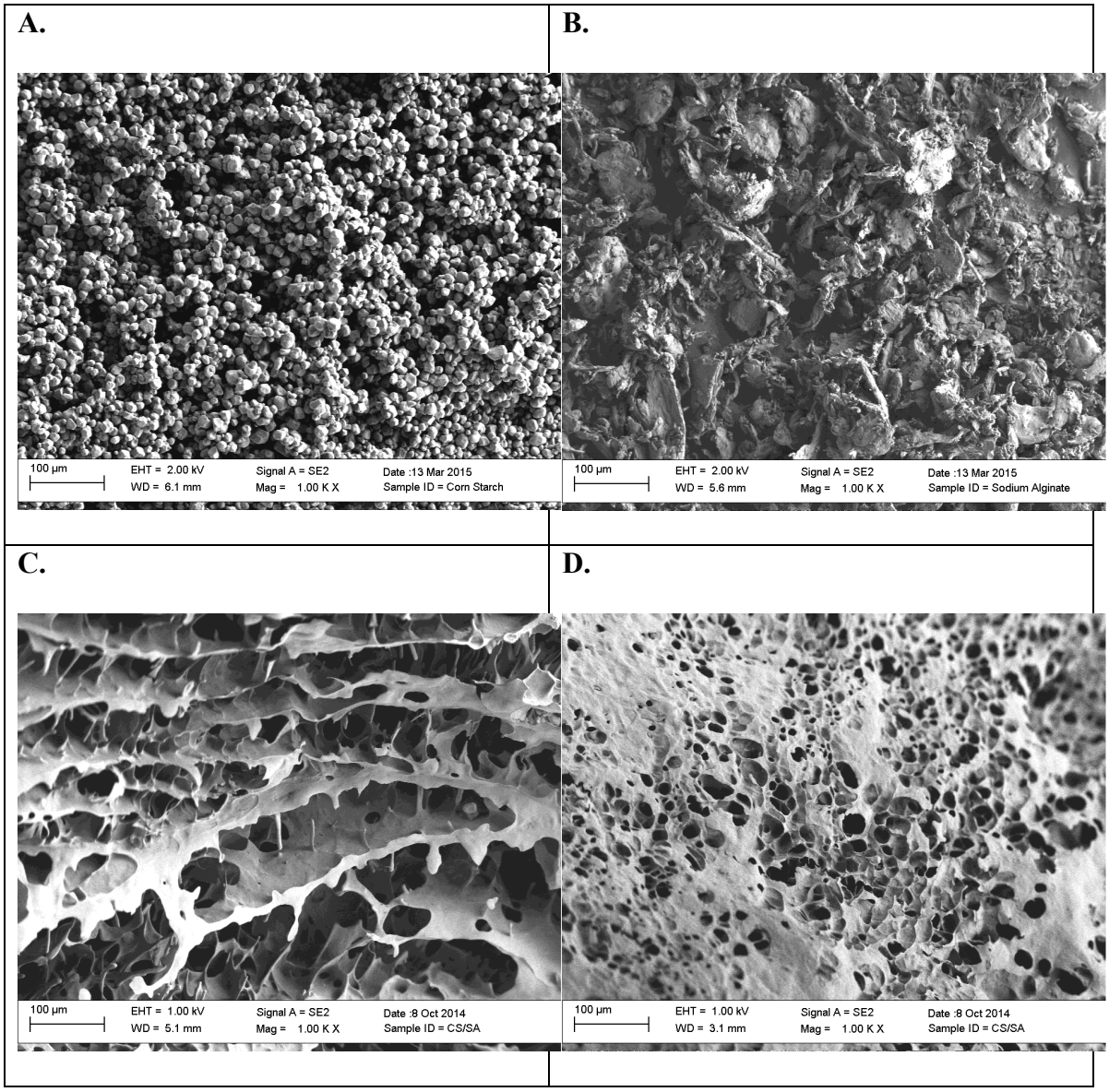

Figure 13: SEM images pertaining to CS-SA scaffold (A) CS powder, (B) SA powder, (C) side view of CS-SA scaffold, and (D) surface image of CS-SA scaffold.

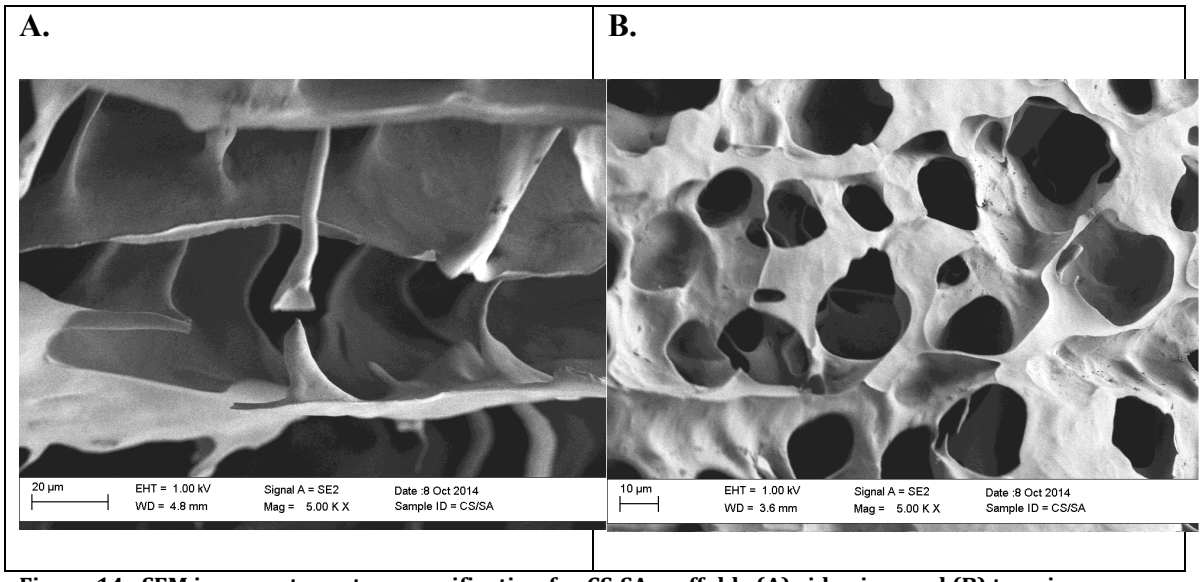

Figure 14: SEM images at greater magnification for CS-SA scaffolds (A) side view and (B) top view.

SEM/EDS Corn Starch-Chitosan. SEM images for CS-CH scaffolds indicate a porous and permeable morphology. While there is no storied structure as in the previous scaffold type, a sponge-like organization is observed and shows pore sizes well beyond that of 50µm upon observation. Surface roughness can be viewed in figure 15-D, and is favorable for cell adhesion and penetration as well. As with the CS-SA scaffold, EDS readings indicate carbon and oxygen within the range of observance. Figure 16-A and B show higher magnification of the corn starch-chitosan scaffolds.

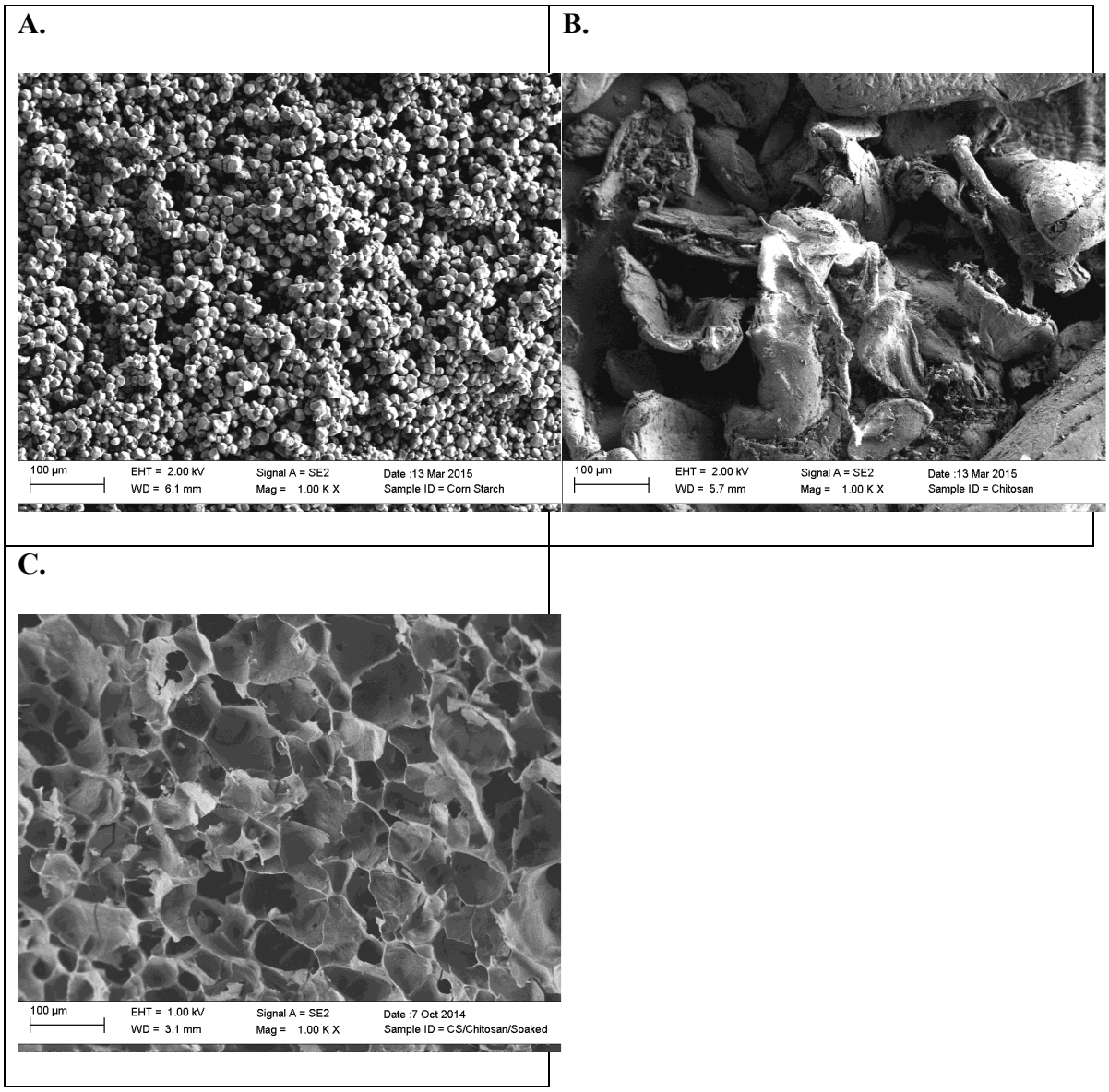

Figure 15: SEM images pertaining to CS-CH scaffold and parent polymers, (A) CS polymer, (B) CH polymer, (C) side view of CS-CH scaffold,

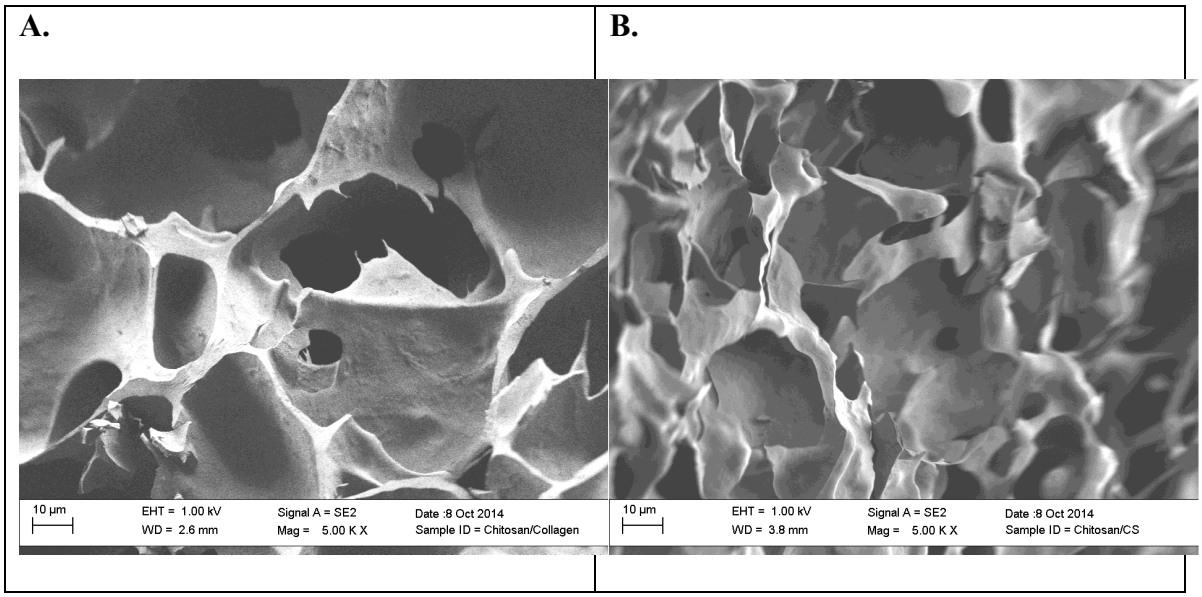

Figure 16: SEM images of CS-CH at greater magnification, (A) side view and (B) alternative location, side view

SEM/EDS TEO Treated Chitosan. SEM observation of chitosan TEO treated scaffolds show morphology analogous to that of fallen and stacked leaves atop each other. Pores are present, but don't seem to be as prevalent as in the cause of the corn starch based irradiated specimens. However, favorable surface conditions exist for cell attachment based off the rough nature of the scaffolds. EDS results are pending as well as an SEM view of the scaffold prior to TEO treatment.

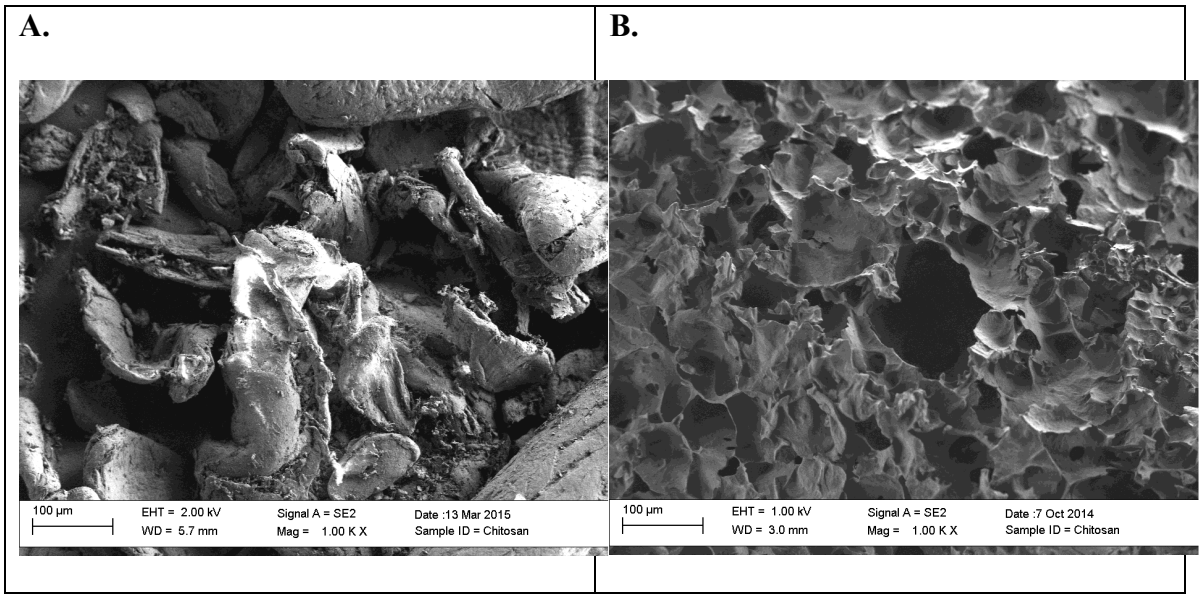

Figure 17: SEM images pertaining to TEO treated CH scaffolds. (A) CHpowder, (B) pre-TEO treated CH, (C) TEO treated CH scaffold

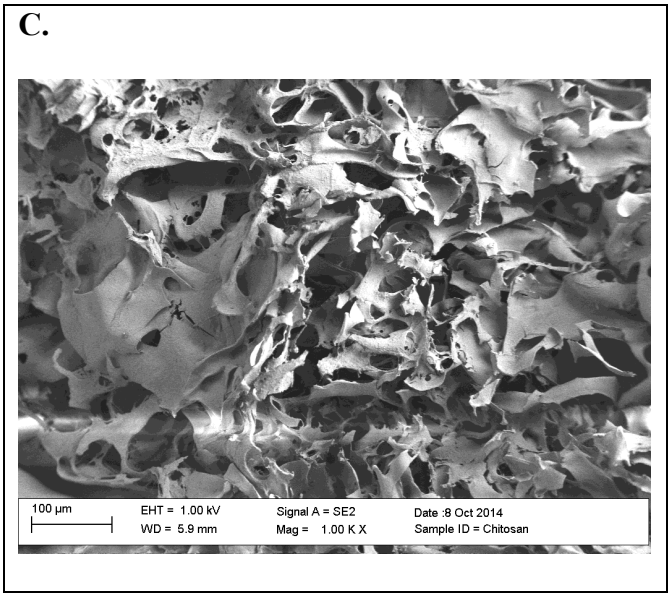

SEM/EDS Chitosan Collagen TEO Treated. Indication of a porous morphology is present by the SEM images taken of CH-Coll TEO treated scaffolds. However, a large presence does not exist in this particular study, with respect to the treated scaffold (figure 18-D). Figure 18-C, is an SEM image of the untreated scaffold of CH-Coll, which is more comparable to the morphology of the microwave irradiated CS irradiated group of

scaffolds. Perhaps another experiment involving more SEM pictures would reveal more pores and evidence of permeability in the treated samples. Nonetheless, surface roughness looks to be accommodating for cell attachment. EDS results indicate carbon and oxygen at the surface.

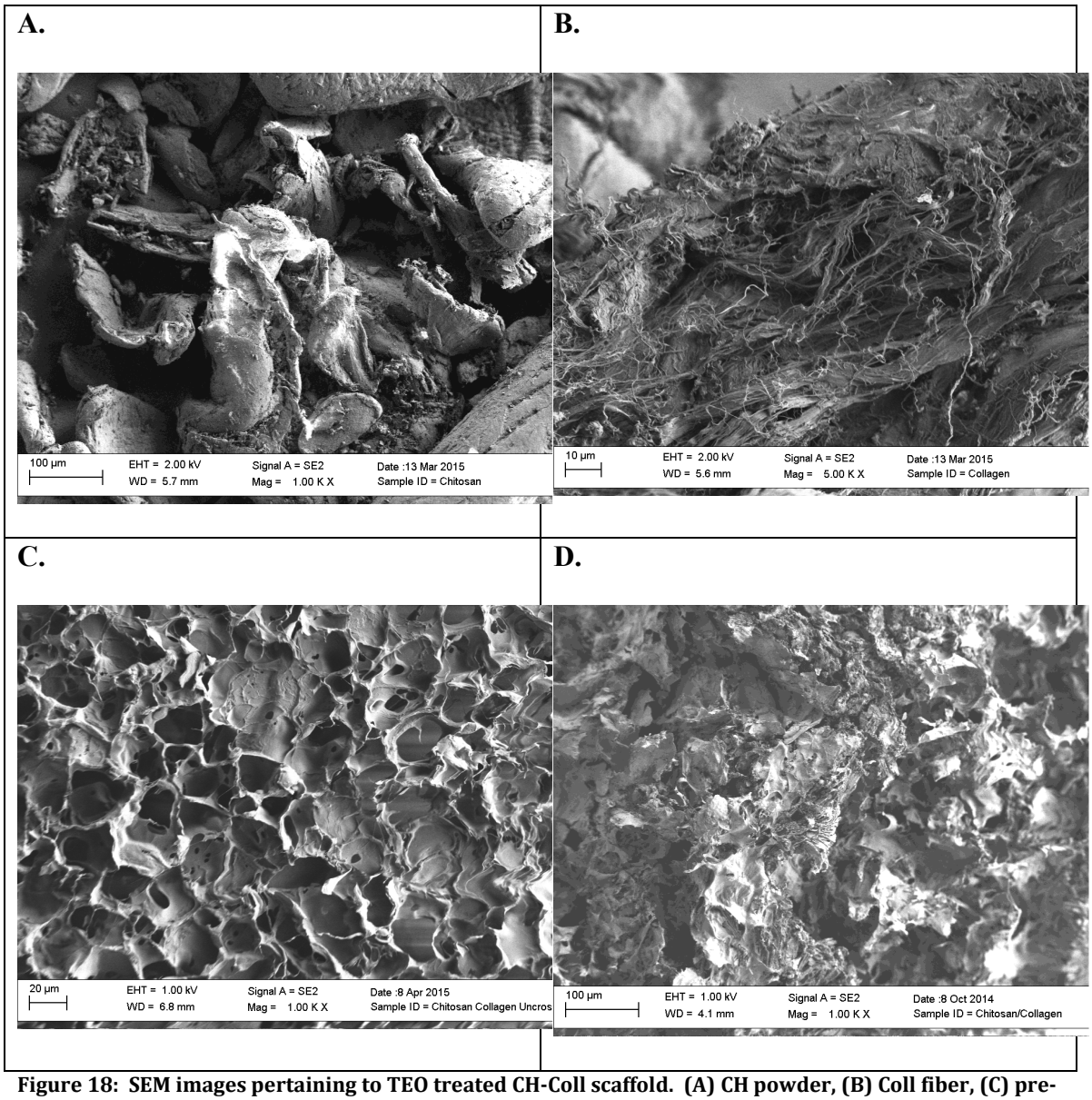

Figure 18: SEM images pertaining to TEO treated CH-Coll scaffold. (A) CH powder, (B) Coll fiber, (C) pre-TEO treated CH-Coll scaffold, (D) TEO treated CH-Coll Scaffold.

SEM/EDS Collagen TEO Treated Scaffolds. Figure 19-B shows the morphology of the un-treated scaffold, which seems to possess morphology more similar to that of the

natural extra-cellular matrix. It appears this morphology however, falters as a result of either the TEO treatment or the second lypholization process, as can be seen in figures 19-C and D. Again, surface roughness looks favorable to cell adhesion in the scaffold image. EDS results also share some new elemental constituent members. Carbon, oxygen, nitrogen, sodium, and sulfur were all found in the surface of the scaffold.

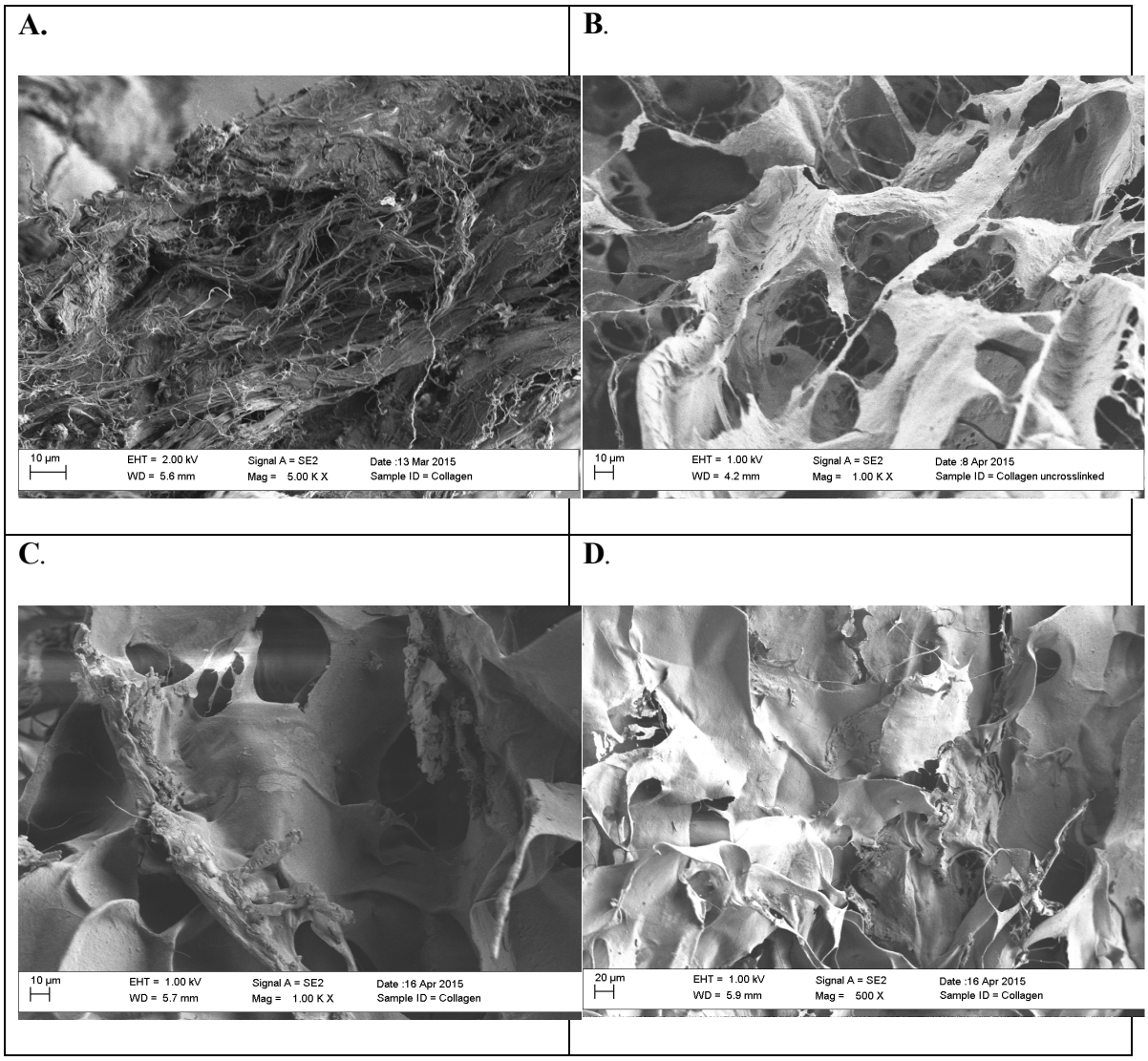

Figure 19: SEM images pertaining to TEO treated Coll scaffold. (A) Coll fiber, (B) pretreated TEO treated Coll scaffold, (C) and (D) TEO treated Coll scaffold.

Swelling Ratio

Swelling Ratio. Absorbability of the scaffolds was assessed through a swelling ratio study. Taken from a study conducted by Sajesh et al. in *Biocompatible conducting chitosan/polypyrrole-alginate composite scaffold for bone tissue engineering*, the swelling ratio was attained by first weighing and recording the dry weights of each scaffold. The study proceeded by submerging all the scaffolds in phosphate buffer solution (PBS), in separate and labeled vials to help distinguish each specimen. The scaffolds (now in vials) were placed in an incubator at 37ºC for 28 days to simulate body temperature and condition. The wet weight was noted for each specimen and was gained after pat drying the scaffold surface to remove excess PBS. During the coarse of the 28 day study, the wet weight was recorded at days 1, 7, 14, 21, and 28. Swelling ratio was derived from the following equation:

$$Swelling\ Ratio\ = \frac{Wet\ Weight - Dry\ Weight}{Dry\ Weight}\ (100)$$

Table 1: 28 day swelling ratio percentages for scaffolds tested

Scaffold	Specimen	Day 1	Day 7	Day 14
MW Irradiated Corn Starch Scaffolds				
	1	464%	462%	465%
	2	424%	458%	457%
MW Irradiated Corn Starch-Sodium Alginate Scaffolds				
	1	565%	547%	515%

	2	535%	522%	509%
MW Irradiated Corn Starch-Chitosan Scaffolds				
	1	663%	726%	669%
	2	404%	434%	486%
TEO Treated Chitosan-Collagen Scaffolds				
	1	340%	238%	203%
	2	403%	217%	191%
TEO Treated Collagen Scaffolds				
	1	461%	556%	497%
	2	209%	237%	161%

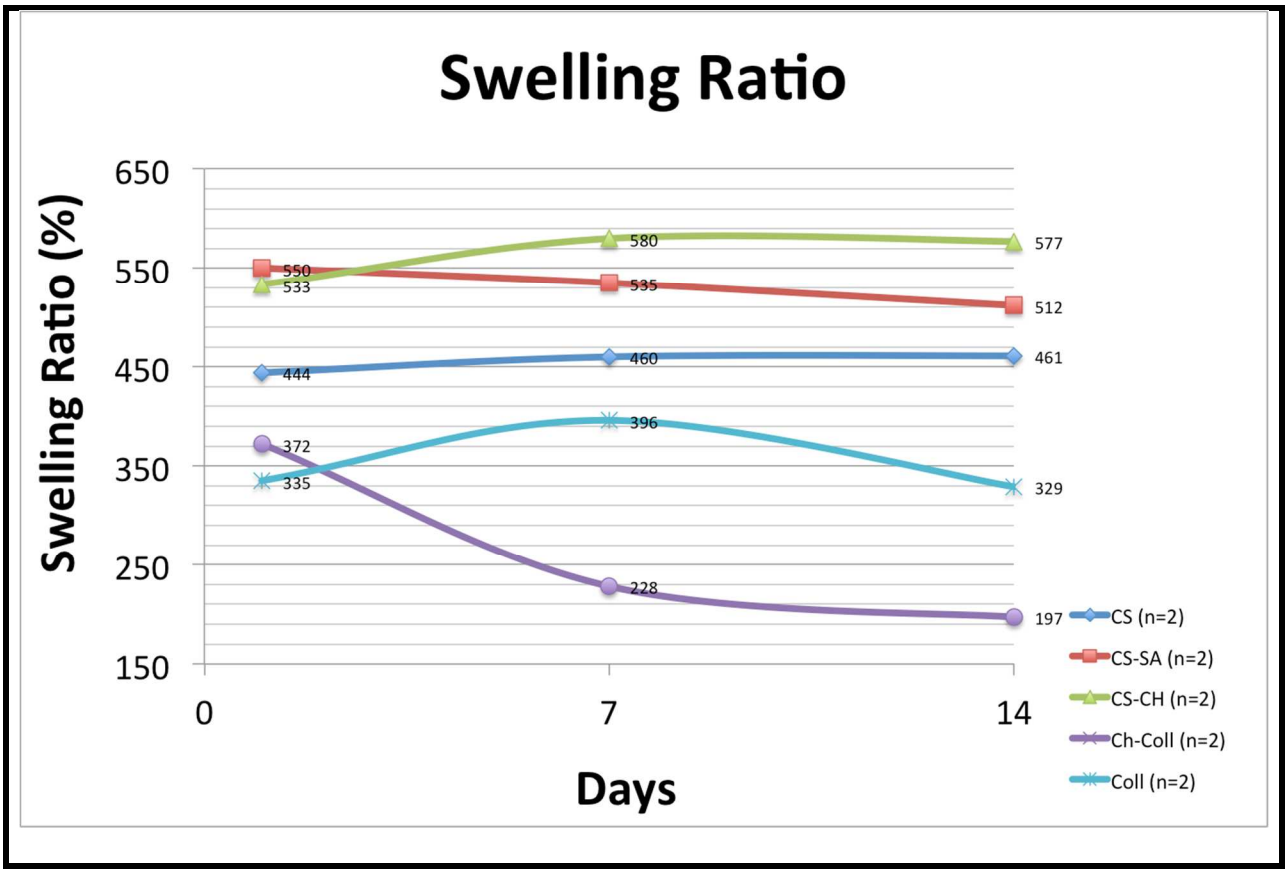

Figure 20: Swelling ratio comparison chart.

Degradation Study. The degradation study was carried out in conjunction with the swelling ratio. The dry weights taken at the beginning of the swelling ratio tests were compared with the dry weight at the conclusion of the swelling ratio test, after the scaffolds were kept in a desiccator for two days. The desiccator effectively dried out the absorbed PBS in the scaffolds. The following table depicts the initial weights and the final dry weights of the scaffolds. Degradation was calculated by:

$$Degradation = \frac{inital\ dry\ weight - final\ dry\ weight}{inital\ dry\ weight} X\ 100$$

Table 2: Degradation of Microwaved Irradiated Scaffolds: initial and final weights of scaffolds and degradation percentage for MW irradiated scaffolds

	Corn Starch Scaffolds		CS-SA Scaffolds		CS-CH Scaffolds	
	Specimen 1	Specimen 2	Specimen 1	Specimen 2	Specimen 1	Specimen 2
Initial (g)	.0736	.1172	0.0438	0.0493	.0554	.06312
Final (g)	.0751	.1185	0.0314	0.0456	.0529	.0521
Degradation (%)	+2%*	+1%	-28%	-7%	-4.50%	-17.5%

***(+) indicates increase in weight, (-) indicates decrease in weight**

Table 3: Degradation of TEO Treated Scaffolds: initial and final weights of scaffolds, and degradation percentage for TEO Treated scaffolds

	Chitosan-Collagen Scaffolds		Collagen Scaffolds	
	Specimen 1	Specimen 2	Specimen 1	Specimen 2
Initial (g)	0.0235	0.0231	.0159	.0175
Final (g)	0.0112	0.0108	.0099	Broke apart
Degradation (%)	-52%	-53%	-37%	Inconclusive

Table 4: Average Degradation: Microwave Irradiated Scaffolds

	Scaffold Type		
	CS (n=2)	CS-SA (n=2)	CS-CH (n=2)
Average Degradation	+1.5%	-17.5%	-11%

Table 5: Average Degradation: TEO Treated Scaffolds

	Scaffold Type	
	CH-Coll (n=2)	Coll (n=1)
Average Degradation	-52.5%	-37%

BIO-ASSESSMENTS

Fluorescence Cell Imagining. Fluorescence cell imagining was done using an EVOS cell imaging microscope. All scaffolds were initially sterilized with 70% ethanol washes followed by placement in a laminar flow hood with the a UV light in operation. Scaffolds were exposed to UV light for 15 minutes on each side. The scaffolds were then placed in individual culture cells of a 24 well culture plate and submerged in their respective medias (i.e. fibroblast media or osteoblast media). The scaffolds were left submerged for 1 to 2 days in an incubator, at 37ºC, with 5% CO_2 to simulate biological conditions, to insure media absorbance throughout the scaffold. After the submergence, the media was aspirated out under disinfected laminar flow hood conditions, at which point the appropriate cell lines were added to the surface of the scaffold. Cells were counted using Almar Blu staining reagent and cell counting technique in conjunction with the EVOS microscope. 50,000 cells were applied to each scaffold surface for this particular study and subsequently stored in the incubator with conditions described above. After four days, dimethlsufoxide (DMSO) was added to the scaffold surface for 20 minutes at room temperature to stain the healthy nuclei. Subsequently, the DMSO was aspirated and MitoTracker Red was added to the scaffold surface for 25 minutes in incubation-pretexted conditions, to stain the mitochondria. Scaffolds were then taken out of the incubator and examined under the fluorescence microscope where mitochondria and nuclei pictures were taken separately and then over laid on each other to produce the images presented.

Corn Starch Scaffolds with MC3T3 Cells. A large population of MC3T3 cells is apparent in both images regarding CS scaffolds, concluding that cell attachment took place, figure below. While cell-cell communication is hard to observe, cell proximity with respect to neighboring cells and their prevalence, seems to elude that communication is taking place, a necessity for proliferation. The cell population, considering the four days of incubation, also suggests that scaffold toxicity does not exist or is insignificant. These images suggest that the corn starch scaffolds are viable for MC3T3 cells. Cell nuclei are indicated by the blue structures where the mitochondria are stained red.

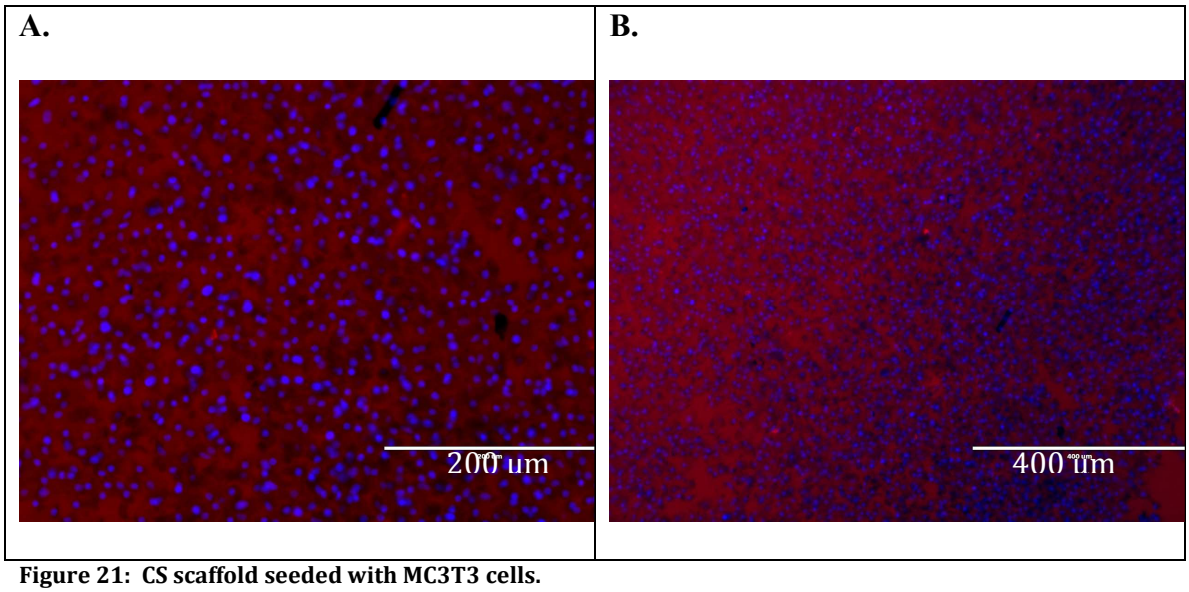

Figure 21: CS scaffold seeded with MC3T3 cells.

Corn Starch-Sodium Alginate Scaffolds with MC3T3 Cells. CS-SA scaffold images also yield promising results. Figure 22-A, shows a highly populated cell cluster on the scaffold surface that reflects the actin regions and cytoskeletal regions of the cell

manifestation, as indicated by the red "cloud like" haze contrasting with the black background. A closer image, as shown in figure-B, focuses more on the cells where both lamellipodium and filopodium are especially observable. The lamellipodium is a thin extension of cytoplasm produced on all sides of migrating cells that enable the cell to move along (American Heritage Medical Dictionary). Filopodia are thin, actin-rich plasma-membrane protrusions that function as antennae for cells to probe their environment, thus, making them important for cell migration (Mattila and Lappalainen). The mitochondria and nuclei of the cells are also more visible in figure 22-B and show that the cells have good structure. The high presence of cells, healthy structure, and evidence of proliferation, is thus indicative of a viable scaffold with permissible toxicity levels.

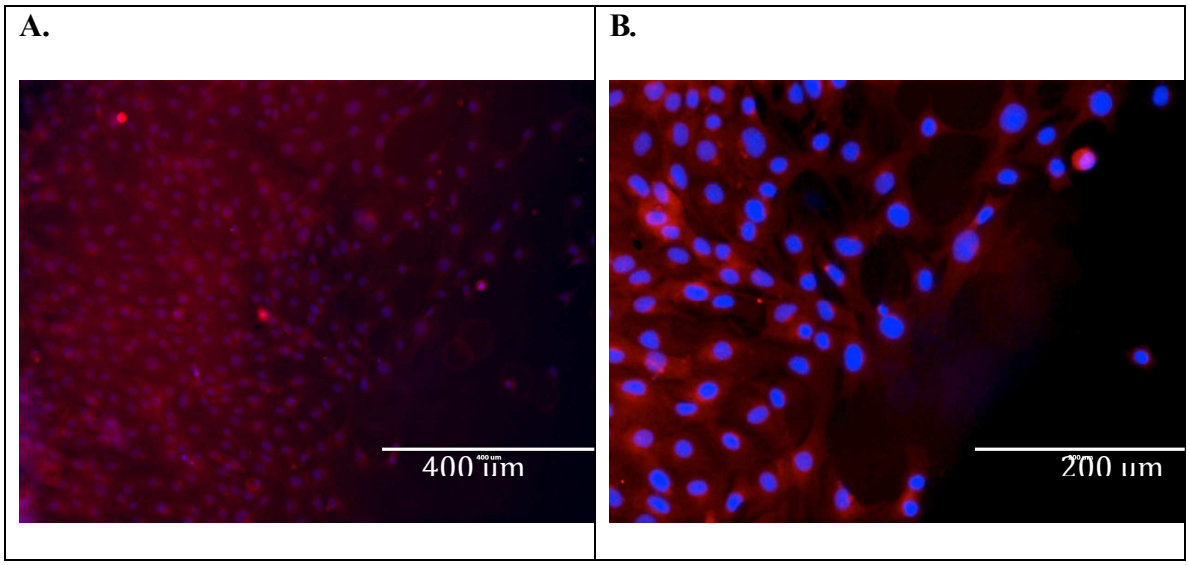

Figure 22: CS-SA scaffolds seeded with MC3T3 cells.

Corn Starch-Chitosan Scaffolds with MC3T3 cells. Fluorescence images depicting MC3T3 cells on CS-CH scaffolds show large cell population, which can be seen in figure 23-A. Cell-cell communication is also evident in both figures 23-A and B,

as well as cell structure, lamellipodium, and filopodia. Due to the high population and health cell structure with evidence of cell mobility, CS-CH scaffolds are suggested as viable scaffolds for MC3T3 cell line.

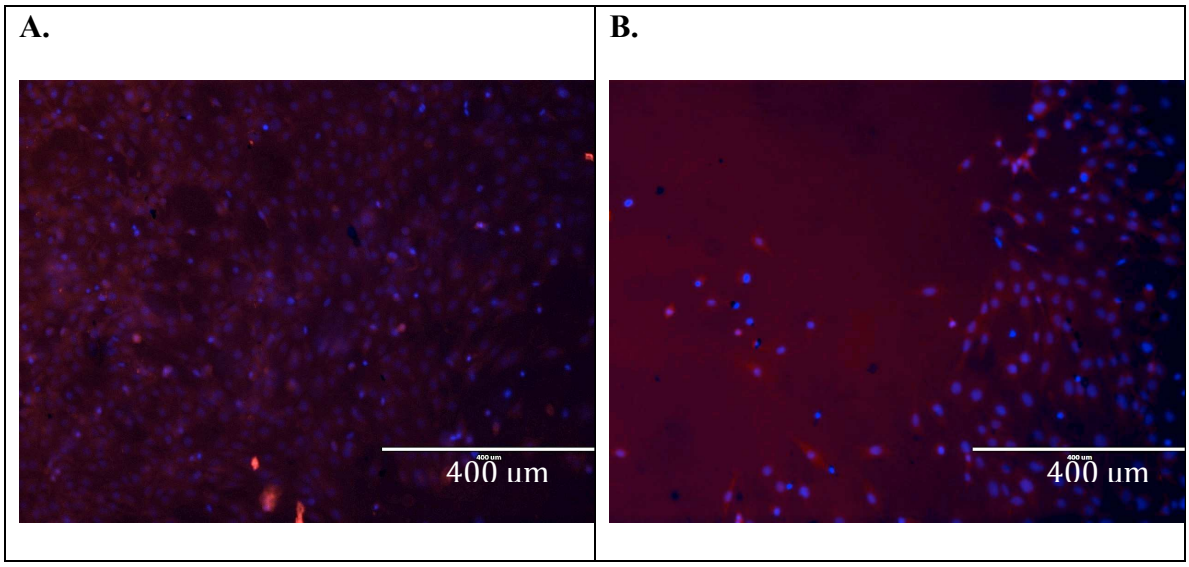

Figure 23: CS-CH scaffolds seeded with MC3T3 cells.

TEO Treated Chitosan-Collagen Scaffolds with Osteoblast MC3T3. CH-Coll TEO treated scaffold fluorescence images detail high levels of cell confluence. In the depicted regions, it can be argued that 100 % confluence has been reached on the scaffold surface. As a result, lamellipodium and filopodia organelle systems are not present, as the cells have grown close to each other. What does become apparent due to this high level of confluence is the appearance of cell walls, which outline the individual cells. These observations prove promising that cell proliferation is taking place and that toxicity levels are also insignificant.

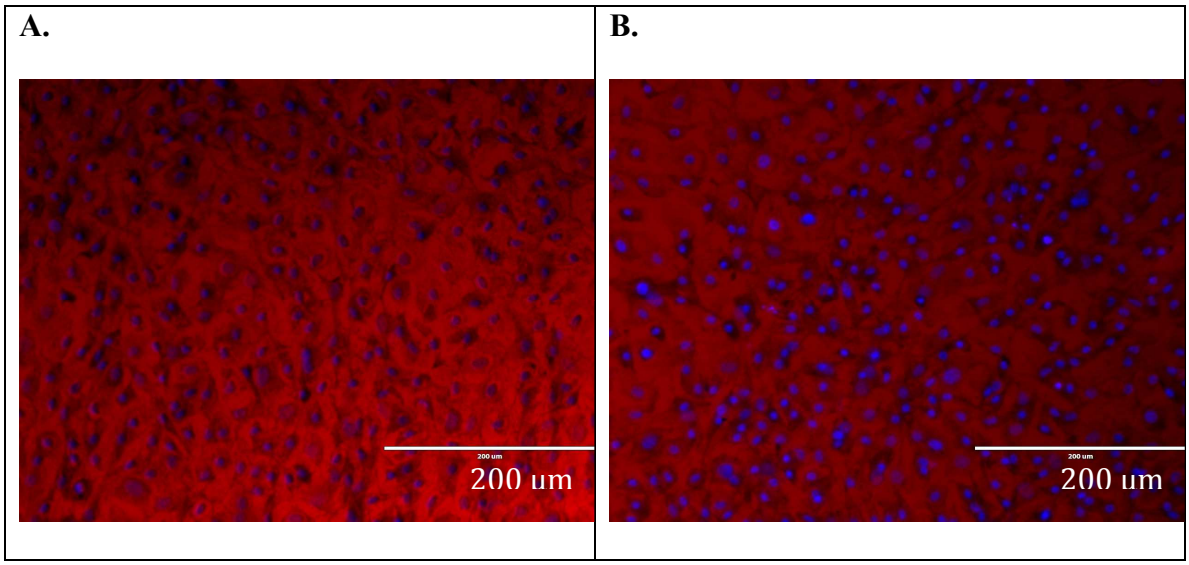

Figure 24: TEO treated CH-Coll scaffolds treated with MC3T3 cells.

Collagen TEO Treated with Osteoblast MC3T3. Figure 25-A, emphasizes the presence of MC3T3 cells on the surface of the collagen TEO treated scaffold, by offering a slanted view of the surface. This image allows visual evidence of cell attachment on the surface where the bottom left corner of A. is the forefront and the top right is the background of the image. Figure-25-B, is a fluorescence image laminating a MC3T3 nuclei landscape on the scaffold surface. Both images depict prevalent cell existence and suggest viability as tissue engineering scaffolds, in regards to toxicity and allowing cell attachment and proliferation.

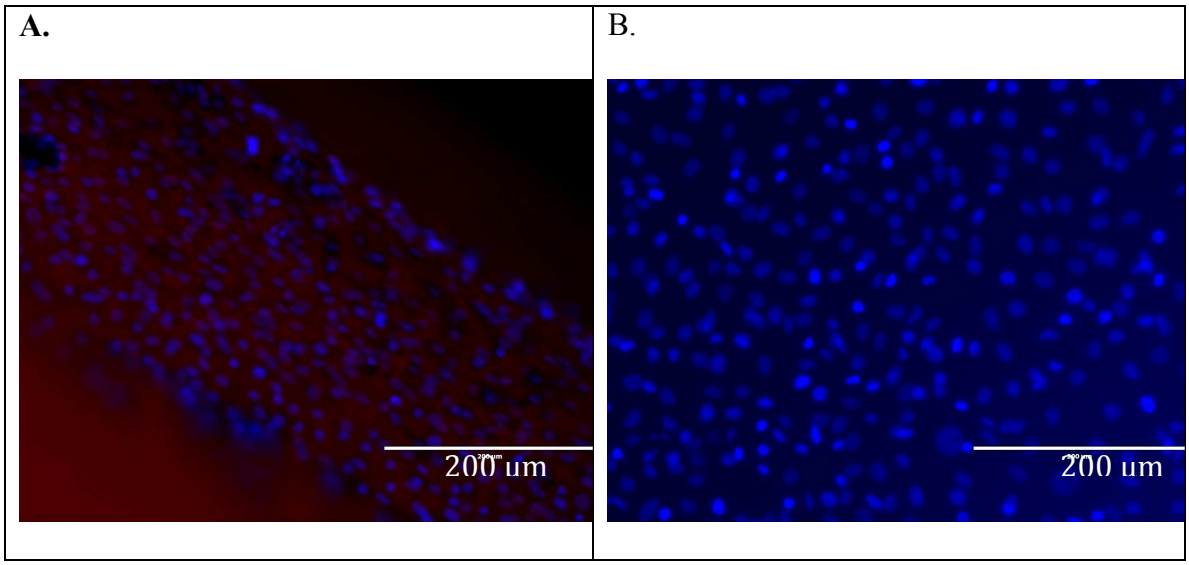

Figure 25: TEO treated Coll scaffolds seeded with MC3T3 cells.

Corn Starch Scaffolds with Fibroblast Cells. Figures 26-A and B indicate fibroblast cell lines are also viable on the corn starch irradiated scaffolds. Image A shows a low confluence area on the scaffold surface however, does offer visual confirmation of healthy cell structure and cell-cell communication. Image B shows better evidence of this with a closer magnification at a different location on the scaffold. In this image, cell alignment may indicate cell proliferation in a particular manner and direction. Moreover, cell lamellipodium and filopodia are present demonstrating cell migration and proliferation is taking place.

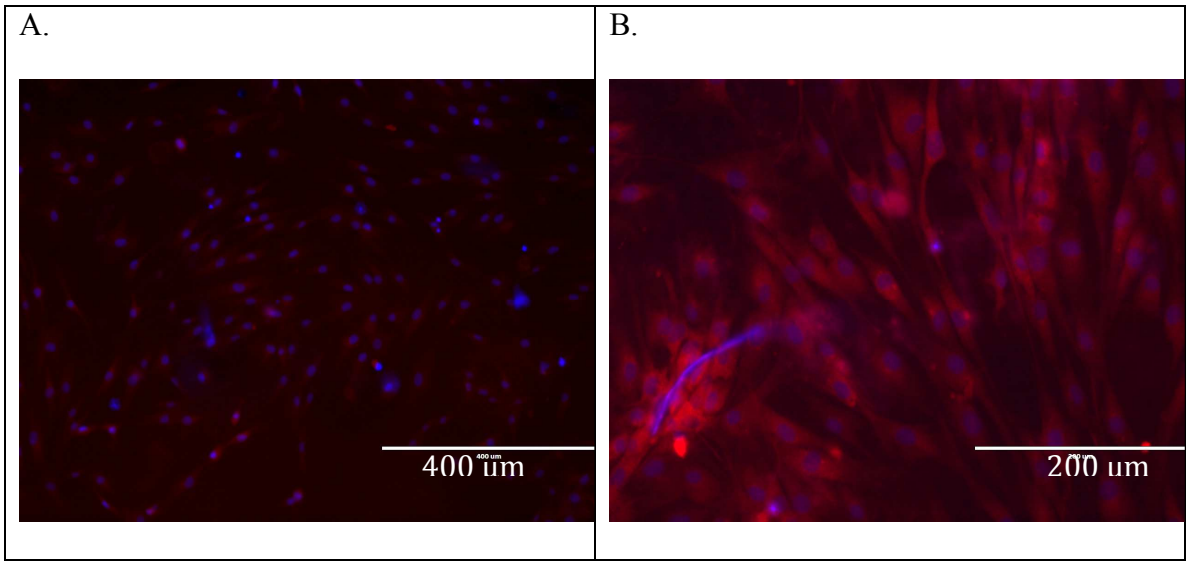

Figure 26: CS scaffolds seeded with fibroblast cells

Corn Starch-Sodium Alginate Scaffolds with Fibroblast Cells. Fibroblast cell growth was also prevalent on the CS-SA scaffold surface. As perceived in figure 27-A, which is the only specimen that facilitated emergent cellular growth. This mass growth of fibroblast cells, at the present time, is not known to be suggestive of beneficial importance or not. However, it reflects cell-cell communication and highlights that cell proliferation is ongoing. Another landscape on the surface of the scaffold is shown in image B below. Here, we can also see cell-cell interaction taking place and evidence of growth coming from a particular area, around the bottom right side of the image.

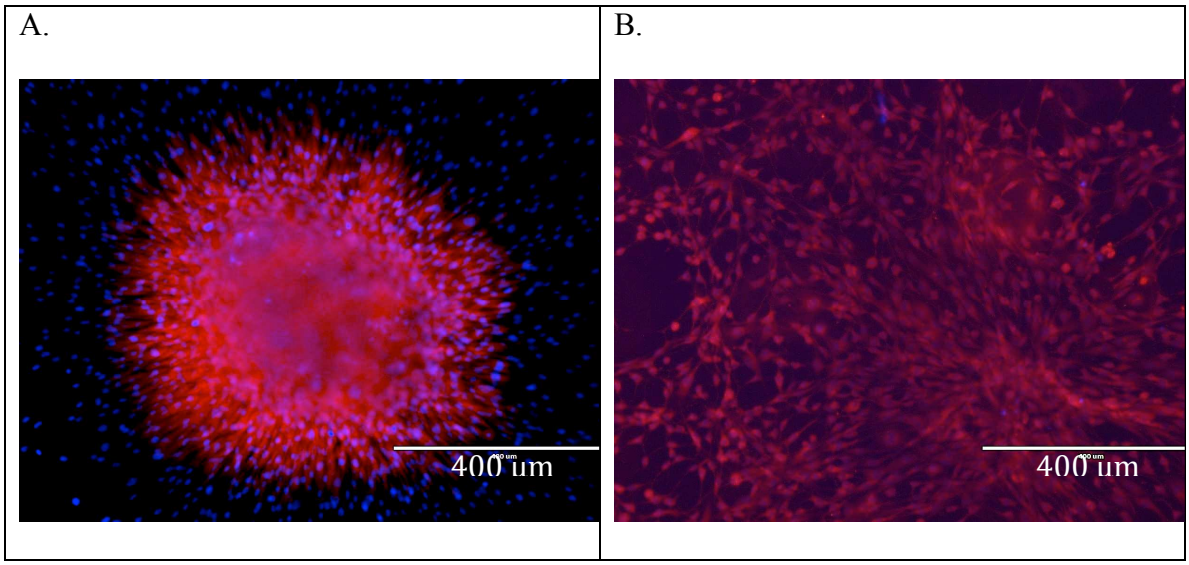

Figure 27: SEM images of CS-SA scaffolds seeded with fibroblast cells.

Corn Starch-Chitosan Scaffolds with Fibroblast Cells. Low and high confluent landscape images were taken on the CS-CH scaffolds with fibroblast cell lines. Figure 28-A, the lower confluent image, shows the cells in more detail along with the lamellipodium and filopodia organelle systems. Also, cell-cell interaction can be observed. In image B, the high population of cells indicates fibroblast cell viability for the CS-CH scaffolds.

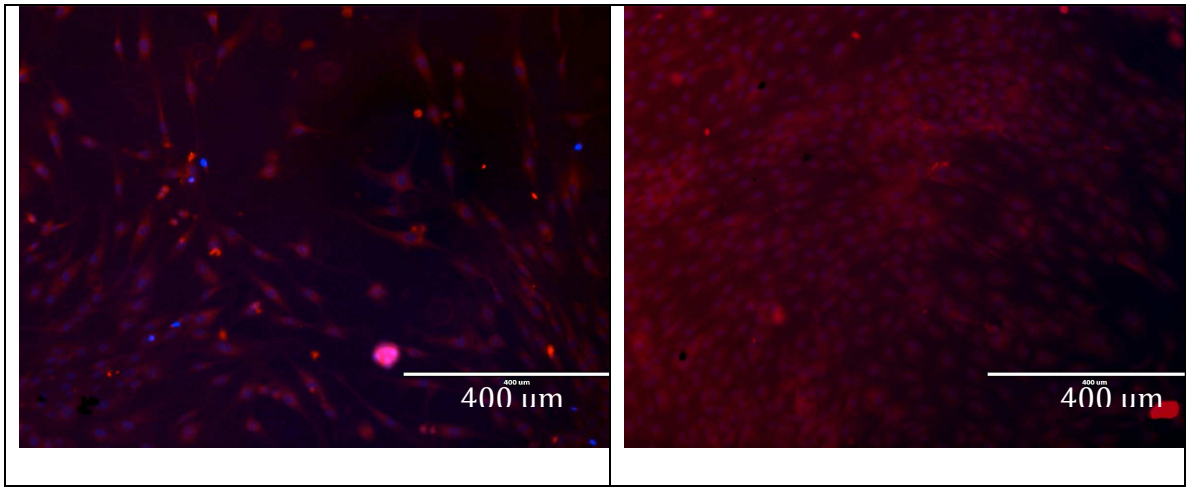

Figure 28: SEM images of CS-CH scaffolds seeded with fibroblast cells.

CHAPTER IV

SUMMARY AND DISCUSSION

The synthesis of two varieties of porous TE scaffolds via lyophilization technique was conducted for characterization and bio-assessment studies. Alternative methods of crosslinking the scaffolds before the lyophilization process, was a great aspect of the project, as crosslinking is shown to add mechanical stability, aid in degradation rates, and correlate well to favorable swelling ratios, which influence pore size, morphology, and permeability. Distinction of the two varieties is chiefly related to the methods in which crosslinking was accomplished. The first variety, primarily derived of cooking grade corn starch, were subjected to microwave irradiation via conventional microwave heating. It was projected this synthesis approach would offer an economical and relatively easy means of producing viable tissue engineering scaffolds, as corn starch is of low monetary value and microwaves are readily available. The second variety, utilized a solution of triethyl orthoformate as a novel crosslinking agent to crosslink the parent polymers together.

SEM was used to study the general morphologies of the scaffolds. Specifically to offer insight into pore size and pore distribution throughout the morphology. Moreover it helped to suggest and establish interconnectivity within the pores, a necessary trait in promoting cell penetration and proliferation.

XPS, EDS, and FTIR, were integrated in the study to ascertain elemental composition and functional groups present in all parent polymers used. This foundation helped establish a base criterion for acceptable biocompatible elements and functional groups, as it's known that all unprocessed parent polymers used, held a high degree of biocompatibility. This basis was then used to compare the XPS, EDS, and FTIR results (i.e. elemental composition, functional groups) of the synthesized scaffolds to help predict biocompatibility based off the composition and functional groups present. Finally, FTIR spectra comparison was used to help oversee any changes incurred by the crosslinking methods. This was primarily to help facilitate the argument that crosslinking was either occurring or not and to attempt to chemically characterize the crosslinking event.

A bio-assessment finalized the experiment aspect of this thesis to help suggest the scaffolds as viable candidates for future tissue engineering studies and programs. Swelling ratios and biodegradation rates where attained for each scaffold via submersion tests. Swelling ratios are used to establish the degree of fluid absorbability the scaffold holds, which can foretell a favorable morphology after the lyophilization process. These ratios were easily attained by simple mathematical formulation.

The biodegradation study was conducted to help decipher the contingency of degradation and its rates in a fluid that mimics that of the ionic concentration found in the human body. For 28 days, scaffolds were submerged in PBS and at the conclusion of the test, the initial dry weights and final dry weights were compared and a material degradation percentage was calculated.

Fluorescence imaging concluded the study as a qualitative viability test. The natures of the images attainted provided insight as to cell adhesion, cell-scaffold interaction, and cell-cell interaction on the scaffolds. From these images, evaluations regarding scaffold viability, proliferation, and scaffold toxicity were made, qualitatively speaking. Moreover, by studying the mitochondria and nuclei structures through the staining process of the cells, cell health was also assessed. The fluorescence study involved both MC3T3 and human fibroblast cell lines, to facilitate both bone and skin viabilities.

In order to facilitate the migration of cells and adequately permit vital cellular processes to occur, scaffolds should possess a micro-porous and permeable morphology. The SEM captured images, presented in this defense, provide key evidence of prospective venues and avenues for such processes and cell attachment. The microwaved irradiated cornstarch scaffold variety, possess the best evidence of porous and permeable networks, strictly in respect to their SEM images. Out of all the MW irradiated types, the CS irradiated scaffolds exhibited the least amount and perhaps the smallest pores of all the other varieties. Pore size for this variety seemed to be around the magnitude of 15 microns. The SEM images for CS-SA scaffolds figure 13, seemed to depict the best evidence of possible cell pathways of all the varieties of the study. In fact, they were the only scaffolds variety to have a somewhat layered or stacked morphology that gave rise to ample amounts of free space within the scaffold. This free space can provide ease of passage for cells to proliferate while accompanying the movement of metabolic wastes secreted by the cells. Clearance between stacked layers at some points indicate magnitudes over 100 microns in length, while small clearance windows were shown to be

as low as 20 microns, which would still be significant for cell passage. Moreover, there was a substantial amount of evidence depicting communication between the stacked layers in the scaffold as well. Thus, suggesting that cell transport is viable in all directions. The CS-CH irradiated samples are thought to be the second best variety of the CS type, with respect to the SEM study. The morphology shown in figure 15 seems to aptly meet the morphological requirements for viable scaffolds, where pore size was within the range of 20 to 100 microns as well as indications of a permeable morphology.

SEM images of the chemically treated scaffold varieties, didn't show as much promise in pore size, permeability, and pores in general, as can be seen in figures 17, 18, and 19. Its hypothesized that the collapsed morphologies of the TEO family of scaffolds is due to the synthesis process which involved soaking, freezing, and lyophlizing the scaffolds twice, before their end result. This phenomena was documented by Ma et al. in *Collagen/chitosan porous scaffolds with improved biostability for skin tissue engineering.* Where, it was observed that the rehydration and relyophilization process, when crosslinking collagen and chitosan with glutaraldehyde, caused a collapsed morphology and elongated pores [i]. Therefore, while not visible, collapsed pores may be present in the scaffolds. However, attention needs to be pointed to the fact that these SEM images were conducted on dry specimens, where prior storage was in a desiccator. Therefore, moisture within the scaffolds was highly mitigated, as moisture should be during SEM analysis. This dry scaffold nature is completely contradictory as to how the scaffold would actually be used when cell scaffold interaction is ongoing. That said, the ideal environment would be that of a highly soaked state, where fluid absorption is isotropic throughout the scaffold. Under a condition where scaffold absorption is met, it must be

considered that volume change in the scaffold would transpire as absorption takes place, giving rise to larger pores or the recovery of collapsed cells within the dry scaffolds. Therefore, all SEM images may only present a small degree of pore size that may actually interact in cell-scaffold conditions.

The surface conditions provided by the SEM test also indicated that cell adhesion should be viable based on surface roughness conditions. In particular, a suitable roughness is depicted in figure 12 for the CS irradiated sample. Small hook like appendages that alter the surface height in the area, are visible around the pores. This landscape was unique in the CS scaffold as they were not as prominent as in the CS-SA and CS-CH scaffolds. The result of this, may be behind the more prevalence of cell adherence as shown in the fluorescence images for CS, over the CS-SA and CS-CH images, with respect to the MC3T3 fluorescence test, figure 21. In addition, more cell confluence is present on the CH-Col TEO and Coll TEO scaffold MC3T3 fluorescence images, figures 24 and 25. This may also related to their higher degree of roughness, as seen in SEM imagery and as indicated in SEM figures, figures 18 and 19. Nonetheless all fluorescence images acquired yielded promising results as cell adhesion and proliferation were evident with all scaffolds. In addition, it suggests low or insignificant degrees of cyto-toxicity levels from the scaffolds. Healthy cells and relatively high populations were captured for all scaffolds tested.

Again, one of the main objectives of the study was to produce crosslinked scaffolds to accommodate more sustainable degradation rates in physiological conditions and to produce favorable absorption characteristics. Therefore it was suggested that by incorporating FTIR technique, spectra comparison between parent polymers and

scaffolds would permit the monitoring of chemical modifications that may arise due to any crosslinking events. In spectra obtained for the corn starch irradiated scaffolds, preliminary findings did not indicate new peak transmittance. Of all the corn starch varieties, the scaffold spectra appeared very similar to the corn starch parent spectra. Arguably, assumptions can attribute this to the higher amount of corn starch used in scaffold preparation, which was higher in concentration than either SA or CH concentrations. Moreover, by comparing the CS, CS-SA, and CS-CH scaffold spectra, observation can be made that the spectra resemble each other and clearly indicate that the scaffolds spectra is heavily influenced by the majority material, corn starch. With this observation presented, and the fact that no new peak developments seem to have transpired, it's more likely that crosslinking didn't occur during the microwave irradiation process as previously thought. This coincides with Torres et al, where in *Microwave Processing of Starch-Based Porous Structures for Tissue Engineering Scaffolds*, its hypothesized that pure cornstarch molecules are not expected to form crosslinks during microwave heating. In addition, the high swelling ratios that were attained from the swelling ratio study may also validate this claim, with respect to the CS irradiated scaffolds. Table 6 compares the swelling ratio averages for day one and day seven. For all scaffolds tested it can be seen that the ratios from the CS based scaffolds are higher than ratios attained from the TEO treated scaffolds. It can be thus argued, that the high swelling ratios from the CS irradiated scaffolds, could be the result of an absence of a crosslinked polymer network. In effect, that there is low resistance to scaffold volume change attributed to the expansion caused by fluid absorption. The same phenomenon was noted in *Increasing Mechanical Strength of Gelatin Hydrogels by*

Divalent Metal Ion Removal, by Xing et al. where after chemically crosslinking hydrogels, the swelling ratios decreased for all samples, as a result of the formation of a rigid network.

In contrast FTIR analysis may very well mark crosslinking events, as a result of drastic modifications in the spectra for TEO treated scaffolds to their parent spectra. In addition, TEO treated scaffolds yielded lower swelling ratios than their irradiated counterparts (figure 6). Thus, suggestion can be made that these lower swelling ratios may be indicative of a more ridged network produced by crosslinking within the scaffold morphology. Future endeavors, which may help in validating this claim may involve either; setting up an experiment where scaffolds are exposed to a gradient study involving altering TEO concentration, or increasing the scaffold soaking time in the TEO solution. Then, subjecting the specimens to additional swelling ratio tests and monitor the differences in ratios. Should swelling ratios alter to either increasing concentrations or exposure time, a stronger argument may then exist in suggesting crosslinking is occurring as a result of TEO chemical treatment. The following tables (tables 7, 8, and 9) help illustrate how functional groups present in parent polymers used to make the scaffold changed and/or appear (it they do) in the final scaffold. Again, while pinpoint crosslinking has not yet been attained, the following tables may help bring to light some areas of interest that may do so. For example, in figure 7 below, peaks at 1153 cm^{-1} and 890 cm^{-1}, are evidence of the sugar backbone of saccharide structure of the chitosan. The fact that these two peaks are still present in the TEO treated scaffold, can facilitate the argument that the backbone polymer chain of the chitosan was not affected by the crosslinking. The broadening in the NH_2 and CH_2 range, for the same polymer and

scaffold, may hint at either H_2O present in the scaffold when tested or additional hydrogen bonding as a consequence of crosslinking. Moreover, the chitosan backbone chain was also contained in the spectra for the TEO treated CH-Coll scaffold as well. Thus, the chitosan backbone may not have been affected by being treated with TEO.

Table 6: FTIR- Functional Groups and Peak Change for CH powder and TEO treated CH scaffold

Chitosan Powder		TEO Treated Chitosan Scaffold
Wavenumber (cm^{-1})	**Functional Group**	
3413	NH_2 Stretching	Broadened
2861, 2906	CH_2	Broadened
1654	Amide I band, –C=O	Intensified
1565	NH_2	Intensified
1420, 1311	OH, CH Vibration	No change
1022, 1079	C-O stretching in acetamide	Shadowed by broad peak from 1270-940 cm^{-1}
1153, 890	Indicates backbone of chitosan -C-O-C in glycosidic linkage	Still present in spectra

Table 7: FTIR- Functional Groups and Peak Change for CH and Coll polymers and TEO treated CH-Coll scaffold

Wavenumber (cm^{-1})	Functional Group	TEO Treated CH-Coll
Collagen Fiber		
3415	NH_2 Stretching	No correlation
2929, 2863	C-H Stretching	No correlation
1650	Amide I band, -C=O	Not present
1542	Amide II band	Not present
1384	Amide III	Not present or shadowed by peak
1234	C-N Stretch of Amine	Not present
Chitosan Powder		
3413	NH_2 Stretching	No correlation
2861, 2906	CH_2	Broadened
1654	Amide I band, –C=O	Not present
1565	NH_2	Decreased in intensity
1420, 1311	OH, CH Vibration	1311- not present

1022, 1079	C-O stretching in acetamide	Shadowed by large peak
1153, 890	Indicates backbone of chitosan	890- still present 1153- maybe over shadowed by large peak

Table 8: FTIR Functional Groups and Peak Change for Coll fiber and TEO treated Coll scaffold

Collagen Fiber		**TEO Treated Collagen Scaffold**
Wavenumber (cm^{-1})	**Functional Group**	
3415	NH_2 Stretching	Broadened
2929, 2863	C-H Stretching	Broadened
1650	Amide I band, -C=O	Decreased in intensity
1542	Amide II band	Decreased in intensity
1384	Amide III	Unchanged
1234	C-N Stretch of Amine	Disappeared

Degradation rates for scaffolds tested reveal that the MW irradiated scaffolds degraded at lower percentages than all TEO treated scaffolds. In fact, both CS MW irradiated scaffolds tested actually acquired more weight 2% and 1% for specimen 1 and 2, respectively. CS-SA and CS-CH had degradation rates of -17% and -11%, respectively. Thus CS scaffolds were the only type that had an increase in weight. Caution should be made however and attention should be drawn to the fact that permeability of the scaffold could have played a factor in this. At the conclusion of the degradation study all scaffolds were placed in a glass desiccator for the extension of 3 days. Moreover, scaffolds were placed in the desiccator at the same time and removed at the same time. The idea presented, is there is a possibility that the CS scaffolds may have had a less permeable morphology than that of the CS-SA and CS-CH scaffolds and that H_2O may still be present in the scaffold after the three day desiccation as a result of lower fluid mobility throughout the CS scaffold. To back this up, the swelling ratio of the CS

scaffold depicted in figure 20, shows that from day 1 to day 7, the PBS absorption of the CS was ongoing. After 1 day in PBS, the CS scaffold has a swelling ratio of 335% and on day 7, the swelling ratio increased to 396%, by far the largest increase in the first 7-day study, indicating that H_2O may have still been migrating into the scaffold. Nonetheless, the MW irradiated scaffolds still seem to show more stability in the PBS media than the TEO treated scaffolds. Suggesting they may be better apt to stage cellular process for tissues with longer tissue growth. The degradation rates for TEO treated CH-Coll and TEO treated Coll, were 52.5% and 37%, respectively. Thus, degradation of TEO treated CH-Coll and TEO treated coll, significantly out pace the MW irradiated cornstarch based scaffolds, indicating a greater degree of stability in PBS solution for the MW irradiated scaffolds.

CHAPTER V

CONCLUSION

The synthesis, characterization, and bio-assessment of two types of tissue engineering scaffolds was presented. While, crosslinking attainment was one of the more sought endeavors of the study, results indicate that the microwaved irradiated scaffolds more than likely did not crosslink via irradiation. This was primarily postulated by the examination of results off Fourier Transform Infrared spectroscopy and swelling ratio results. On the other hand, the same methodologies indicated that the triethyl orthoformate treated varieties may have caused crosslinking to occur as a result of the treatment. Crosslinking was initially deemed of importance in order to provide improved mechanical integrity to the scaffold, to permit high degrees of fluid absorption and to facilitate expansion via cell proliferation. It was also thought that it would deliver more stable degradation rates in simulated body studies, where high fluidity environments are present. Interestingly, the MW irradiated scaffolds yielded lower degradation rates and higher swelling ratios and did not burst as a result of fluid intake as it swelled, all while showing no crosslinking evidence.

Energy dispersive spectroscopy and X-ray photoelectron spectroscopy characterization also indicated that the templates seemed to be molecularly similar at the surface to that of their parent polymer used, where the parent polymers are all known to be biocompatible in nature. This was important in that it suggested biocompatibility

amongst the scaffolds before *in vivo* endeavors. As projected all scaffolds deliberated, indicated viability and non-cytotoxic traits via the *in vitro* fluorescence study. Moreover, the fluorescence images indicated that there was commencement of cell attachment while providing evidence of cell proliferation by the identification of key cellular organelle systems.

Finally, scanning electron microscopy gave light to the morphological geologies attributed from the scaffold synthesis methods. Porous morphology existed in corn starch microwave irradiated scaffolds while porous and permeable networks existed in in the corn starch-sodium alginate and corn starch-chitosan scaffolds. The TEO chemically treated scaffolds however did not show was much porous and permeability as with the microwave irradiated scaffolds. However, attention was brought to the fact that a collapsed porous and permeable network may exist and may reconstruct as fluid absorption initiates, analogous to the blowing up of a balloon. Nonetheless, scaffolds studied thus far seem to indicate that avenues exist for cell proliferation through the surface and throughout the scaffold.

While these assessed templates are long from actual application programs, they indicate promise thus far as viable tissue engineering scaffolds. Future prospects include pinpointing where crosslinking in the TEO treated scaffolds may be taking place and the type of bonding responsible, again if crosslinking is occurring. In addition, to help improve the mechanical integrity to oppose shear stresses, it's thought that a fiber mesh could help by being employed throughout the scaffold morphology. Forcespinning technology or electrospinning processes may be viable options in attaining such biocompatible reinforcing fibers.

REFERENCES

1. Florida Institute of Technology. Biomedical-engineering welcome page. Retrieved October 2013, coe.fit.edu/biomedical-engineering/

2. Ratner, B. D., Hoffman, A. S., Schoen, F. J., & Lemons, J. E. (1996). Biomaterials Science: An Introduction to Materials in Medicine. San Diego, CA: Academic Press.

3. Yunos, D. M., Bretcanu, O., & Boccaccini, A. R. (2008). Polymer-Bioceramic Composites for Tissue Engineering Scaffolds. Commonality of Phenomena in Composite Materials, J Mater Sci. (43) pp. 4433-4442.

4. Hubbell, J. A., & Langer, R. (1995). Tissue Engineering. Chemical & Engineering News, 73, pp. 42-54.

5. Thayer, S. M. (2011). Biology's approach to construction: The developement and use of scaffolds in tissue engineering. Illumin, 14 (3).

6. Karp, J. M. (2003). Scaffolds for tissue engineering. Materials Research Society Bulletin, 28, pp. 301-306.

7. Chan, B., & Leong, K. (2008). Scaffolding in tissue engineering: general approaches and tissue specific considerations. European Spine Journal, 17.4 pp. 467-479.

8. Ackbar, R., & al., e. (2007). Scaffolds for skeletal tissue engineering. The University of Sheffield [online] http://iadr.confex.com/iadr/bsdr07/techprogram/abstract_95076.htm 2007.

9. Martin, I., Wendt, D., & Heberer, M. (2004). The role of bioreactors in tissue engineering . Trends in Biotechnology, 22 (2), pp. 80-86.

10. Martin, Y., & Vermette, P. (2005). Bioreactors for tissue mass culture: design, characterization, and recent advances. Biomaterials, 26 (35), pp. 7481-7503.

11. Plunkett, N., & O'Brian, F. (2011). Bioreactor in Tissue Engineering. Technology and Health Care,19, 55-69.

12. Mekala, N. K., Baadhe, R. R., & Parcha, S. R. (2011). Review on bioreactos in tissue engineering. Bio Technology: An Indian Journal, 5 (4), pp. 246-253.

13. Lee, S., & Shin, H. (2007). Matrices and Scaffolds for Delivery of Bioactive Molecules in Bone and Tissue Engineering. Advanced Drug Delivery Reviews, 59, 339-359.

14. Fishman, J. M., Tyraskis, A., Maghsoudlou, P., Urbani, L., Tontonelli, G., Birchall, M. A., et al. (2013). Skeletal muscle tissue engineering: Which cell to use? Tissue Engineering Part B: Reviews, 19 (6), pp. 503-515.

15. Gartner, L. P., & Hiatt, J. L. (2006). Color Atlas of Histology (4th ed.). Baltimore, Maryland: Lippincott Williams & Wilkins.

16. Loh, Q. L., & Choong, C. (2013). Three-dimensional scaffolds for tissue engineering applications: Role of porosity and pore size. Tissue Engineering Part B: Reviews, 19 (6), pp. 485-502.

17. Hutmacher, D. W. (2000). Scaffolds in Tissue Engineering Bone and Cartilage . Biomaterials, 21 (24), pp. 2529-2543.

18. Yang, S., Leong, K.-F., Du, Z., & Chua, C.-K. (2001). The design of scaffolds for use in tissue engineering. Part I. Traditional Factors. Tissue Engineering, 7 (6), pp. 679-689.

19. Clyne, Alisa Morss Thermal Processing of Tissue Engineering Scaffolds. *Journal of Heat Transfer* (March 2011) Vol. 133

20. Chung, H. J., and Park, T. G., (2007) Surface Engineered and Drug Releasing Pre-Fabricated Scaffolds for Tissue Engineering. Adv. Drug Delivery Rev., 59 (4–5), pp. 249–262.

21. Tuzlakoglu, K., and Reis, R. L., (2009) Biodegradable Polymeric Fiber Structures in Tissue Engineering, Tissue Eng. Part B Rev., 15(1), pp. 17–27.

22. Weigel, T., Schinkel, G., and Lendlein, A., (2006) Design and Preparation of Polymeric Scaffolds for Tissue Engineering. Expert Review of Medical Devices, 3 (6), pp. 835–851.

23. Yang, S., Leong, K.-F., Du, Z., and Chua, C.-K., (2001) The Design of Scaffolds for Use in Tissue Engineering. Part I. Traditional Factors. Tissue Eng., 7 (6), pp. 679–689.

24. Kim, B.S., and Mooney, D.J., 1998, Engineering Smooth Muscle Tissue with a Predefined Structure. J. Biomed. Mater. Res., 41 (2), pp. 322-332

25. Lee, S. J., Oh, S. H., Liu, J., Soker, S., Atala, A., and Yoo, J. J., 2008, "The Use of Thermal Treatments to Enhance the Mechanical Properties of Electro-spun Poly-Caprolactone Scaffolds, Biomaterials, 29 (10), pp. 1422–1430.

26. Murugan, R., Huang, Z. M., Yang, F., and Ramakrishna, S., (2007) Nanofibrous Scaffold Engineering Using Electrospinning. J. Nanosci. Nanotechnol. 7 (12), pp. 4595–4603.

27. Wnek, G. E., Carr, M. E., Simpson, D. G., and Bowlin, G. L., (2003) Electro-spinning of Nanofiber Fibrinogen Structures. Nano Lett., 3(2), pp. 213–216

28. Min, B.-M., Lee, G., Kim, S. H., Nam, Y. S., Lee, T. S., and Park, W. H., (2004) Electrospinning of Silk Fibroin Nanofibers and Its Effect on the Adhesion and Spreading of Normal Human Keratinocytes and Fibroblasts In Vitro. Biomaterials, 25 (7–8), pp. 1289–1297

29. Li, M., Mondrinos, M. J., Chen, X., Gandhi, M. R., Ko, F. K., and Lelkes, P. I., (2006) Co-Electrospun Poly(Lactide-co-Glycolide), Gelatin, and Elastin Blends for Tissue Engineering Scaffolds, J. Biomed. Mater. Res. Part A, 79 (4), pp. 963–973.

30. Xu, Fenghua, Weng, Baicheng, Materon, Luis Alberto, Gilerson, Robert, Lozano, Karen Large-scale production of ternary composite nanofiber membrane for wound dressing applications. Currently under review for publication.

31. Padron S, Fuentes AA, Caruntu DI, Lozano K. Experimental study of nanofiber production through forcespinning. J Appl Phys (2013); 113:024318.

32. Sarkar K, Gomez C, Zambrano S, Ramirez M, Hoyos E, Vasquez H, Lozano K. Electrospinning to forcespinning™. Mater Today (2010) 13 (11): pp. 12–14.

33. Lozano K, Sarkar K. U.S. Pat. 8231378 (2012)

34. Ramakrishna S. An introduction to electrospinning and nanofibers technology. World Scientific Publishing Co. Singapore, (2005) pp. 130.

35. Cima, L. G., Vacanti, J. P., Vacanti, C., Ingber, D., Mooney, D., and Langer, R., (1991), Tissue Engineering by Cell Transplantation Using Degradable Polymer Substrates. J. Biomech. Eng., 113 (2), pp. 143–151.

36. Whang, K., Thomas, C. H., Healy, K. E., and Nuber, G., (1995) A Novel Method to Fabricate Bioabsorbable Scaffolds. Polymer, 36 (4), pp. 837–842.

37. Whang, K., Healy, K. E., Elenz, D. R., Nam, E. K., Tsai, D. C., Thomas, C. H., Nuber, G. W., Glorieux, F. H., Travers, R., and Sprague, S. M., (1999) Engineering Bone Regeneration with Bioabsorbable Scaffolds with Novel Microarchitecture. Tissue Eng., 5(1), pp. 35–51.

38. Baker, S. C., Rohman, G., Southgate, J., and Cameron, N. R., (2009) The Relationship Between the Mechanical Properties and Cell Behavior on PLGA and PCL Scaffolds for Bladder Tissue Engineering. Biomaterials, 30 (7), pp. 1321–1328.

39. Spiller, K. L., Laurencin, S. J., Charlton, D., Maher, S. A., and Lowman, A. M., (2008) Super Porous Hydrogels for Cartilage Repair: Evaluation of the Morphological and Mechanical Properties. Acta. Biomater., 4 (1), pp. 17–25

40. Sachlos, E., Czernuszka, J.T. Making tissue engineering scaffolds work. Review on the application of solid freeforming fabrication technology to the production of tissue engineering scaffolds. European Cells and Materials Vol. 5. (2003) pp. 29-40

41. Dagalakis N, Flink J, Stasikelis P, Burke JF, Yannas IV (1980) Design of an artificial skin. Part III. Control of pore structure. Biomaterials (14) pp. 511-528.

42. Doillon CJ, Whyne CF, Brandwein S, Silver FH. (1986) Collagen-based wound dressings: Control of the pore structure and morphology. J Biomed Mater Res 20: pp. 1219-1228.

43. Schoof H, Apel J, Heschel I, Rau G (2001) Control of pore structure and size in freeze-dried collagen sponges. J Biomed Mater Res-A 58: pp. 352-357.

44. Schoof H, Burns L, Fisher A, Heschel I, Rau G (2000) Dendritic ice morphology in unidirectionally solidified collagen suspensions. J Crystal Growth 209: pp. 122-129.

45. Mooney DJ, Baldwin DF, Suh NP, Vacanti JP, Langer R (1996) Novel approach to fabricate porous sponges of poly(D,L-lactic co-glycolic acid) without the use of organic solvents. Biomaterials 17: pp. 1417-1422.

46. Callister, W. D. (2007). Material Science and Engineering an Introduction (7th Edition). Wiley & Sons, Inc.

47. Yusop, A., Bakir, A., Shaharo, N., Kadir, M. A., & Hermanwan, H. (2012). Porous biodegradable metals for hard tissue scaffolds: A review. International Journal of Biomaterials, (2012).

48. Yoshida, Y., Dhandayuthapani, B., Maekawa, T., & Kumar, D. S. (2011). Polymeric Scaffolds in Tissue Engineering Application: A Review. International Jounal of Polymer Science, (2011).

49. Huang, J., Lin, Y. W., Fu, X. W., Best, S. M., Brooks, T. A., Rushton, N., et al. (n.d.). Development of Nano-sized Hydroxyapatite Reinforced Composites for Tissue Engineering Scaffolds. J Mater. Sci: Mater Med, 18, pp. 2151-2157.

50. Bruice, Paula Yurkanis. Organic Chemisitry-5th Edition. Upper Saddle River, NJ: Pearson Prentice Hall, (2007), Textbook

51. Solomans, T.W. Graham Fryhle, Craig B., Organic Chemistry 8th Edition. Wiley & Sons, Inc, (2004), Textbook

52. Ratner B.D., Bryant S.J. Biomaterials: Where we have been and where we are going. Annu. Rev. Biomed. Eng. (2004) vol. 6: pp. 41-75.

53. Khan, F., Ahmad, S., Polysaccharides and Their Derivatives for Versatile Tissue Engineering Application. Macromolecular Bioscience Journals. (2013), 13, pp 395-421

54. Shelke, N. James, R. Laurencin, C. Kumbar, S. Polysaccharide biomaterials for drug delivery and regenerative engineering. Polymers Advanced Technologies. (2014)

55. K.M. Colvin, V.D. Gordon, K. Murakami, B. R. Borlee, D. J. Wozniak, G. C. L. Wong, M. R. Parsek, PLoS Pathog. (2011), 7(1), e1001264

56. M. M. H. Huisman, H.A. Schols, A.G. J. Voragen, Carbohydrate Polymers (1999), 38(4), pp. 299-307

57. I. Mkedder, C. Travelet, A. Durand-Terrasson, S. Halila, F. Dubreuil, R. Borsali, Carbohydr. Polym. (2013) 94(2), pp. 934-939

58. M. G. Peter, chitin and CS from Animal Sources, in Biopolymers, Vol. 8 (Ed: A. Steinbuchel), Wiley-VCH, Weinheim (2002) pp. 481-574

59. Ko, Hsu-Feng, Sfeir, Charles, Kumta, Prashant N. Novel synthesis strategies for natural polymer and composite biomaterials as potential scaffolds for tissue engineering Philosophical Transaction of the Royal Society A (2010) 368, pp. 1981-1997

60. Bo Fang, Yi-Zao Wan, Ting-Ting Tang, Chuan Gao, and Ke-Rong Dai. Tissue Engineering Part A. May (2009) 15(5): pp. 1091-1098. doi:10.1089/ten.tea.2008.0110

61. Gao, Chuan, Wan, Yizao, Yang, Chunxi, Dai, Kerong, Tang, TingTing, Luo, Honglin, Wang, Jiehua preparation and characterization of bacterial cellulose sponge with hierarchal pore structure as tissue engineering scaffolds. J Porous Mater (2011) 18: pp. 139-145

62. R. Jayakumar, Menon, Deepthy, Manzoor, K., Nair, S.V., Tamura, H. Biomedical applications of chitin and chitosan based nanomaterials- A short review Carbohydrate Polymers 82 (2010) pp. 227-232

63. Cho YW, Jang J, Park JR, Ko SW. Preparation and solubility in acid and water of partially deacetylated chitins. Biomacromolecules (2000); 1: pp. 609–14.

64. Jayakumar R., Prabaharan, M., Nair, S.V., Tamura, H. Novel chitin and chitosan nanofibers in biomedical applications. Biotechnology Advances 28 (2010) pp. 142-150

65. Kurita K. Controlled functionalization of the polysaccharide chitin. Prog Polym Sci (2001) 269; 1921-1971

66. Jayakumar R, Tamura H. Synthesis, characterization and thermal properties of chitin-g- poly(caprolactone) copolymers using chitin hydrogel. Int J Biol Macromol (2008);43: 32–6.

67. Nagahama H, Kashiki T, Nwe N, Jayakumar R, Furuike T, Tamura H. Preparation of biodegradable chitin/gelatin membranes with GlcNAc for tissue engineering applications. Carbohydr. Polym. (2008) a;73: pp. 456–63.

68. Nagahama H, Nwe N, Jayakumar R, Koiwa S, Furuike T, Tamura H. Novel biodegradable chitin membranes for tissue engineering applications. Carbohydr Polym (2008)b;73: pp. 295–302.

69. Min BM, Lee SW, Lim JN, You Y, Lee TS, Kang PH, et al. Chitin and chitosan nanofibers: electrospinning of chitin and deacetylation of chitin nanofibers. Polymer (2004);45: pp. 7137–42.

70. Di Martino, A., Sittinger, M. & Risbud, M. V. (2005) Chitosan: a versatile biopolymer for orthopaedic tissue- engineering. Biomaterials 30, pp. 5983–5990. (doi:10.1016/j.biomaterials.2005.03.016)

71. Suh, J.-K. F. & Matthew, H. W. T. (2000) Applications of chitosan-based polysaccharide biomaterials in cartilage tissue engineering. Biomaterials 21, pp. 2589–2598. (doi:10.1016/S0142 9612(00)00126-5)

72. Hejazi, R. & Amiji, M. (2003) Chitosan-based gastrointestinal delivery systems. J. Control. Release 89, pp. 151–165. (doi:10.1016/S0168-3659(03)00126-3)

73. Li, J. & Xu, Z. (2002) Physical characterization of a chitosan-based hydrogel delivery system. J. Pharm. Sci. 91, pp. 1669–1677. (doi:10.1002/jps.10157)

74. Zhang, Y. & Zhang, M. (2001) Synthesis and characterization of macroporous chitosan/calcium phosphate composite scaffolds for tissue engineering. J. Biomed. Mater. Res. A 55, pp. 304–312. (doi:10.1002/1097-4636(20010605)55:3<304::AID-JBM1018>3.0.CO;2-J)

75. Kim, S. E., Park, J. H., Cho, Y. W., Chung, H., Jeong, S. Y., Lee, E. B. & Kwon, I. C. (2003) Porous chitosan scaffold containing microspheres loaded with transforming growth factor-b1: implications for cartilage tissue engineering. J. Control. Release 91, pp. 365–374. (doi:10.1016/ S0168-3659(03)00274-8)

76. Lee, K. Y., Kwon, I. C., Kim, Y. H., Jo, W. H. & Jeong, S. Y. (1998) Preparation of chitosan self-aggregates as a gene delivery system. J. Control. Release 51, pp. 213–220. (doi:10.1016/S0168- 3659(97)00173-9)

77. Roy, K., Mao, H. Q., Huang, S. K. & Leong, K. W. (1999) Oral gene delivery with chitosan–DNA nanoparticles generates immunologic protection in a murine model of peanut allergy. Nat. Med. 5, pp. 387–391. (doi:10.1038/7385)

78. Peter, M., Binulol, N. S., Nair, S. V., Selvamurugan, N., Tamura, H., & Jayakumar, R. (2010). Novel biodegradable chitosan-gelatin/nano-bioactive glass ceramic composite scaffolds for alveolar bone tissue engineering. Chemical Engineering Journal, 158, pp. 353–361

79. Peter, M., Ganesh, N., Selvamurugan, N., Nair, S. V., Furuike, T., Tamura, H., et al. (2010). Preparation and characterization of chitosan-gelatin/ nanohydroxyapatite composite scaffolds for tissue engineering applications. Carbohydrate Polymers, 80, pp. 414–420.

80. L. Kong, Y. Gao, G. Lu, Y. Gong, N. Zhao, X. Zhang. A study on the bioactivity of chitosan/nano-hydroxyapatite composite scaffolds for bone tissue engineering. Eur. Polym. J. 2006, 42, 3171-3179.

81. Panjian, L., Ohtsuki, C., Kokubo, T., Nakanishi, K., & Soga, N. (1992). Apatite forma- tion induced by silica gel in a simulated body fluid. Journal of American Ceramic Society, 75, pp. 2094–2107.

82. Karlsson, K. H., Froberg, K., & Ringbom, T. (1989). A structure approach to bone adhering of bioactive glasses. Journal of Non-Crystalline Solids, 112, 69–72.

83. Lee, Kuen Yong, Mooney, David J. Alginate: Properties and biomedical applications. Progress in Polymer Science 37 (2012) pp. 106-126

84. Cattalini, JP., Garcia, J., Boccaccini, A.R., Lucangioli, S., Mourino, V. A new calcium releasing nano-composite biomaterial for bone tissue engineering scaffolds. Procedia Engineering (2013) 59, pp. 78-84.

85. Marsich, E., Bellomo, F., Turco, G., Travan, A., Donati, I., & Paoletti, S. (2013). Nano-composite Scaffolds for Bone Tissue Engineering Containing Silver Nanoparticles: Preparation, Characterization and Biological Properties. Journal of Material Science: Material Medicine, 24, pp. 1799-1807.

86. Chen, J., Li, X., Cui, W., Xie, C., Zou, J., & Zou, B. (2010). In situ grown fibrous composites of poly(Dl-lactide) and hydroxyapatite as potential tissue engineering scaffolds. Polymer. (51) 26, pp. 6268-6277

87. Nejati, E., Mirzadeh, H., & Zandi, M. (2008). Synthesis and characterization of nano-hydroxyapatite rods/poly(L-lactide acid) composite scaffolds for bone tissue engineering. Composites: Part A, 39, pp. 1589-1596.

88. Wei, G., & Ma, P. (2004). Structures and properties of nano-hydroxyapatite/polymer composite scaffolds for bone tissue engineering. Biomaterials , 25, pp. 4749-4757.

89. Zhang, L., Liu, W., Yue, C., Zhang, T., Li, P., Xing, Z., et al. (2013). A tough graphene nanosheet/HA composite with improved in vitro biocompatibility. Carbon 61, pp. 105-115.

90. Mishra, S., Rajyalakshmi, A., & Balasubramanian, K. (2012). Compositional dependence of hematopoietic stem cells expansion on bioceramic composite scaffolds for bone tissue engineering. J Biomed Mater Res Part A, pp. 2483-2491.

91. Zhang, Q., Mochalin, V. N., Neitzel, I., Knoke, I. Y., Han, J., Klug, C. A., et al. (2011). Fluorescent PLLA-Nanodiamond composites for bone tissue engineering. Biomaterials, 32, pp. 87-94.

92. Barbieri, D., Yuan, H., Luo, X. F., Grijpma, D. W., & Bruijn, J. D. (2013). Influence of polymer molecules weight in osteoinductive composites for bone tissue regeneration. Acta Biomaterialia. July

93. Britto, V., Tiwari, S., Purohit, V., Wadgaonkar, P., Bhoraskar, S., Bhonde, R., et al. (2009). Composites of plasma treated poly(etherimide) films with gold nanoparticles and lysine through layer by layer assembly: a "friendly-rough" surface for cell adhesion and prolideration for tissueengineering applications. Journal of Materials Chemistry, pp. 544-550.

94. Yang, Z., Xu, L., Yin, F., Shi, Y., Han, Y., Zhang, L., et al. (2012). In vitro and in vivo characterization of silk fibroin/gelatin composite scaffolds for liver tissue engineering . Journal of Digestive Diseases.

95. Liu, Jin. Yang, Rendang. Yang, Fei. Effect of the starch source on the performance of cationic starches having similar degree of substitution for papermaking using deinked pulp. Bioresouces 10(1), pp. 922-931

96. Kizil, Ramazan, Irudayaraj, Joseph, Seetharamn, Koushik. Characterization of irradiated starches by using FT-Raman and FTIR spectroscopy. Department of agricultural and Biological Engineering, 227 agricultural engineering building, the Pennsylvania state university, University Park, Pennsylvania 16802, USA. Journal of Agricultural and Food Chemistry 08/2002; 50(14):3912-8

97. lamellipodium. (n.d.) The American Heritage® Medical Dictionary. (2007). Retrieved May 13, 2015 from: http://medicaldictionary.thefreedictionary.com/lamellipodium

98. Mattila, Pieta, Lappalainen, Pekka (2008) Filopodia: molecular architecture and cellular functions Nature Reviews Molecular Cell Biology 9, pp. 446-454

99. Ma, Lie, Gao, Changyou, Mao, Zhengwei, Zhou, Jie, Shen, Jiacong, Hu, Xueqing, Han, Chunmao. (2003) Collagen/chitosan porous scaffolds with improved biostability for skin tissue engineering Elsevier Biomaterials 24, pp. 4833-4841

100. Torres, Fernando G., Boccaccini, Aldo R., Troncoso, Omar P. (2007) Microwave Processing of Starch-Based Porous Structures for Tissue Engineering Scaffolds. Journal of Applied Polymer Science 103, pp. 1332-1339

101. Xing, Q, Yates, Keegan, Vogt, Caleb, Qian, Zichen, Frost, Megan, Zhao, Feng. (2014) Increasing Mechanical Strength of Gelatin Hydrogels by Divalent Metal Ion Removal. Scientific Reports 4: 4706 DOI: 10.1038/srep04706

BIOGRAPHICAL SKETCH

Marcos Rene Villarreal was born into a scientific and educationally driven family on September 26, 1984 in Edinburg, Texas. Residing in South Texas his entire life, Marcos enrolled and attended The Science Academy of South Texas (Sci-Tech) in Mercedes, Texas where he graduated in May of 2003 with his high school degree. It was during his tenure at Sci-Tech where Marcos first contemplated a future as an engineer, first finding interest in tissue engineering and subsequently structural engineering. After high school, he decided to pursue his engineering career. Admitted into both the University of Texas-San Antonio and The University of Texas-Pan American, he eventually graduated with his bachelor degree in mechanical engineering from the University of Texas Pan American in 2010. After graduation an opportunity in teaching with McAllen ISD was presented which set the foundation for a future in even higher education. After one year in teaching, Marcos tried for the oil and gas industry working with FESCO Ltd as a electric wire line operator . With the rigorous and spontaneous nature of the oilfield, the motivation acquired from the high school students he mentored, and the new family forged with his wife, Candace Michelle Villarreal, he set to acquire a masters degree in mechanical engineering from the University of Texas Pan American. After admittance in the fall of 2013, he started research work under the guidance and mentorship of Dr. Waseem Haider, who helped devise an exciting thesis study involving tissue engineering scaffolds for biomedical applications. Marcos R. Villarreal received his MS degree from the University of Texas-Pan American in July 2015 with a 3.66 GPA and is currently seeking a PhD program in engineering

or medical school program. Marcos Villarreal's permanent mailing address is that of his parents physical address, Dr. John and Nelinda Villarreal 5107 North Victoria Road in Donna, Texas, 78537.